THE INFLUENCE OF A PACIFIC INVASIVE SPONGE ON CORAL REEF DYNAMICS IN HAWAIʻI

A DISSERTATION SUBMITTED TO THE GRADUATE DIVISION OF
THE UNIVERSITY OF HAWAIʻI AT MĀNOA IN PARTIAL FULFILLMENT OF THE
REQUIREMENTS FOR THE DEGREE OF

DOCTOR OF PHILOSOPHY

IN

OCEANOGRAPHY

AUGUST 2018

By

Joy Leilei Shih

Dissertation Committee:

Brian N. Popp, Chairperson
Matthew J. Church
Richard E. Zeebe
Ruth D. Gates
Les Watling

Keywords: Marine sponges, nitrogen cycling, stable isotopes, Hawaiʻi, invasive species

For 奶奶

The matriarch of our family over multiple generations. Your dream was that we could fulfill our dreams in life. We are doing that, because of you.

ACKNOWLEDGEMENTS

First and foremost, I'd like to thank my advisor Brian Popp who introduced me to the exciting world of stable isotope biogeochemistry and guided me patiently throughout my project. Through your immense knowledge you both inspired and challenged me. I am indebted to your mentorship. I also want to extend my sincerest gratitude to my committee members who provided invaluable feedback and encouragement. Ruth Gates, no one can share the wonder of corals and impart the importance of these magnificent organisms like you. Thank you for letting me be a part of the magic in your lab. Richard Zeebe, your unparalleled knowledge in the field of carbon chemistry has inspired me from day one. The bars you set would be intimidating if not for your friendly and sincere desire to help others set and reach their own bars. Matt Church, your expertise in microbial nitrogen cycling has been essential to my development as a scientist. I am truly grateful to the willing time you always took to always answer questions and discuss my research. Les Watling, your always thoughtful perspective helped my project take shape, thank you for your graciously provided guidance. It has been an honor and privilege to work with every one of you.

Graduate school is a long and arduous journey and is one I would not have been able to complete without the wisdom, nurture, and enthusiasm of my past academic mentors, James Graham, James Leichter, and Dimitri Deheyn. I am also enormously appreciative to Laura Nunez Pons, who taught me much that I know about conducting research on sponges in the field, and Michael Cooney for his welcoming mentorship and support.

Throughout this challenging undertaking, every step was illuminated with the unwavering and unconditional support of my dearest friends, Tracy Chen, Ali Firouzi, Rawson Glover, Roxanne Rivero, Scott Higgins, and Jennivine Lee. My success would have been impossible without your support, and for that I am eternally grateful. While in Hawai‘i, I met a group of individuals who have become lifelong friends. Robert and Reina Harris, Joshua and Malia Wisch, and Chris Lee, it is a great understatement to say that you are all doing amazing things to change the world. I am so honored and humbled to share friendships with you that have included everything from shoulders to cry on, brainstorming ideas that would become groundbreaking legislation, and laughing so hard it hurts while playing Bears vs. Babies. Truly, you have all been essential to the preservation of my physical and mental health throughout my graduate career.

Of course, I would not have been able to go down this path without the unconditional support of my mother Judy Chin and father K.C. Shih. Many other members of my family were equally critical to my success. Especially essential to this achievement was my brother Kingstone Shih, my grandfather Robert Liu, and my aunt Christina Shih for their unconditional love and sources of inspiration.

Last but not least, I would like to thank Alexander Mouldovan, the light in my life, and Kalia, the apple of my eye.

Financial support for the research presented in this dissertation was provided by NOAA Sea Grant #NA14OAR4170071. Supplemental funds were provided by the University of Hawai‘i at Mānoa Graduate Student Organization Grants and Awards program.

ABSTRACT

Sponges are ecologically important components of many benthic ecosystems and are abundant on coral reefs. Many sponges host a diverse consortium of microbes and are known to rely on their symbiotic microbial communities for a variety of functions including nutrition, metabolic waste removal, and the production of secondary metabolites for chemical defense. *Mycale grandis* is an alien invasive sponge that first appeared in Hawai‘i in the late 1990s and is found within several partially degraded shallow water coral ecosystems throughout the main Hawaiian Islands. In surveys of south Kāne‘ohe Bay, *M. grandis* benthic coverage was found to range from 2% on fringing coral reefs to 32% in mangrove ecosystems. I report seawater pumping rates (0.016 L seawater s^{-1} kg^{-1} sponge (dry mass)) and ammonia oxidation rates (21.2 nM $g^{-1}h^{-1}$) for *M. grandis*, which are the first such rates measured in a Pacific sponge. Combining pumping rates, biomass estimates, and nitrogen flux rates for *M. grandis* with depth and circulation parameters in south Kāne‘ohe Bay indicates that it is the most significant benthic source of dissolved inorganic nitrogen to the water column in the environments studied. Individual amino acid $\delta^{13}C$ and $\delta^{15}N$ values suggest that *M. grandis* acquires nutrition from its associated bacteria through direct assimilation of bacterially-synthesized amino acids. Statistically indistinguishable ΣV indices and trophic position of microbial and sponge cells also support this dietary strategy. These results strongly suggest that the *M. grandis* microbial consortia assimilate DOM, resynthesize the organic material, and pass on nutrition to the sponge in the form of amino acids through translocation. The vulnerability of native and endemic species to invasive reef species coupled with the threats of increased anthropogenic activity, ocean acidification, and ocean warming have growing implications for ecosystems throughout Hawai‘i. It is evident that where sponges are abundant members of the reef community, the sponge holobiont can play important

roles in organic matter recycling and can significantly alter nutrient profiles within the water column through their rapid rate of seawater circulation and biogeochemically active microbiome.

TABLE OF CONTENTS

LIST OF TABLES

LIST OF FIGURES

CHAPTER 2

CHAPTER 3

CHAPTER 4

LIST OF ABBREVIATIONS

DW, WW: Dry weight and wet weight of sponge

^{15}N: Stable heavy isotope of nitrogen used in tracers

N+N: Combined concentrations of NO_3^- + NO_2^-

DIN: Dissolved inorganic nitrogen; includes NH_4^+, NO_2^-, and NO_3^-

TN: Total nitrogen; all nitrogenous material which passes through a glass fiber filter (~0.7 μm nominal pore size; inorganic and organic compounds)

DOC: Dissolved organic carbon; operationally defined as organic carbon which passes through glass fiber filter

DON: Dissolved organic nitrogen; all nitrogenous material which passes through a glass fiber filter minus inorganic nitrogen (DON = TN – DIN)

DOM: Dissolved organic matter, all material that passes through a glass fiber filter inclusive of both carbon and nitrogen

POM: Particulate organic matter; all material retained on a glass fiber filter inclusive of both carbon and nitrogen

HMA: High microbial abundance (see Hentschel et al. 2006); referring to species of sponges hosting large tissue microbial communities

LMA: Low microbial abundance (see Hentschel et al. 2006); referring to species with tissue microbial densities similar to surrounding seawater.

Δ[analyte]: Refers to the ambient seawater concentration minus the excurrent concentration of the stated analyte

FCM: Flow cytometry methods

SYN: *Synechococcus*

HBACT: Heterotrophic bacterial cells

AA: Amino Acid(s)

CSIA: Compound specific isotopic analysis

ΣV: An index for microbial resynthesis of amino acids determined by the sum of variance among individual $\delta^{15}N$ values of trophic amino acids

TP: Trophic proxy; determined from the difference in averaged $\delta^{15}N$ values between trophic and source amino acids

TL: Trophic level; estimate based on the $\delta^{15}N$ values of measured amino acids and $\delta^{15}N$ amino acid values of assumed primary producers and assumed trophic enrichment factors

CHAPTER 1:

Introduction

Sponges are an abundant and ecologically important component of coral reefs, yet research on the biogeochemical roles of these ubiquitous members of the benthic habitat is limited for the Pacific. Investigating how these filters feeders affect the biogeochemistry of the overlying water column through their active pumping rates and metabolic activities is crucial to understanding the role sponges play in ecosystem dynamics. Given the abundance of sponges in Hawai‘i and the diverse and active microbial symbioses observed in sponges, investigating the influence of invasive sponges on these ecosystems has great implications for our understanding of the ecology and biogeochemistry found on tropical reefs.

In Hawai‘i, sponges account for about one third of the total alien marine species (Eldredge and Carlton 2002). *Mycale grandis*, an invasive sponge from the Indo-Pacific region, was unintentionally introduced to Hawai‘i in the late 1990s. It is the most abundant and most aggressive invasive sponge found on Hawaiian reefs (Coles et al. 2007). Biomass of the sponge increased throughout the mid 2000s and the sponge remains a prominent member of the benthic community in Kāne‘ohe Bay and other partially degraded shallow coral reef ecosystems in Hawai‘i.

Globally, sponges are one of the most successful multicellular organisms in the ocean. The resilience of siliceous sponges like *M. grandis* has been long exemplified by their survival through mass extinctions that eliminated many other organisms (Botting et al. 2017). Their resiliency suggests sponges will continue to be competitive in compromised ecosystems such as coral reefs under future regimes of ocean warming and ocean acidification (Bell et al. 2013) and decreased sunlight (Botting et al. 2017) while calcifying organisms are particularly vulnerable to

rising ocean acidity and temperatures (Hoegh-Guldberg et al. 2007, Fabry et al. 2008, Hofmann et al. 2010). Associations between sponges and microbes have a remarkable history of at least 600 million years in the fossil record making them one of the first symbioses between microbes and Metazoa (Wilkinson 1984). The largest and most internally consistent reconstruction of a metazoan-scale superalignment of 1,719 genes confirmed that sponges are the sister group to all other multicellular animals (Simion et al. 2017). Sponges owe their unique adaptability to a variety of conditions and environments to their ability to use both dissolved and particulate matter as nutritional sources, and to their close relationship with their symbiotic microbial communities. Sponges use their array of microbial symbionts for functions such as nutrient acquisition, conversion of their own metabolic wastes into less harmful substrates, and to attain secondary metabolites for chemical defense (Taylor et al. 2007a).

This study focuses on Kāneʻohe Bay in Oʻahu, Hawaiʻi. Considered a model system, many variables are richly documented in the bay. Because Kāneʻohe Bay is typically a nitrogen limited environment except for short bursts following heavy rainfall (De Carlo et al. 2007) any perturbation to the N balance in the bay has the ability to affect the overall ecosystem, potentially favoring some reef species over others. Increases in dissolved inorganic nutrients and/or reductions in the numbers of herbivores may allow algae to outcompete and overgrow living coral (Smith et al. 2010), in turn creating an optimal environment for the opportunistic sponge to grow. As *M. grandis* is able to overgrow compromised coral heads, it can further enhance the cycling of DIN to support continued macroalgal growth. Indeed previous studies in Kāneʻohe Bay Hawaiʻi show its history of nutrient enrichment supported the growth of various invasive macroalgae (Stimson and Larned 2000). Reefs in the future may no longer represent their

pristine shapes in terms of water quality, elevated CO_2, and warmer temperatures. A more comprehensive understanding of this prominent member of partially degraded reefs in Hawai‘i would complement existing literature on the changes in the bay throughout its history of runoff, algal dominance and recovery, sedimentation, and more recently, coral bleaching events. ***The overarching goal of this research is to characterize the influence of* M. grandis *on biogeochemical cycling on coral reef ecosystems in Kāne‘ohe Bay, O‘ahu, Hawai‘i through assessing biomass, seawater pumping rates, and microbially mediated nitrogen transformations performed by the sponge holobiont. Furthermore, an understanding of the sponge’s nutritional strategies and how its dietary behavior relates to its microbial symbionts would reveal the affiliation of the sponge to its environment and other reef organisms, and provide insight on the sponge’s ability to adapt and establish itself on Hawaiian coral reefs.***

Sponges are known to drive a number of biogeochemical processes and have been found to be a significant source of DIN on coral reefs in the Caribbean (Southwell et al. 2008b, Fiore et al. 2013), however little research has been done on the biogeochemical role of Pacific sponges and in particular in Hawai‘i. Sponge-mediated nitrification has been shown to be a potentially important source for bioavailable N to organisms in a variety of benthic environments (Corredor et al. 1988, Jiménez and Ribes 2007). The rates of sponge-mediated DIN flux measured in this study are over an order of magnitude greater than other reported fluxes of DIN in Kāne‘ohe Bay and other coral reef environments.

The ability of sponges to influence seawater chemistry is directly tied to their active pumping and water filtration processes. Sponges have been measured to sustain pumping rates of up to

10,000 times their body volume daily (Weisz et al. 2008) to facilitate water flow for substrate acquisition and metabolic waste removal. As a result of their active pumping, sponges circulate large amounts of overlying water through their microbially rich interior mesohyl. The functional roles of microbes associated with alien invasive sponges in the Pacific has not been previously studied. Dynamic biogeochemical transformations such as nitrification (Diaz and Ward 1997, Jiménez and Ribes 2007, Southwell et al. 2008a, b), nitrogen fixation (Mohamed et al. 2008), and N_2 production (Schlappy et al. 2010, Mohamed et al. 2010) have been observed to be performed by microbial communities hosted within Atlantic sponges. Because Kāneʻohe Bay is typically an N limited system (De Carlo et al. 2007) the role of sponges in active N transformations is an integral part of understanding the biogeochemical cycling of coastal coral reef ecosystems.

Sponges are also important drivers of organic matter recycling in an ecosystem through their effective uptake of both dissolved and particulate organic matter (DOM and POM) (de Goeij et al. 2008b). Though coral reef ecosystems are characterized by low nutrients (Webb et al. 1975) with typical dissolved inorganic nitrogen and phosphorus concentrations of <0.5 and <0.1 μM, respectively (Furnas et al. 2005, Cox et al. 2006), coral reefs are able to support extremely high productivity through the sponge loop (de Goeij et al. 2013). Sponges can uptake DOM otherwise unavailable to organisms at higher trophic levels and facilitate the transfer of carbon through the rapid shedding and regeneration of choanocytes (sponge water filtering cells) that are then fed upon by detritivores. Through this process, sponges sustain food webs in oligotrophic systems by this rapid and efficient DOM - to - POM recycling (de Goeij et al 2013).

This dissertation addresses the fundamental questions regarding the role of sponges in coastal coral reef ecosystems in Hawai‘i and in particular the biogeochemical influence of an invasive sponge on overlying reef waters. Chapter 2 provides a comparison of *M. grandis* biomass within different environments in south Kāne‘ohe Bay where this sponge is most abundant and provides the first updated biomass surveys of the alien invasive sponge in over a decade. Sponge coverage assessments are paired with sponge-mediated biogeochemistry ascertained in the following chapters to determine a magnitude of influence of the sponge in the bay. Through these observations I describe life history of the sponge and discuss the controls on biomass within the sponge. The ecological effects due to the presence of *M. grandis* in the extended phase shift from coral dominance to dominance by the green alga *Dictyosphaeria cavernosa* observed in Kāne‘ohe Bay (Stimson 2014) are pertinent to developing ecosystem based management strategies in Hawai‘i.

Chapter 3 discusses how *M. grandis* can influence biogeochemistry on coral reefs. Pumping rates and DIN flux rates determined for *M. grandis* were combined with depth and circulation parameters in south Kāne‘ohe Bay for a discussion of sponge influence on the biogeochemistry in the overlying water on different environments in south Kāne‘ohe Bay. These rates are the first description of ammonia oxidation in a Pacific sponge and the first seawater pumping rates measured for *M. grandis.*

Chapter 4 examines the dietary behavior and trophic position of *M. grandis* through bulk $\delta^{15}N$ values of whole sponge samples and separated sponge and microbial cells as well as carbon and nitrogen compound specific isotopic analysis of amino acids (CSIA) of separated sponge and

microbial cells. Broad characteristics of the diverse consortia of microbes found in association with *M. grandis* were classified through flow cytometry methods (FCM). The dietary contribution of associated symbionts to the host sponge as described through amino acid isotopic patterns and trophic relationships appears to dominate the nutritional needs of the sponge cells.

These observations on the invasive and pervasive sponge *M. grandis* suggest that the sponge is an important and understudied component of Pacific shallow water tropical benthic communities. The research presented here comprises a significant contribution to the understanding of the biogeochemical role of invasive sponges in tropical Pacific ecosystems. In addition, I reveal insights into the dietary relationship between the sponge and its associated microbes and the mechanism of transfer of nutrition from symbiont to the sponge. I provide evidence that the ability of sponges to uptake DOM is facilitated by bacterial intermediates, and that specifically bacterially synthesized amino acids, including nonessential amino acids, are directly assimilated by the sponge.

This research is important because little is known about the role of sponges in coastal N biogeochemical cycles, yet they are prevalent in shallow coastal ecosystems throughout the Hawaiian Islands. Invasive, introduced sponge species such as *M. grandis* are of particular threat to Hawaiian habitats because of unique and limited ecosystems characterized by endemic and often endangered species. Because sponges are capable of affecting the N biogeochemistry of its habitat through high seawater pumping rates and active microbial communities, the impact of sponges is not limited to just spatial competition with native species. As coral reefs are oligotrophic environments, and because Kāneʻohe Bay is nitrogen limited (De Carlo et al. 2007,

Drupp et al. 2011), and community structure can be shaped by nutrient levels (Hunter and Evans 1995, Dudgeon et al. 2010), a change in the nutrient profile caused by an introduced sponge has the potential to alter community dynamics. Details about the feeding strategy of tropical Pacific sponges provide additional insight into the ecological ties between sponges, microbial symbionts, and other reef organisms. Future climate change and environmental degradation may differentially affect resilient sponges and less adaptable coral species within Kāneʻohe Bay. An understanding of these community dynamics would help predict how coral reef ecosystems may be impacted by future regimes and guide future directions for the protection and preservation of these important living resources.

CHAPTER 2:

An Assessment of an Invasive Tropical Sponge on Coral Reefs in Hawai'i

Abstract

Sponges are an ecologically important component of many marine ecosystems and are found abundantly within the benthic fauna on coral reefs. Although sponges perform important functions on the reef such as seawater filtration, uptake of particulate and dissolved organic matter, and the recycling of nutrients, some reefs have been observed to shift from more coral dominated habitats to more sponge dominated habitats, raising questions about the increasing influence of sponges on ecosystem dynamics. For example, many Caribbean reefs are largely dominated by sponges hosting biogeochemically active microbial communities. Tropical sponges in the Pacific have not been comparably well studied. Importantly, *Mycale grandis* is an alien invasive sponge now found on many partially degraded shallow water coral ecosystems in Hawai‘i. *M. grandis* is known to compete spatially with dominant native reef building coral such as *Montipora capitata* and *Porites compressa*. Since its appearance in the late 1990s, *M. grandis* has been observed to spread and establish itself in a number of coral reef ecosystems around the main Hawaiian Islands. This study provides the current status of *M. grandis* abundance within Kāne‘ohe Bay, O‘ahu and considers factors that may contribute to its continued success on these reefs. Within south Kāne‘ohe Bay, sponge coverage was found to be 4.6% on patch reefs, 2.1% on fringing reefs, and 32.3% within mangroves habitat along the northern edge of Coconut Island. Furthermore, first details of life history of the sponge are described. The study of *M. grandis* in Kāne‘ohe Bay serves as a model system for studying the impacts and future trajectories of coral reefs that will more likely resemble Kāne‘ohe Bay than pristine reefs in the future.

Introduction

Coastal ecosystems worldwide contribute substantial direct economic benefits (e.g., fisheries and tourism) and provide important ecosystems services (Jackson et al. 2001, Doney 2010). However, they are being increasingly compromised such that many of these systems no longer resemble their more pristine states (Jackson et al. 2001, Lotze et al. 2006). The appearance of invasive sponges such as *Mycale grandis* are of particular interest because sponges can affect nitrogen recycling and flux on a reef (Jimenez and Ribes 2007, Southwell et al. 2008b). Sponges, especially in the Pacific tropical region, are understudied and underappreciated. On tropical reefs, introduced sponges compete spatially with coral but do not provide the same reef building structure or ecosystem function as stony coral and may further alter ecosystem balance by influencing the nutrient profile and community structure within their environments. Some reefs have experienced a shift in baseline environments to macroalgal dominated systems under effects of increased runoff, sedimentation, ocean warming, ocean acidification, fishing, recreational use, and introduced species. Kāneʻohe Bay on Oʻahu in Hawaiʻi has experienced well-documented phase shifts from coral dominance to dominance by the green alga *Dictyosphaeria cavernosa* (Stimson 2014) and the appearance of highly successful alien invasive arthropods (Eldredge and Smith 2001). *M. grandis* is an unintentionally introduced sponge prevalent in several shallow water coral reef communities around the main Hawaiian Islands and is considered the most successful and aggressive alien sponge in Kāneʻohe Bay (Coles et al. 2007).

Mycale grandis is an opportunistic species and overgrows compromised coral infrastructure, and has been observed to overgrow living coral heads. Although it is not the only invasive sponge in Hawaiʻi, it is the most widespread and is a threat to overgrowing some coral reefs. Recent

surveys by the Smithsonian's Marine Global Earth Observatory program (MarineGEO) found 150 previously unseen sponge species in Hawai‘i, among those of which a third are new species (https://marinegeo.si.edu/place/kane%CA%BBohe-bay-O‘ahu, see also Nunez Pons et al. 2017). Research on *M. grandis* establishes a foundation for future hypothesis-driven studies aimed at better understanding the role of sponges in ecological and biogeochemical processes on tropical Pacific coral reefs.

Marine sponges are essential to driving the high productivity observed on nutrient poor coral reefs via the "sponge loop" which occurs through rapid turnover of sponge cells that are shed and consumed by reef fauna (de Goeij et al. 2013), thereby enabling dissolved organic matter to become available to higher trophic levels.

Here I present (i) updated biomass surveys in over a decade of the alien invasive sponge *M. grandis* since the Coles et al. (2007) surveys, including (ii) a comparison of the biomass of *M. grandis* within different environments in Kāne‘ohe Bay, (iii) a discussion of controls on the biomass of *M. grandis* in south Kāne‘ohe Bay, and (iv) descriptions of life history of the sponge. Through this study I aim to provide more details to major questions regarding the invasive alien sponge as a member of the benthic community under the current extended phase shift in Kāne‘ohe Bay and what continued ecological role *M. grandis* will play in the long term within Kāne‘ohe Bay and other shallow water coral reef ecosystems in Hawai‘i.

Study site

Kāne‘ohe Bay, a semi-enclosed body of water with the only barrier reef in the Hawaiian archipelago, is 13 km long and 4 km wide with an extended coral reef system located on the

northeast coast of Oʻahu, Hawaiʻi (21° 26' 0.59" N, 157° 47' 10.79" W) (Figure 2.1). It has served as a model system for studying the impacts and recovery of coral reefs and has undergone significant changes in water quality due to periods of heavy discharge and sustained heavy human activity within the bay (Hunter and Evans 1995). Because it is such a well-studied ecosystem, Kāneʻohe Bay is also a model system to study future impacts under projected climate regimes. Degraded reefs in the future are more likely to resemble Kāneʻohe Bay than pristine reefs. Reef flats extend over much of the area and are characterized by macroalgae, coral, coral rubble, sands and muds. Patch reefs and fringing reefs are also distributed throughout the bay, including in the south bay, the area of focus for this study. The bay experienced a shift from coral to algal dominance during 25 years of sewage discharge that ended in 1977-1978 followed by a recovery to coral after the cessation of discharge, although it remains a partially degraded ecosystem with continued overgrowth of invasive macroalgal species. Water is exchanged with the open ocean through two main channels via the partially dredged Ship Channel in the north of the bay and the shallower Sampan Channel in the south. Water movement across the bay is dominated by wind-driven waves and swell that bring water to the reef with nutrient profiles of typical tropical oceanic waters (Atkinson 1987). The residence time of seawater in southern Kāneʻohe Bay, the site of interest for this study, is between 30 days and 2 months (Lowe et al. 2009). Findings from the study "Assessment of Invasiveness of the Orange Keyhole Sponge *Mycale armata* in Kāneʻohe Bay, Oʻahu, Hawaiʻi" funded by the Hawaiʻi Coral Reef Initiative (HCRI) from 2004-2006 indicated that the sponge had maximal abundance in the south-central region of the bay near the Hawaiʻi Institute of Marine Biology (HIMB) pier and Coconut Island.

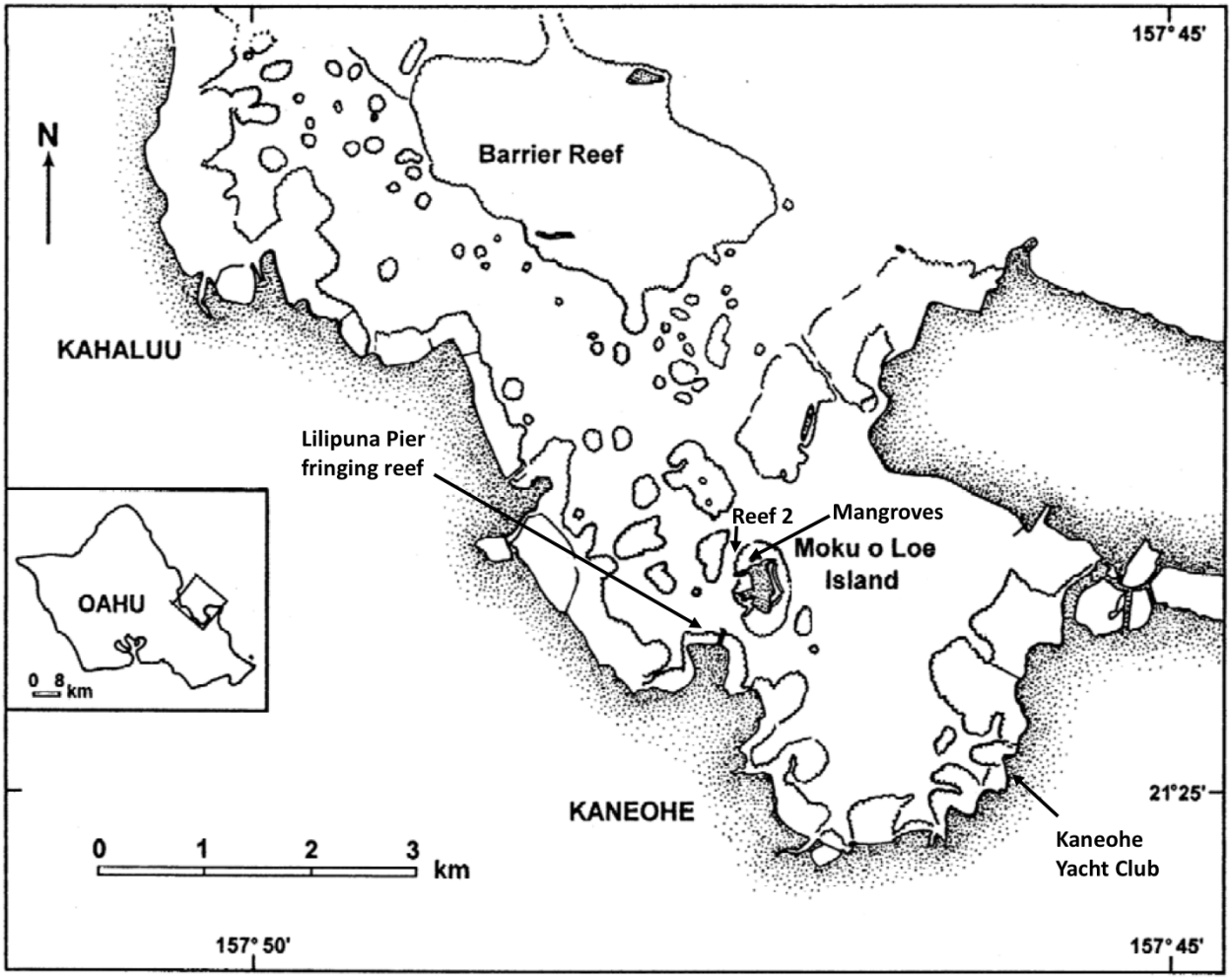

Figure 2.1: Map of Kāneʻohe Bay and Moku o Loʻe, Oʻahu (modified from Stimson and Larned 2000) including the main sites for this study. Outlined areas represent fringing reefs, patch reefs, and the barrier reef.

History of Mycale grandis

Mycale grandis, (also formerly referred to as *Mycale armata*), is native to Australia, Indonesia, Malaysia, and India and spread to Hawai‘i as biofouling on ships’ hulls. The initial inoculation point was most likely on O‘ahu in Honolulu Harbor or Pearl Harbor where there is heavy shipping traffic (Coles 2007). The first official account of *M. grandis* in Hawai‘i was reported for Pearl Harbor in 1996 (Coles et al. 1997, Coles et al. 1999). It is unlikely that this sponge would have been missed in historical accounts and previous surveys because of its shallow water habitat and striking orange coloration. There was no report of *M. grandis* in the de Laubenfels surveys in Kāne‘ohe Bay or elsewhere in Hawai‘i (de Laubenfels 1950 and 1951). The first preliminary abundance studies of *M. grandis* in Kāne‘ohe Bay were undertaken in 1996 and 2000 (Coles et al. 1999, Coles and Eldredge 2002). *M. grandis* is predominantly found in shallow-water fouling communities of major harbors or associated disturbed habitats, but has now appeared throughout Kāne‘ohe Bay, although predominantly in the south basin of Kāne‘ohe Bay (Coles et al. 2007). The higher abundance of these sponges in south bay are likely due to conditions favorable to sponges such as higher nutrients and particulate organic matter compared to the mid or northern portions of the bay.

M. grandis appears as a bright orange, thickly encrusting, and firm but cushiony sponge. Individuals observed in Kāne’ohe Bay usually range from several cms to 0.2 m across, although the sponge is known to reach 1 m across and 0.5 m or more in thickness. The inner cavities often harbor clusters of the brittle star *Ophiactis savignyi*. The surface is smooth but textured and uneven and is covered with unevenly distributed oscula and smaller keyhole shaped ostia. *M. grandis* overgrows reef building coral species such as *Montipora capitata* and at least one endemic species (*Porites compressa*) (Coles et al. 2007) (See Figure 2.2).

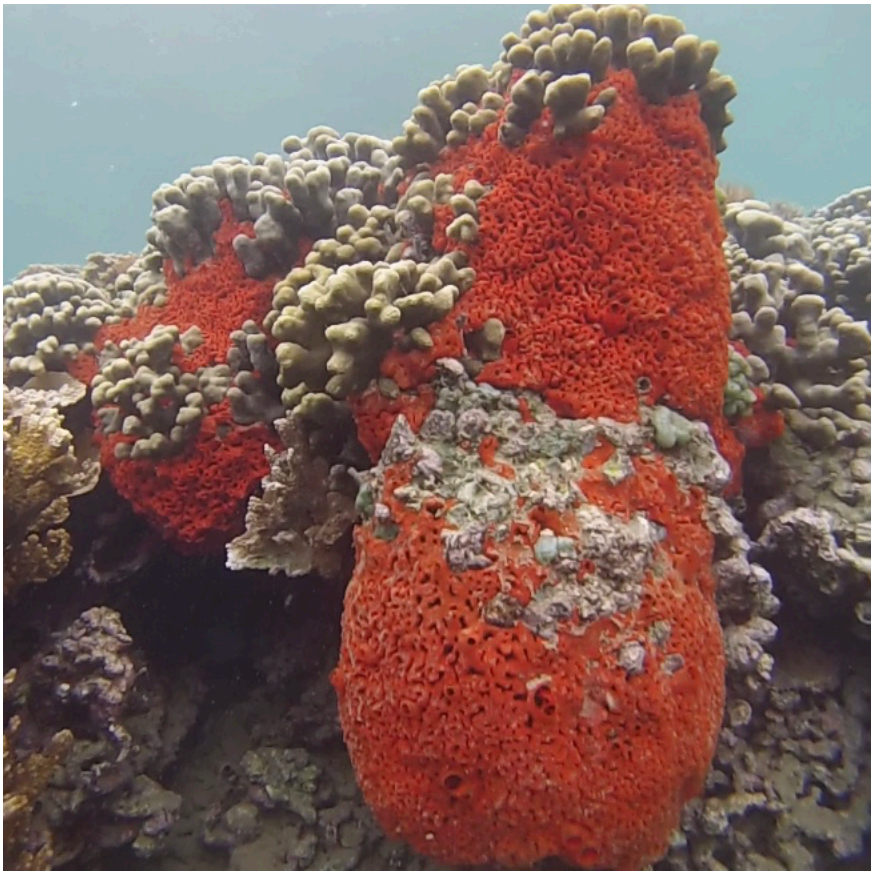

Figure 2.2: *M. grandis* overgrowing living *Porites compressa* on the Lilipuna Pier fringing reef in south Kāneʻohe Bay.

Methods

Biomass surveys

Coverage of *M. grandis* in south Kāneʻohe Bay was assessed by 25 m video belt transects of the fringing reef running perpendicular to Lilipuna Pier, with two transects along the reef crest in each direction and two transects over the reef flat in each direction for a total of 8 transects, and by 65 semi-quantitative rapid assessment estimates of 1 m^2 quadrats all along the inner and outer

reef crests of Coconut Island Reef 2, and 3 semi-quantitative rapid assessment estimates of 1 m^2 quadrats in the mangroves on the northern edge of Moku o Lo‘e (Coconut Island) (see Figure 2.3).

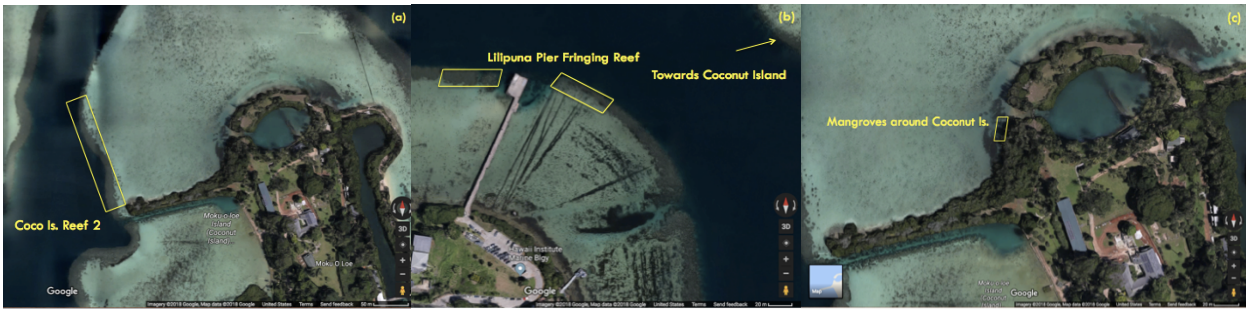

Figure 2.3: Areas surveyed for *M. grandis* coverage. (a) Photo quadrats on Reef 2 (b) belt transects on Lilipuna Pier fringing reef (c) quadrats in mangroves on Moku o Lo‘e.

Abundance surveys in south Kāne‘ohe Bay by Coles and Bolick (2006) and Coles et al. (2007) were performed using rapid assessment manta board surveys (in 2004-2005 only), and in digital photo analyses of permanently marked 0.66 m^2 quadrats along 25 m belt transects on the reef slope located on the southeast perimeter of Coconut Island in the vicinity of Coconut Island Reef 2. This study sought to approximate those methods using biomass assessments along linear transects as well as photo quadrat assessments.

Twenty permanently marked photo quadrats from the Coles and Bolick (2006) 2004-2005 study were established in October 2004 on the reef slope along the southeast perimeter of Coconut Island in the vicinity of the Coconut Island Reef 2 transects. During their study, eleven of these quadrats remained in 2006. Two and then later four additional quadrats were established in 2007.

These previously marked quadrats from the Coles and Bolick (2006) and Coles et al. (2007) studies no longer existed so new quadrats were selected and assessed within the same region for this study.

For video transects of *M. grandis* coverage, 25 m of transect tape were laid along the reef and anchored at both ends with lead dive weights. The swimmer then proceeded slowly along one side of the tape while recording a video transect with a GoPro Hero 3 in one direction, and recording along the opposite side of the tape in the other direction. Percent coverage of *M. grandis* on the reef was estimated by assessing the transect video frame by frame roughly every 0.5 m. Estimate of coverage is reported by the 2D percent coverage of *M. grandis* versus other substrate as viewed from directly above. The depth of the reef ranged from 1 m to 3 m along the reef crest and the GoPro was maintained at a depth of 1 m above the reef to the best of the swimmer's ability. The width of the transect included in determining sponge coverage was 0.66 m outwards from each side of the transect tape.

For the semi-quantitative rapid assessment biomass estimates, quadrats were chosen by random over the inner and outer reef crests of Reef 2. The depth of the reef ranged from 0.5 m to 2 m deep. The sponge growing around the roots of *Rhizophora mangle* were at a depth of approximately 0.3 m depth. A 1 m by 1 m PVC frame was placed over the area and two snorkelers separately estimated the percentage of *M. grandis* cover. The average of the two estimates was recorded as the semi-quantitatively determined 2D *M. grandis* coverage within each quadrat.

Collection of M. grandis

Specimens of *M. grandis* were collected from under the Lilipuna Pier in south Kāneʻohe Bay to assess rates of sponge growth. Pieces of sponge ranging from 6 to 10 cm across were carefully excised using a razor and transferred into a bucket without exposure to air. The sponges were then immediately moved to Coconut Island by boat and placed into outdoor seawater flow through water tables where the sponges were exposed to natural daylight cycles for an acclimation period of one week. The flow through water tables at the Hawaiʻi Institute of Marine Biology have continuous seawater with similar ambient profile pumped in from the eastern edge of the island in the southern portion of Kāneʻohe Bay, which is an area where *M. grandis* is found abundantly. Water tables were scrubbed of any visible algae and siphoned of detritus twice weekly and the day before experiments. The water tables are approximately 150 cm long, 75 cm wide, and 15 cm deep with water flowing in from one end and exiting at the opposite end. Residence time of seawater in the flow through water tables were calculated and adjusted to *ca.* three hours to ensure turnover of any particulate detritus.

Growth rates

Change in mass was measured in five *M. grandis* samples collected from under the Lilipuna Pier. Sponges were tagged with color-coded zip ties and maintained in outdoor seawater flow through tables. Wet weight of the five sponges were measured on an analytical scale at the HIMB Wet lab over a ten week period spanning from late winter to early spring of 2018. Sponges were collected specifically for growth rate assessment and were not subject to other experiments.

Results

Sponge Abundance

Average coverage of *M. grandis* along the reef crest of Coconut Island Reef 2 was 2.1% on the inner reef crest and 9.2% on the outer reef crest with an average coverage of 4.6% on the reef ranging from 0% to 30% coverage. The average cover of *M. grandis* on the transects on the fringing reef running perpendicular to Lilipuna Pier in south Kāne'ohe Bay was 2.9%. *M. grandis* was found in all transects. Average coverage of *M. grandis* around the roots of *Rhizophora mangle* along the northern edge of Moku o Lo'e was 32.3% (Table 2.1).

Site	N	Mean coverage	SD
Inner Reef	40	2.09^{a}	2.5^{e}
Outer Reef	22	9.19^{b}	10.85^{g}
Fringing Reef	100	7.02^{b}	4.68^{f}
Mangroves	3	32.33^{c}	4.04

Table 2.1: Area coverage percent. Note: Mean marked [a] lower than means marked [b] in independent-sample t tests; mean marked [c] higher than means marked [a] and [b] in one-sample t tests. Variance (SD^2) was significantly lowest for group marked [e] and significantly highest for group marked marked [g].

One-sample t tests were used to compare the area percentage of sponge coverage in the mangrove locations ($N = 3$, $M = 32.33$) to area percentage in the inner reef ($N = 40$, $M = 2.09$). The sponge coverage in the mangroves was statistically greater, $t = -76.44$, $df = 39$, $p = 0.00$,

than the inner reef. The mangroves also had statistically greater sponge coverage than the outer reef ($N = 22$, $M = 9.19$), $t = -10.01$, $df = 21$, $p = 0.00$.

The percent area of coverage in photographed and unphotographed transects did not differ significantly. Kolmogorov-Smirnov tests for normality showed that the data for number of sponges and percent area of coverage were normally distributed within each reef setting, and so independent sample t tests could be used to make comparisons across settings. Table 2.2 shows that the number of sponges and percent area of coverage were both significantly greater in the outer reef areas. However, the number of sponges per area covered did not differ significantly in the inner and outer reefs. In paired-sample t tests where data from the inner reef and the outer reef in the same transects were paired, the results showed the same pattern of significance. In the paired-sample t tests for data within the same transects, there were also no significant correlations between (a) inner reef and outer reef number of sponges, (b) inner reef and outer reef percent area coverage, or (c) inner reef and outer reef number of sponges per area covered.

	N	*M*	*SD*	Range	*t*	*df*	*p*	Mean difference (95% CI)
Number of sponges					-2.98	18.96	0.01	-11.68 (-19.89, -3.48)
Inner reef	25	6.44	6.65	0-33				
Outer reef	16	18.13	14.75	2-50, many				
Area % coverage					-2.78	15.7	0.01	-7.88 (-13.91, -1.86)
Inner reef	25	1.57	2.14	0.00-8.26				
Outer reef	16	9.45	11.21	0.12-43.00				
Sponges per m^2					1.43	39	0.16	0.15 (-0.03, 0.33)
Inner reef	25	0.22	0.42	0.00-1.94				
Outer reef	16	0.07	0.1	0.10-0.29				
Paired transects (*N*= 16)								
Number of sponges					-3.53	15	0	-13.31 (-21.34, -5.28)
Inner reef		4.81	3.62	1-12				
Outer reef		18.13	14.75	2-50, many				
Area % coverage					-2.57	15	0.02	-7.59 (-13.89, -1.28)
Inner reef		1.86	2.47	0.04-8.26				
Outer reef		9.45	11.21	0.12-43.00				
Sponges per m^2					1.25	15	0.25	0.05 (-0.03-0.12)
Inner reef		0.11	0.1	0.01-0.25				
Outer reef		0.07	0.1	0.10-0.29				

Table 2.2: Number of sponges, percent area of coverage, and sponges per m^2 on the inner and outer reef crests of Reef 2 compared using independent sample t tests. *N* is number of measurements, *M* is average % coverage, and SD is standard deviation. Transects on the inner and outer reef were evaluated separately and also evaluated in pairs. Note: On the outer reef, six transects contained too many individual (uncountable) sponges and were not included in the analyses. This could have affected the level of significance in the analysis for sponges per m^2.

Growth rates

All five *M. grandis* specimens maintained in the water tables over a ten week period exhibited loss in biomass. All sponges remained alive and otherwise appeared healthy. Over the first four weeks, the sponges lost an average of 16% by weight, ranging from 6 to 28% loss by weight. Results for individual sponges are reported in the Appendix in Table A.1. Over a ten week period, all sponges exhibited a loss in biomass with an average loss of 24% for all five sponges ranging from 17 to 35% in wet weight.

Discussion

The appearance of *M. grandis* in the coral reef environment of Kāneʻohe Bay differed from previous appearances of the sponge in environments such as major harbors and significantly disturbed environments. Two decades after it was first observed in 1996, this invasive sponge remains a conspicuous member of the reef community in south Kāneʻohe Bay. *M. grandis'* ability to alter seawater chemistry (Shih, this volume, Chapter 3) coupled with active seawater pumping raises questions about the ecological influence of *M. grandis* on reefs where the sponge can be found. The observed long-term sustained biomass implies the adaptability of this invasive sponge to Kāneʻohe Bay.

Unlike other alien sponges reported in Hawaiʻi which appear to be relatively benign introductions, *M. grandis* may present a true threat to corals and the reef communities in Hawaiian waters (Coles and Bolick 2006). The sponge has been observed to not only overgrow living coral, but is observed to weaken its calcium carbonate skeleton, the stony part of the reef that provides habitat for other marine animals and is part of a double incursion on coral as macroalgae smothers from above (McCook et al. 2001) and sponges intrude from below. Algae

can further indirectly cause coral mortality by enhancing microbial activity via the release of dissolved compounds high in organic carbon (Smith et al. 2006). Thus far the threat is limited to the central and southern portions of Kāneʻohe Bay. Coles et al. (2007) noted that *M. grandis* was not found near the Kāneʻohe Yacht Club despite the environment's resemblance to other areas *M. grandis* had become established. Instead, the fact that they found *M. grandis* predominantly by the pier and around the Hawaiʻi Institute of Marine Biology led to speculation that the point of introduction of *M. grandis* could have been from Lilipuna Pier or HIMB.

Sponge abundance

Results of the sponge coverage surveys were comparable to the abundance of *M. grandis* on the reefs measured by Coles et al. in 2004 - 2005 and 2007. These most recent surveys focused on south Kāneʻohe Bay as Coles et al. (2007) found that coverage decreased substantially in all directions from south bay, with less than 1% coverage beyond the 1 - 3 km Moku o Loʻe "epicenter". The Coles et al. (2006) assessment in 2004 - 2005 included 20 permanent quadrats on Reef 2. Of those they repeated 11 of the quadrat assessments in 2006. As the quadrats from those studies were no longer present these follow up quadrats were placed at random along Reef 2. Also to note for comparison purposes, their quadrats were 0.66 m^2 whereas the quadrats for this study were 1 m^2 quadrats, therefore the data from this study and the Coles and Bolick (2006) and Coles et al. (2007) studies are not directly comparable but serve as a record of updated observations. Percent coverage observed in this study was comparable to mean coverage observed in the Coles and Bolick (2006) study (an average of 4.6% versus 4.5 - 5% on the Coconut Island and HIMB dock reefs nearby in 2004 - 2004) and less than the mean cover of 12.2% observed on Reef 2 in 2006.

Larger clusters of *M. grandis* are present in shaded areas such as along pier pilings and docks but also grows in clear and shallow locations on the reef. It is not readily obvious if *M. grandis* prefers shade or if shade and turbidity inhibit the growth of coral and thereby provide an opportunity for sponge to grow. Areas around docks and piers also tend to be disturbed environments and again may compromise the localized health of coral. In addition, low light penetration may aid in sponge proliferation as it also inhibits the growth of light-dependent macroalgae. Kāneʻohe Bay is also subject to turbidity, which can smother coral whereas sponges can actively block pores from sediment as well as actively expel small particles. Turbidity may also reduce light levels for algal growth.

M. grandis was also found to grow prolifically on the roots of the nonindigenous Red Mangrove, *Rhizophora mangle* (Figure 2.4), native to Florida, West Indies, and South America, and is also abundant in Pearl Harbor and Keehi Lagoon. In this situation one invasive species is providing habitat for another invasive species, enabling a co-evolved community shift.

Figure 2.4: Example of *M. grandis* growing on the roots of the invasive mangrove *Rhizophora mangle.*

Current *M. grandis* biomass on Coconut Island Reef 2 aligns with observation that the appearance of the sponge has seemed to stabilize rather than completely overgrow live coral, which had been a point of concern when it first aggressively appeared and then doubled in abundance from 2005 to 2006. The presence of this invasive alien sponge on the reef is nonetheless a departure from the baseline community structure, potentially altering resource dynamics, and influencing seawater chemistry. Sponge growth and reproduction must be balanced by predation or other forms of turnover. The "sponge loop" is at least partially responsible for limiting the growth rate of tropical sponges. Sponges retain organic matter on reefs through their rapid uptake of DOM on tropical reefs (de Goeij et al. 2013). However, some tropical sponges have been measured to respire only 42% of the carbon taken up from the water column. If the remaining 58% is used for growth, a biomass increase of 38% of body carbon per day (more than a doubling of biomass every 3 days) would be expected (de Goeij et al. 2008a). However, the net growth of some sponges is near zero due to rapid turnover of old choanocyte cells shed as particulate organic matter, which enables the transfer of DOM to higher trophic levels. This implies that sponges use the majority of carbon uptake to replenish their choanocytes used in their water pumping system and to maintain these high rates of cell turnover. Phase shifts to more sponges may cause carbon release rates on reefs to increase (de Goeij et al. 2013), which could play an important role in restructuring higher trophic levels within an ecosystem (Silveira et al. 2015). The net growth of spatially constrained sponges such as cryptic species in the Caribbean is considered to be zero (de Goeij et al. 2008a) whereas the same assumption cannot be made for the asconoid and vertical sponge *Xestospongia muta* which shows considerable annual growth (McMurray et al. 2008). Sponges in cryptic habitats may be severely space limited and, by consequence, could be driven to allocate more energy towards functions

other than growth. As an encrusting sponge, *M. grandis* experiences spatial competition and may tend towards function rather than growth. These results also suggest that as the sponge occupies an area its rate of growth may slow down relative to the remaining habitable space.

Growth rates

Sponges kept in the outdoor flow through water tables did not exhibit net growth and overall decreased in mass over the ten week observation period. Although not reported in units of mass, Coles et al. (2007) found increases in coverage biomass on reefs over the 2004 to 2006 study period suggesting growth. The decline in mass of sponge individuals in the water tables was most likely due to a number of environmental differences such as changes in insolation (partially shaded tanks versus unshaded reef) that may affect phytoplankton-derived sources of nutrition to the sponge and the water flow in the tables compared to water movement on the reef. Sponges have the ability to grow in response to water flow and optimize their morphology to conform to their environment (Wilkinson and Vacelet 1979). The flow regime in the water tables differ from water movement on the reef, as the residence time of seawater in the table was calculated to be *ca.* 3 hours versus the 30 days characteristic of south Kāneʻohe Bay. Additionally, the flow of water in the tables is unidirectional versus varying with wind and tides. Creating conditions in the water tables identical to the flow regime and nutrient sources on the reef is not realistic for these aquaria. The sponges may also have experienced partial starvation due to less particulate organic matter or sources of dissolved organic matter in the water that is supplied to the facilities. Many sponges are observed in intimate contact with corals and it is known that coral mucus can be used as a nutrient source by sponges (Rix et al. 2016, Rix et al 2017). Tropical sponges also undergo rapid shedding of choanocyte cells (de Goeij et al. 2013) thus sponge

growth is not necessarily retained as biomass. Also, a review of quarterly measurements by Coles et al. (2007) suggests that sponge growth is not constant but is in spurts, sometimes interspersed with periods of moderate regression, and that *M. grandis* was observed to increase in abundance and habitat overall within Kāneʻohe Bay in the mid 2000s. Finally, these samples were collected around the same period that sponge eggs were discovered within the mesohyl of some sponge samples. If there are reproductive seasons for *M. grandis*, the sponge may be allocating more energy towards reproductive strategies than towards net growth.

Vicente et al. (2016) also observed a decrease in biomass of 25 - 35% in *M. grandis* specimens that were collected and kept in shaded tanks over a 26 day period, although their sponges were subject to pCO_2 and temperature experiments. Although positive net growth rates were not observed in their sponges either, they did exhibit internal silica biomineralization. *M. grandis* requires silica uptake to support its densely spiculated siliceous skeleton (see Figure 2.5). Because lower levels of silica were measured in their experimental tanks compared to ambient seawater in the bay, it was suggested that *M. grandis* growth was potentially limited by silica in this experiment. Vicente et al. (2016) further suggested that diatom uptake of silica in the tanks may have been responsible for reducing available silica. Silica uptake rates for *M. grandis* increased proportionally when tanks were spiked with silica (Vicente et al. 2016). Future longer term studies performed using caged experiments on the reef would better constrain representative growth rates under ambient environmental conditions. Observations over different seasons and time periods could account for differential growth phases and seasonal differences.

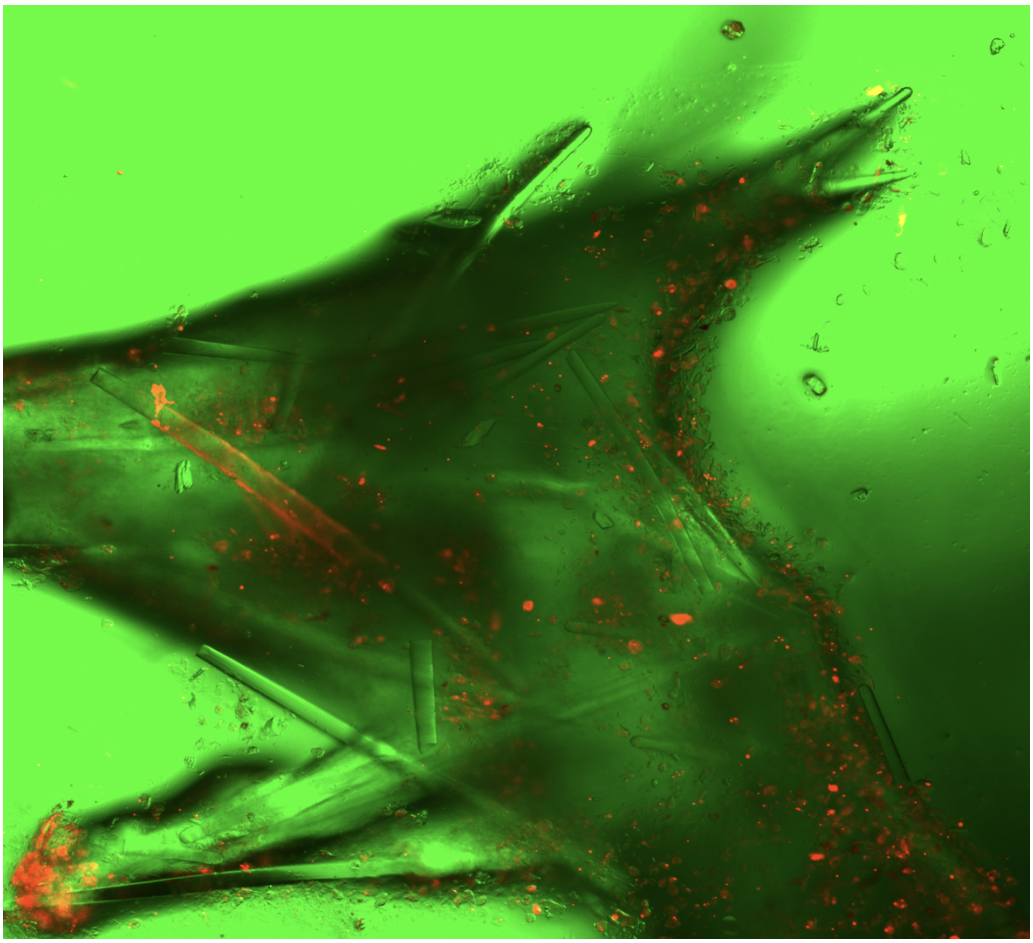

Figure 2.5: Transmitted and fluorescent light confocal microscope image of *M. grandis* showing siliceous spicules. Red pigment is from natural fluorescence of chlorophyll from associated phytoplankton.

The only sponge to have been studied and observed to displace coral in the Pacific is *Terpios hoshinota* in Guam (Rutzler and Muzik 1993). This aggressive sponge grows 23 mm month^{-1} and rapidly spread around the west and south reefs of Guam from 1971 to 1973, dominating shallow submerged reefs (Bryan 1973, Plucer-Rosario 1987). *M. grandis* has spread more aggressively than other known invasive sponges in Hawai‘i which appear to have minimal impact (*Gelliodes fibrosa, Suberites zeteki, Zygomycale parishii,* and *Haliclona caerulea*), and

has the potential to pose a threat to native reef-building corals in south Kane‘ohe Bay (Coles et al. 2007). While *M. grandis* is the most prevalent and widespread sponge in Hawai‘i, its abundance on Hawaiian reefs appears to have stabilized with similar reef coverage in south Kāne‘ohe Bay since 2007.

Reproduction

Reproductive strategies of *M. grandis* were previously unknown, although it is assumed that like most sponges it is capable of asexual reproduction by fragmentation (Eldredge and Smith 2001). During the preparation of sponge tissue samples clusters of sponge eggs were observed within the mesohyl of some specimens (Figure 2.6), indicating that *M. grandis* is also capable of sexual reproduction. Some sponges are able to reproduce sexually by capturing sperm that has been released into the water column by an adjacent sponge. Samples in which eggs within the mesohyl were observed were collected in the spring of 2017. It is unknown if *M. grandis* has specific spawning seasons. The discovery of gamete cells is important as many organisms spawn under duress and attempts to physically remove or otherwise perturb *M. grandis* may induce spawning and cause further proliferation.

Figure 2.6: Eggs within the mesohyl observed in samples of *M. grandis* collected in May of 2016.

Management of the sponge in the bay

Coles et al. (2007) attempted to remove *M. grandis* mechanically but the results yielded no net effect due to regrowth of the sponge and inadvertent damage to live coral. Further trials included the injection of compressed air into the sponges which proved to be an effective method to control proliferation, however eradication of the sponge would require expensive and extremely labor intensive efforts (13 to 23 man hours per m^2 depending on the method) (Coles et al. 2007). Although compressed air is an effective treatment, *M. grandis* does not appear to be significantly impacted by exposure to atmospheric air. Clusters of *M. grandis* can be found exposed for hours on pier pilings and reefs during lower tides.

Invasive sponges are likely in competition with invasive macroalgae and native coral. Rapidly growing macroalgae smothers coral and compromised coral heads are susceptible to invasion by opportunistic *M. grandis.* Unlike the top-down control on both sponges and macroalgae that are observed on Caribbean reefs (Pawlick 2013), both *M. grandis* and macroalgae such as *D. cavernosa* owe their success partially to the fact that they both experience low grazing pressure within Kāneʻohe Bay (Stimson and Larned 2000, Stimson 2014). Coles et al. (2007) reported that the principle bycatch obtained by the "Supersucker" for mechanical removal of the invasive macroalga *Gracilaria salicornia* was *M. grandis*. Fragments of *G. salicornia* that are easily moved on by waves may provide a mechanism by which *M. grandis* could be spread to new areas in the bay. Because of evidence of sexual reproduction of the sponge, uncontrolled manual and mechanical removal of the sponge should be approached with caution so as to not induce spawning. Even sponges with relatively low growth rates are able to dominate on reefs provided there is little-to-no predation (Gonzalo-Rivero et al. 2011). One potentially positive role of *M. grandis* is based on the observation that *M. grandis* does not appear to be a boring sponge.

Because it grows on the surface of reefs and on coral rubble, it is possible that the sponge could temporarily bind rubble or hold together the reef against mechanical breakdown and from bioerosion by other organisms (Wulff and Buss 1979).

Overall, management of algal species in the bay has allowed significantly for the recovery of corals. This reduction of algae has reduced the opportunity for sponge to further establish because coral is less compromised and remains spatially competitive. *Dictyosphaeria cavernosa* also declined dramatically throughout the bay between February and June 2006 (Stimson and Conklin 2008) as the result of heavily overcast and very low irradiance levels during an unusual 42-day period of continuous rain. There has been no major resurgence of the alga since 2008 and is a rare example of a reverse phase shift from an algal-dominated to a coral-dominated community structure on a reef (Stimson and Conklin 2008). It is worth noting that *M. grandis* may have begun to spread less aggressively around this time. If macroalgae do aid in the proliferation of sponges on coral reefs (McCook et al. 2001, Smith et al. 2006), this may be one explanation for the stabilization of *M. grandis* coverage in Kāneʻohe Bay as well as the lack of growth when sponges were isolated and incubated in the flow through seawater tanks. Furthermore, previous increases of sponge within the bay may have altered the balance of nitrogen substrates available to macroalgae and further reduced the pressure of algal overgrowth on coral because of macroalgal preference for energetically favorable NH_4^+ over oxidized forms of N (Rees 2007) released by the sponge (Shih, this volume, Chapter 3). Preferential use of NH_4^+ is observed when NH_4^+ is available at only a few μM or less (Glilbert et al. 2015). Sponge-hosted microbially mediated NH_4^+ also converts N into forms available to N loss processes, potentially enhancing the N limitation already observed in the bay.

Predators

There are no *in situ* observations of nor physical evidence for natural predators for *M. grandis* in Kāneʻohe Bay, however the Tiger Cowry *Cypraea tigris* will consume the sponge if provided as a food source in an aquarium (current project being undertaken by Jan Vicente and Andrew Osberg at HIMB) (see Figure 2.7). It is not known whether cowries will preferentially consume the sponge if given other natural food options. However, predation could be one of the controls behind the limited net growth observed in *M. grandis* on the reef. Some species of sea turtles (e.g. *Eretmochelys imbricata*) and fish (angelfishes (Pomacanthidae), wrasses (Labridae), (leatherjackets (Monacanthidae), boxfishes (Ostraciidae) and pufferfishes (Tetraodontidae)) are known to be spongivores though there has been little evidence of these species acting as local controls on *M. grandis* in Hawaiʻi. While purely speculation, some species may interpret the bright orange coloration as aposematic warning, though there can be little or no actual connection to chemical or physical defenses (Pawlick et al. 1988). The coloration of sponges is often acquired from cyanobacterial symbionts, such as *Synechococcus* in the red-orange Caribbean sponge *Xestospongia muta*. *Synechococcus* is also found in the tissue of *M. grandis* (this study, Chapter 4) as well as abundantly throughout Kāneʻohe Bay (Selph et al. 2018).

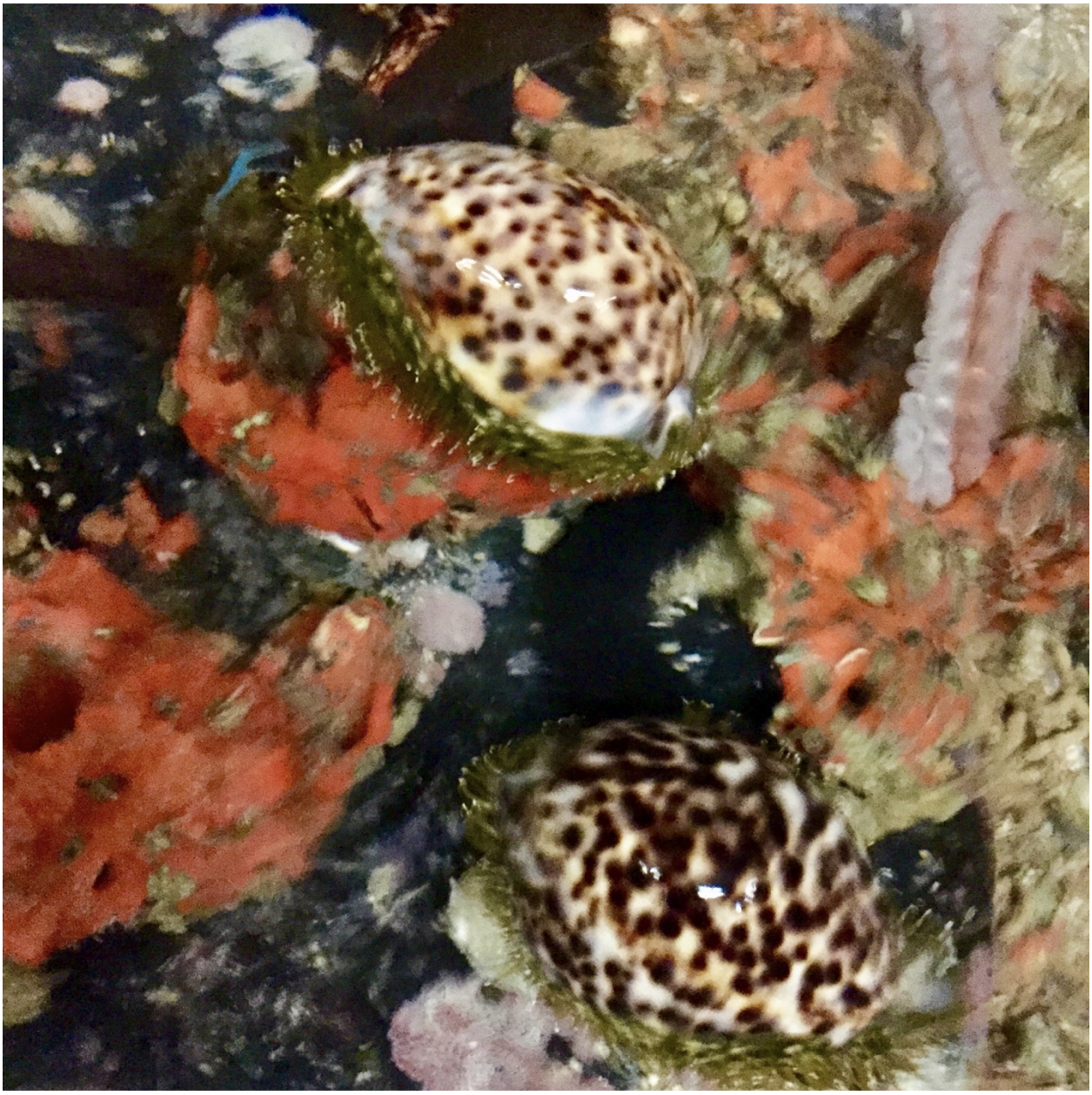

Figure 2.7: *Cypraea tigris* feeding on *M. grandis* in enclosed seawater flow through tables at HIMB.

Conclusion

Results of this study indicate that the coverage of *M. grandis* in Kāneʻohe Bay appears to have stabilized in recent years, and while the sponge does not appear to be spreading at aggressive rates as previously feared, there appears to be no viable options for full eradication. The current abundance of *M. grandis* on the reef is likely to persist especially as part of the extended phase shift or alternative steady state found in Kāneʻohe Bay. However, invasion by the persistent alien sponge could be exacerbated by changing climate. While coral are expected to be "losers" under future climate regimes, sponge growth rates of six Caribbean species were not affected by pH or warmer temperatures (Duckworth et al. 2012), and *M. grandis* has displayed exceptional ability to withstand pCO_2 and temperature conditions that are stressful to many other organisms, suggesting that this invasive sponge will continue to be a competitor on coral reefs in Hawaiʻi in a warmer and more acidic ocean (Vicente et al. 2016). Vicente et al. (2016) did not observe a difference in silica uptake or growth rates in *M. grandis* under projected levels of elevated CO_2 and temperature. In fact, studies have shown that some sponges may even benefit from predicted conditions of acidified oceans. Spiculated sponges are able to tolerate warmer seawater temperatures and ocean acidification and actually accelerate their attachment rates to substrates (Duckworth et al. 2012). Decreased pH will favor the speciation of $Si(OH)_4$ and HCO_3^- which could make $Si(OH)_4$ and HCO_3^- more available for the Na^+/HCO_3^- symporter protein to transport and facilitate uptake of silica through the cell membranes (Zeebe and Wolf-Gladrow 2001) of organisms such as *M. grandis*. In addition, rates of bioerosion on the reef are anticipated to increase with decreasing pH (deCarlo et al. 2015). A shift to greater coverage of *M. grandis* on the reef away from stony coral reduces the availability of hard reef infrastructure and habitat, as well as prevents the creation of new rocky reef which has the potential to cause an

entire community shift. Anthropogenic activities in the bay that result in fragmentation of the sponge or inducement of spawning could further propagate the sponge.

M. grandis will likely be present on the reefs of Kāneʻohe Bay and other partially degraded coral reef environments throughout Hawaiʻi for the foreseeable future as these reefs are unlikely to return to pristine conditions due to continued anthropogenic activities, terrestrial inputs, and increasing pressures of climate change. However, there is potential for returning to more baseline conditions based on the history of recovery in Kāneʻohe Bay from previous extreme phase shifts. A favorable outcome is enhanced through management of invasive macroalgae and minimization of artificial nutrient loads in runoff and in submarine groundwater discharge to the bay. The management of algae has allowed coral to recover and may have improved resilience against spatial competition from *M. grandis*. However, *M. grandis* is an opportunist and easily establishes on a variety of substrates in addition to compromised coral. Bleaching induced by elevated seawater temperature is the current greatest threat to coral in the bay, especially over longer time frames that delay recovery or bleaching events that occur over consecutive years. Other threats experienced by coral in Kāneʻohe Bay include light limitation by increased particulate matter in the water column and smothering by macroalgae and sedimentation.

Invasive species management is a priority for the State of Hawaiʻi and the findings of this study could contribute to local ecosystem management and preservation. Coral reefs are one of Hawaiʻi's most valuable natural resources and face the multiple threat of algal overgrowth enhanced by runoff and pollution, invasive species, and climate change. The consequences of an alien invasive species as a permanent and potentially progressively more dominant member of

the local benthic biota under anticipated future regimes should be taken into account as regulatory agencies move towards adopting increasingly proactive climate change policies and ecosystem-based management strategies.

CHAPTER 3:

An invasive sponge as an important driver of nitrogen biogeochemistry on coral reefs in Kāneʻohe Bay, Oʻahu

Abstract

Sponges have long been known to be ecologically important members of the benthic fauna on coral reefs, but there is virtually no information on the role of sponges in nitrogen biogeochemistry of coral reefs in the Pacific. Studies of sponges particularly in the Caribbean and Mediterranean Sea have shown that they can host a variety of microbially-mediated nitrogen transformations. Sponges are prolific filter feeders and pump seawater for the dual purpose of obtaining resources and removing metabolic wastes, and thus come into contact with large amounts of water in their near environment. The alien invasive sponge *Mycale grandis* was measured to pump 0.0027 L seawater $s^{-1}L^{-1}$ sponge or 0.016 L seawater s^{-1} kg^{-1} sponge (dry mass), equivalent to 115 times its own volume per day. Volume and mass normalized rates of $^{15}NH_4^+$ oxidation determined from incubation of $^{15}NH_4^+$ performed on sponges collected from two sites in Kāneʻohe Bay ranged from 3.9 to 75.1 nmol $g^{-1}h^{-1}$ (dry weight) and averaged 21.2 nM $g^{-1}h^{-1}$. Ammonia oxidation rates determined from uptake of NH_4^+ in sponge excurrent compared to ambient seawater ranged from 84.5 to 339.1 nmol $g^{-1}h^{-1}$. These pumping rates, biomass, and flux rates were combined with depth and circulation parameters in south Kāneʻohe Bay to determine the influence of *M. grandis*-facilitated ammonia oxidation on the biogeochemistry of overlying reef water in south Kāneʻohe Bay. These are the first reported ammonia oxidation rates for a Pacific sponge and the first seawater pumping rates measured for *M. grandis.*

Introduction

Coral reefs have long been recognized as one of the world's most biodiverse habitats (Birkeland 1997). These benthic reef communities are composed of hard coral, macroalgae, encrusting

coralline algae, sponges, and other sessile invertebrates. Understanding this biodiversity and how each member contributes to ecosystem function is critical to predicting how reef dynamics will evolve under the trajectory of community shifts catalyzed by climate change and other anthropogenic influences. Sponges and their role on coral reef communities are largely understudied and underappreciated, especially in tropical Pacific regions. Furthermore, previous research focusing heavily on binary coral and macroalgae models as indicators of reef health has ignored key influences of other vital players within the community such as marine sponges (Gonzalez-Rivero 2011).

In addition to an extended history as the first multicellular organism on earth and having survived several mass extinctions that eliminated many marine organisms through episodes of elevated CO_2, acidified oceans, warmer temperatures, and decreased sunlight (Botting 2017), studies suggest sponges including the invasive sponge *Mycale grandis* will be resilient and competitive in compromised ecosystems such as in coral reefs under future regimes (Bell et al. 2013, Vicente et al. 2016). Some reefs have seen a recent shift from coral dominance to sponge dominance (Maliao et al. 2008). Because nutrient levels typically drive productivity and ultimately food web and community structure in ecosystems (Falkowski et al. 2008) sponges and their role in active nitrogen transformations are integral to the understanding the biogeochemical cycles within a coastal ecosystem. Sponges harbor high concentrations of diverse and active microbial communities (Hentschel et al. 2006) known to perform biogeochemical transformations such as nitrification (Diaz and Ward 1997, Jiménez and Ribes 2007, Southwell et al. 2008a, b), N_2 fixation (Mohamed et al. 2008), anammox, and N_2 production (Mohamed et al. 2010). Nitrification is the two-step microbial oxidation of ammonia (NH_3) first to nitrite (NO_2^-) and then to nitrate (NO_3^-). Nitrification, and in particular ammonia oxidation, is of

interest because it is often the rate limiting step in the marine nitrogen cycle and because rates of ammonia oxidation in the ocean have been shown to be affected by declining seawater pH (Beman et al. 2011). The influence of sponge nitrogen flux is enhanced by their extraordinary seawater filtration capacity that can reach upwards of 30 L hr^{-1} per L of sponge (Weisz et al. 2008). Their prolific pumping rates effectively expose large volumes of seawater to biogeochemically active microbial communities within the sponge holobiont. Animal-derived nutrients can be important drivers in structuring nutrient regimes within and between ecosystems when aggregating organisms undergo repetitive behavior creating nutrient hotspots (Shantz 2015).

Sponges also sustain paradoxically high productivity and biodiversity on coral reefs despite being nutrient-poor "marine deserts" by making dissolved organic matter available to higher trophic levels (de Goeij et al. 2013). This "sponge loop", analogous to the well-established microbial loop in the open ocean (Azam et al. 1983) reveals an additional importance of sponges to overall function of coral reefs ecosystems and how they can impact the delicate balance of community structure.

Kāneʻohe Bay in Oʻahu, Hawaiʻi consists of coral patch reefs and a barrier reef and has a long history of heavy use, urbanization, and sewage discharge resulting in shifts to algal dominance and recovery during the 25 years of sewage discharge up until 1977 - 1978 (Hunter and Evans 1995). Considered a model system, many variables are richly documented in the bay. Because Kāneʻohe Bay is a typically nitrogen limited environment except for short bursts following heavy rainfall (De Carlo et al. 2007) any perturbation to the N balance in the bay has the ability to affect the overall ecosystem, potentially favoring some reef species over others.

Mycale grandis was only first reported on Hawaiian coral reefs in 1996 (Coles and Bolick 2007) and is pervasive in Kāne‘ohe Bay. Hawai‘i is particularly susceptible to invasive species because of the high rate of endemism due to the archipelago’s geographic isolation (Kay and Palumbi 1987, Jokiel 1987). Recent surveys by the Smithsonian’s Marine Global Earth Observatory program (MarineGEO) found an astonishing 150 sponge species previously unseen in Hawai‘i, among those of which a third are new species (https://marinegeo.si.edu/place/kane%CA%BBohe-bay-oahu, see also Núñez Pons et al. 2017). The cumulative influence of these sponge species could be even greater than previously imagined and future research efforts should focus on the biogeochemical influence of these ubiquitous benthic organisms in the tropical Pacific.

Coral reefs in the future may resemble Kāne‘ohe Bay more than pristine coral reef ecosystems. Invasive species and climate change are causing entire community baseline shifts and therefore we seek to understand partially degraded systems such as Kāne‘ohe Bay. The goal of this study was to determine the effects of the invasive sponge *M. grandis* on the nitrogen speciation on coral reef environments. I specifically measured the seawater pumping rate of the sponge and measured the net removal or addition of dissolved nutrients in water circulated through the sponge holobiont, as well as specifically determined the microbially-mediated ammonia oxidation rates performed by the sponge microbiome. These pumping rates are combined with biomass estimates (Shih, this volume, Chapter 2) and the production rates of $^{15}NO_3^- + {}^{15}NO_2^-$ from $^{15}NH_4^+$ uptake incubations as well as the drawdown of NH_4^+ between ambient seawater and sponge excurrent to calculate fluxes through two experimental methods. These fluxes are then compared with other sources of NO_3^- found throughout different reef environments within

Kāne‘ohe Bay to evaluate the importance of sponge-mediated NO_3^- production for reef nitrogen biogeochemistry.

High microbial abundance (HMA) sponges have bacterial densities that are two to four orders of magnitude higher than in low microbial abundance (LMA) sponges (Hentschel et al., 2006). In HMA sponges, microbial biomass can comprise up to one third of the total sponge biomass (Vacelet 1975). LMA sponges are characterized by higher pumping rates and higher rates of heterotrophic feeding on particulate organic matter (Weisz et al. 2008, Schläppy et al. 2010, Freeman and Thacker 2011). Based on the encrusting morphology of *M. grandis*, the higher abundance of LMA sponges found in in shallow water (Pawlik et al. 2015), and LMA classification of other *Mycale spp.* (Rutzler 1990, Gloekner et al. 2014), I hypothesized that *M. grandis* is an LMA sponge, and from that further hypothesized that *M. grandis* would have a higher seawater pumping rate. The hypothesis that *M. grandis* in an LMA sponge would have to be further confirmed by transmission electron microscopy to quantify the abundance of microorganisms in the mesohyl matrix or by comparison of the specific diversity of microbes found within *M. grandis* to the differentiation of phylotypes observed and described for other LMA and HMA sponges (Gloecker et al. 2014). Broad categorization of the microbial community associated with *M. grandis* is explored using flow cytometry methods (FCM) and carbon and nitrogen compound specific isotopic analysis (CSIA) of amino acids in Chapter 4 (Shih, this volume). Based on nitrification measured in several Caribbean sponges (Diaz & Ward 1997, Jiménez & Ribes 2007, Southwell et al. 2008a, b) and the presence of *Crenarchaeota* phylotypes in *M. grandis* (Wang et al. 2009) and the high availability of NH_4^+ in the south Kāne‘ohe Bay water column, I hypothesize that the *M. grandis* holobiont performs ammonia oxidation. Finally, due to the shallow habitat of *M. grandis*, its abundances in south Kāne‘ohe

Bay (Coles et al. 2007, Shih, this volume, Chapter 2), as well as the low circulation within the semi-enclosed south bay (Lowe et al. 2009), I hypothesize that *M. grandis* has the potential to be an important driver of local biogeochemical cycling and nitrogen balance in Kāneʻohe Bay.

To our knowledge these are the first reported rates of ammonia oxidation by a sponge in the North Pacific and the first reported rates of seawater pumping and rates of microbially-mediated nitrification by the alien sponge *M. grandis*, the most abundant invasive sponge species on coral reefs in Kāneʻohe Bay. By investigating the importance of *M. grandis* relative to other dissolved inorganic nutrients (DIN) sources reported in literature and examining its representation as an indicator of change on reefs in Hawaiʻi, we can improve efforts in native coral habitat conservation through increased understanding of drivers of biogeochemistry on the reef.

Methods

Site description

Kāneʻohe Bay (Figure 3.1) is the largest sheltered body of water in Hawaiʻi and is on the Northeast coast of Oʻahu. The bay is 12.8 km long by 4.3 km wide with an average depth of 8 m, with a maximum depth of 12 m in the dredged channel, and is characterized by an extensive coral reef system protected from trade wind swells by a barrier reef bordering the windward margin and patch reefs and finger reefs throughout parts of the bay. The physical oceanography of Kāneʻohe Bay and its effect on nutrient delivery to reef organisms is well known from early descriptive studies (Bathen 1968) and from more recent 3D coupled wave-circulation numerical models (e.g. Lowe et al. 2009). *M. grandis* is found in shallow waters throughout Kāneʻohe Bay, on reefs, on or near pier pilings, mangroves, harbors, floating docks or within other shallow areas of the bay. This invasive and introduced sponge threatens lagoon-patch reef communities around

Hawai‘i where it spatially-competes with and can overgrow two of the dominant reef-forming corals in Kāne‘ohe Bay (Coles et al. 2004). *M. grandis* is a bright orange, thickly encrusting, asymmetrical cushiony sponge. Individuals in Kāne’ohe Bay are usually observed to range from several cms to 0.2 m across, although the sponge can reach 1 m across and over 0.5 m in thickness.

Figure 3.1: Map of Kāneʻohe Bay on Oʻahu, Hawaiʻi and the Hawaiʻi Institute of Marine Biology on Coconut Island (Moku o Loʻe). The diamonds mark the collection sites of *Mycale grandis* for $^{15}NH_4^+$ incubations from the reef along Lilipuna Pier and Reef 2, located just northwest of Moku o Loʻe .

Collection of M. grandis *for seawater pumping rates*

Whole sponge pieces of *M. grandis* were collected from under the Lilipuna Pier in south Kāneʻohe Bay. Sponge fragments ranged from 6 to 10 cm across and were carefully excised using a razor and moved into a bucket containing seawater avoiding exposure to air. The sponges were then immediately transferred by boat to the outdoor seawater flow through tables located at Hawaiʻi Institute of Marine Biology where specimens were exposed to natural daylight cycles and allowed to acclimate for one week. Seawater is continuously pumped into the tables from the eastern edge of Moku o Loʻe from a region where *M. grandis* commonly grows, supplying a natural seawater nutrient profile supportive of this sponge. Water tables were cleaned twice weekly of detritus and visible algae and again the day before experiments. The flow through water tables are approximately 150 cm long, 75 cm wide, and 15 cm deep. Residence time of seawater in the flow through water tables was adjusted to be ~3 hours to avoid accumulation of excess particulate detritus in the tables.

Sponge seawater pumping rates

Seawater pumping rates through *M. grandis* were determined for three individuals using techniques modified from Southwell et al. (2008a) and Fiore et al. (2013). The acclimated sponges were visually inspected and healthy sponges were selected based on fully healed surfaces and absence of signs of necrosis or irregular coloration. Sponges were transferred to a clear tank marked with cm and mm tickings along x, y, and z axes. A small amount of Fluorescein dye solution was carefully injected along the perimeter of the sponge (where the ostia are located) using a syringe. Uptake of the dye via active pumping by the sponge was apparent within several seconds and the dye was observed to be expelled in coherent jets by the sponge through its oscula, which are irregularly distributed every few centimeters over the

surface of the sponge. The injection and uptake of the dye was video-recorded and the velocity of the jets ($\Delta x/t$, where x is in cm and t is time in seconds) was estimated by the progress of distinct ripples along markings on the x, y, and z axes by the jets of sponge excurrent (Figure 3.2). The video was slowed to one quarter speed to more accurately constrain the velocity of the jets.

The velocity of the jets perpendicular to the plane of the sponge at the site of the osculum was measured in triplicate and averaged for each observation. Velocity was then multiplied by the area of the excurrent plume (assumed to be πr^2 based on the best estimate of the radius of the plume) to obtain the volume of seawater being pumped by the sponge per second. The volume of pumped seawater was normalized to the volume of the sponge (L seawater s^{-1} L^{-1} sponge) and by dry mass (L s^{-1} kg^{-1} dry weight). To determine the conversion of wet weight (WW) to dry weight (DW) for *M. grandis*, the weights of five samples of saturated sponge were measured, freeze dried (VirTis benchtop freeze dryer) and reweighed. Using this method, the dry weight of *M. grandis* was determined to be 0.16 of the wet weight, (or DW:WW = 1.6:10). The average density of *M. grandis* (wet), determined through volume displacement of water compared to the wet weight of sponge sample is 1.08 g mL^{-1}.

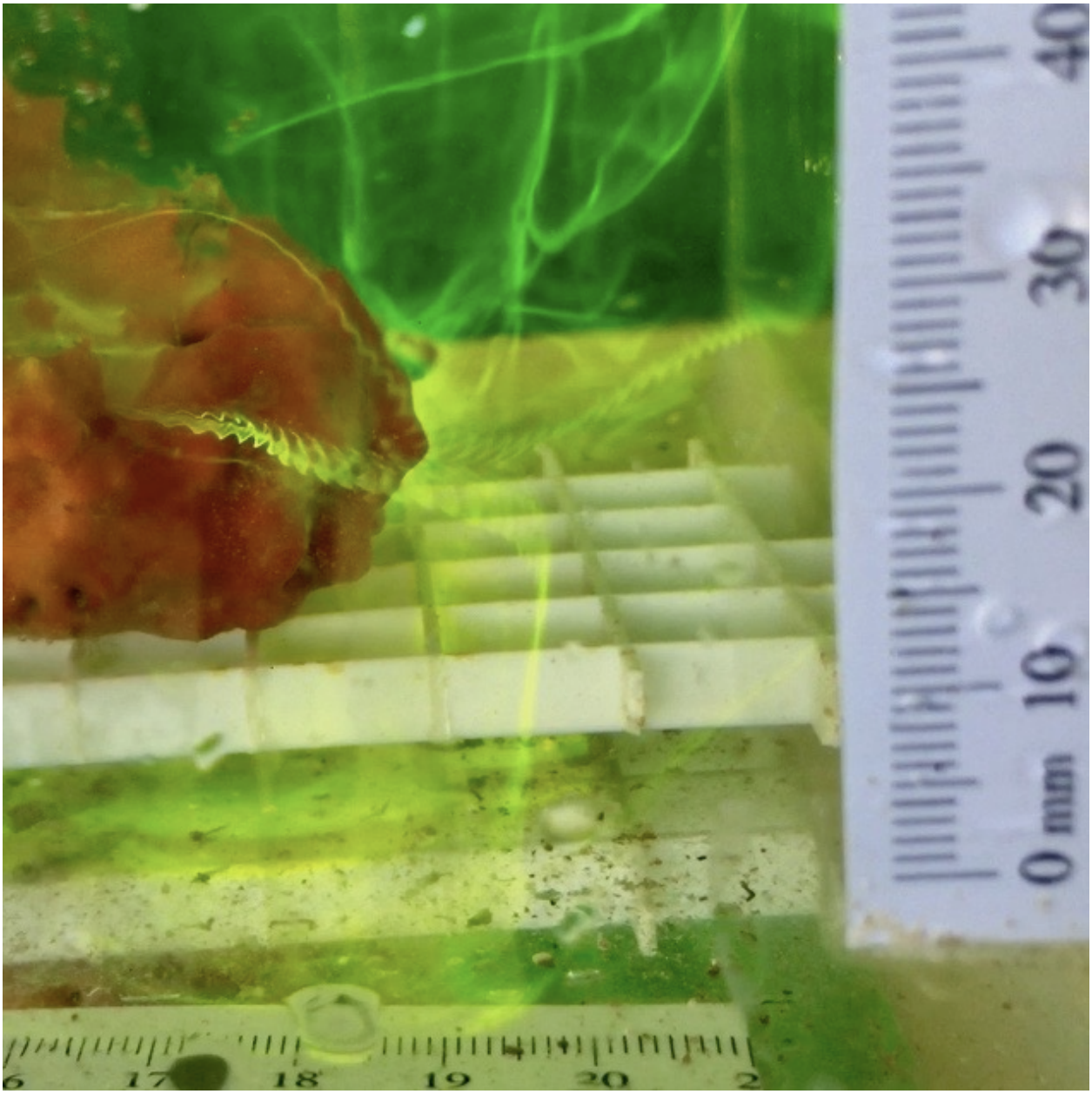

Figure 3.2: Distinct jets of Fluorescein dye expelled from the oscula of *M. grandis* showing ripples used to estimate velocity of jets along *x*, *y*, and *z* axes in cm and mm.

Sponge collection for $^{15}NH_4^+$ oxidation incubations

Specimens of *M. grandis* were collected from under the Lilipuna Pier near Moku o Lo‘e (Coconut Island) and Reef 2 (Fig 3.1) for a total of ten $^{15}NH_4^+$ oxidation rate experiments. Nitrification rates were determined for *M. grandis* by conducting incubations of sponge pieces in $^{15}NH_4^+$ using techniques described in Southwell et al. (2008a). Ammonia oxidation by the sponge is evidenced by the $^{15}NH_4^+$ tracer appearing in the $NO_3^- + NO_2^-$ pool in increasing concentrations over the duration of the incubation as well as an increase in the concentration of $NO_3^- + NO_2^-$.

For the first set of incubations which were performed at a concentration of 5 µM $^{15}NH_4^+$, pieces of sponge were harvested and fastened to segments of weighted PVC with zip ties and left to acclimate *in situ* near the site of collection. After one week, sponge pieces were examined to ensure they were healthy and absent of necrosis. Sponges were transferred into buckets without exposure to air and immediately brought to outdoor facilities at the Hawai‘i Institute of Marine Biology. Incubations were initiated within a half hour of collection and conducted in natural daylight.

Live samples of *M. grandis* for incubations at lower concentration of $^{15}NH_4^+$ (0.1 µM and 1.0 µM $^{15}NH_4^+$) were collected from Lilipuna Pier and Reef 2 and immediately transported in seawater to outdoor open seawater flow through tables at Hawai‘i Institute of Marine Biology for acclimation. Prior to the ammonia oxidation incubations, the sponges were allowed to acclimate for a period of one week and inspected for any signs of necrosis. Tanks were regularly cleaned of algal growth. All sponges remained healthy throughout the acclimation period and were used for the ammonia uptake incubations. Volume and weight of sponge samples for rate calculations

were determined by water displacement and by measuring the wet weight of each sponge sample. Two additional sets of incubations using acclimated sponges were performed each at concentration of $^{15}NH_4^+$ of 5 μM and 10 μM, which minimized effects of isotope dilution due to $^{14}NH_4^+$ production in the experiment (Kanda et al. 1987) .

Ammonia oxidation incubations

The incubations were performed in open top constant volume tanks of known volume containing ambient seawater sourced from the site of sponge collection and were continuously aerated with standard aquarium pumps (Rio Plus 600 Powerhead Aqua Pump) running through an air stone throughout the incubation. To begin the incubation, $^{15}NH_4^+$ (Isotec ammonium-^{15}N chloride 98 atom %) was added to a concentration of 5 μM, which matched ambient levels of NH_4^+ in south Kāneʻohe Bay (measured to be 4 to 13 μM during the sampling periods for this experiment). Two additional sets of ammonia oxidation incubations using identical procedural steps were performed using tracer levels of ^{15}N-labeled NH_4^+ (0.1 μM and 1.0 μM), defined as 10% or less of the typical range of ambient ammonium concentration. Tracer level experiments are designed with the idea of not excessively increasing the concentration of NH_4^+ above ambient levels during the incubation. Additional incubations were repeated at concentration of $^{15}NH_4^+$ of 5 μM and 10 μM $^{15}NH_4^+$, but most of the $NO_3^- + NO_2^-$ pool samples drawn from these incubations could not be analyzed because they contained too much ^{15}N label for reliable measurement (i.e., the working range of the detector on the mass spectrometer during analysis was greatly exceeded). $^{15}NH_4^+$ was also added to control incubations conducted in enclosures without sponges for each set of incubations to account for nitrification that could be occurring in the seawater. Samples of seawater were drawn at the start of the incubation upon addition of $^{15}NH_4^+$

(t_0), 30 minutes, 1 hour, 2 hours, and 4 hours. The incubation was conducted in ambient outdoor conditions and water samples were collected in HCl washed 60 mL HDPE bottles. Collection bottles were rinsed three times with sample seawater before collection and samples were kept on ice during the experiment. Immediately following the incubation, samples were transported to the University of Hawai‘i at Mānoa and stored at -20℃ until analysis.

Sample analysis

Samples were analyzed using the “denitrifier” method (Sigman et al., 2001) using methods as described previously (Popp et al., 1995; Dore et al., 1998). Briefly, $^{15}NO_3^- + {}^{15}NO_2^-$ present in each sample was converted to $^{15}N_2O$ gas through denitrification by *Pseudomonas aureofaciens*, transferred from the reaction vial, cryofocused, and separated from other gases using a CP-PoraBOND Q capillary column (0.32 mm inner diameter × 25 m × 5 μm) held at 20 – 25◦C. $\delta^{15}N$ values of N_2O were analyzed using a ThermoFinnigan MAT 252 isotope ratio mass spectrometer coupled to a modified GasBench II interface (Beman et al. 2008, Christman et al. 2011). Ammonia oxidation rates were calculated from $\delta^{15}N$ values as previously described (Christman et al. 2011, Beman et al. 2012); the detection limit for this measurement (0.001 nM d^{-1}) was determined by using the detection limit for [NH_4] and [NO_x], as well as the uncertainty in stable isotope measurements using this equipment (Beman et al. 2011). Reference materials (USGS-32, NIST-3, and UH $NaNO_3$) and blanks were bookended every 7 - 14 samples. The measured $\delta^{15}N$ values were linearly correlated (R^2 = 0.996 - 0.999) with the accepted $\delta^{15}N$ values of the reference materials. Duplicate analyses of procedural blanks were below the limit of detection.

Ammonia oxidation rates ($^{15}R_{ox}$) from $\delta^{15}N$ values of the accumulated NO_3^- + NO_2^- pool were calculated using the equation (Eq. 3.1) and methods described in Beman et al. (2011) and modified from Ward et al. (1989),

$$^{15}R_{\mathrm{ox}} = \frac{\left(n_t - n_{o_{\mathrm{NO}_x^-}}\right) \times \left[\mathrm{NO}_3^- + \mathrm{NO}_2^-\right]}{\left(n_{\mathrm{NH}_4^+} - n_{o_{\mathrm{NH}_4^+}}\right) \times t} \qquad \text{(Eq. 3.1)}$$

where n_t is the atom % ^{15}N in the NO_3^- + NO_2^- pool measured at time t in the incubation, n_{0NOx-} is the measured atom % ^{15}N of unlabeled NO_3^- + NO_2^- , n_{0NH4+} is the background atom % ^{15}N of NH_4^+, [NO_3^- + NO_2^-] is the concentration of the NO_x^- pool, and n_{NH4+} is the atom % enrichment of NH_4^+ at the beginning of the experiment. The ^{15}N natural abundance of unlabeled NH_4^+ was assumed to be 0.3663 atom % ^{15}N and initial atom % enrichment of the substrate at the beginning of the experiment n_{NH4+} was calculated by isotope mass balance based on measured ambient NH_4^+ concentrations (which ranged from 0.3 to 13.5 μmol L^{-1}) in the seawater used during the incubation. Nutrients were analyzed at the SOEST Laboratory for Analytical Biogeochemistry (S-LAB).

To compliment measurement of rates of $^{15}NH_4$ oxidation, rates of NO_3^- + NO_2^- production were also calculated using the increase in peak area of masses 44 ($^{14}N^{14}N^{16}O$) and 45 ($^{15}N^{14}N^{16}O$ or $^{14}N^{15}N^{16}O$) in samples incubated in the presence of 0.1 μM and 1.0 μM $^{15}NH_4^+$. Peak areas corrected for background were measured using techniques described above from each experimental data point, giving the concentration of N_2O produced, which can only originate from NO_2^- or NO_3^- produced via the denitrifier method used in this analysis (Sigman et al.

2001). Therefore, in these experiments, increases in mass 44 as a function of time is attributed to the formation of $^{14}NO_2^-$ and $^{14}NO_3^-$, whereas mass 45 is attributed mainly to the formation of $^{15}NO_2^-$ and $^{15}NO_3^-$. Calibration was achieved using known quantities of reference materials at the start and end of each analysis sequence as well as after approximately every ten samples. The slope of the regression of the sum of masses 44 and 45 as a function of time was used to calculate the rate of production of $NO_3^- + NO_2^-$.

Concentration of nutrients in excurrent versus ambient reef water

The nutrient profile of sponge exhalent (seawater exiting the sponge) from *M. grandis* was compared to surrounding ambient seawater to determine Δ[analyte], the excurrent concentration of the measured nutrient minus the ambient concentration of the measured nutrient, for analytes NH_4^+, N+N ($NO_3^- + NO_2^-$), total nitrogen (TN), PO_4^{3-}, and silicate ($Si(OH)_4$). Seawater samples representative of sponge excurrent were drawn by carefully inserting a syringe needle 0.5 cm into the cavity of the oscula and slowly drawing (~1 mL s^{-1}) the sponge excurrent water sample. The ambient seawater sample was drawn from the adjacent water column 0.3 m to the side of and away from the sponge. Samples were filtered through 0.22 μM syringe filters (Millex GV Durapore) into sample bottles which were rinsed 3x with sample material before drawing the final water sample. The nutrient samples were placed on ice, transferred to the University of Hawai‘i at Mānoa and stored frozen at -20°C until analysis. Sample 60 mL HDPE bottles and syringe barrels were washed with Liquinox® Detergent, rinsed well with deionized water and soaked in freshly made 10% HCl for 24 hours, rinsed again in DI water and allowed to dry. Syringe plungers were washed with Liquinox® Detergent, rinsed with DI water, soaked in 10% HCl for 10 minutes, rinsed well with DI water and air dried. 18 gauge 1 ½ inch needles were washed in Liquinox® Detergent and rinsed with DI water and allowed to dry. Initial attempts to

collect samples from the field were not successful as surface movement of water on the reef made it challenging to maintain the position of the syringe and the needle would tear the small-sized oscula on the sponges, and therefore the *in situ* method was not conducive to yielding meaningful samples. Therefore, samples were drawn from 5 sponge individuals collected from Reef 2 and kept in the large seawater flow through aquaria at the Hawai‘i Institute of Marine Biology.

DIN analysis

Sponge exhalent and ambient reef water nutrient samples were submitted to the SOEST Laboratory for Analytical Biogeochemistry (S-LAB) at the University of Hawai‘i at Mānoa for analysis of dissolved inorganic nutrients. The S-LAB utilizes methods and procedures outlined by Seal Analytical for the AA3 Nutrient Autoanalyzer (BRAN-LUEBBE, Hamburg, Germany). Ammonium is measured fluorometrically following the method of Kerouel and Aminot (1997). N+N is analyzed via the diazo reaction based on the methods of Armstrong et al (1967) and Grasshoff (1983). Total Dissolved Nitrogen and Phosphorus (TDN and TDP) analyzed under an in-line UV digester following the method developed by the University of Hamburg in cooperation with the Ocean University of Qingdao for the autoanalyzer. The determination of orthophosphate is based on the colorimetric method of Murphy and Riley (1962). Silicate is measured using the method of reduction of silicomolybdate in acidic solution to molybdenum blue by ascorbic acid (Grashoff and Kremling 1983). The mean detection limit (MDL) is defined as three times the standard deviation of the analytical blank as was dependent on the range of the analyte in the sample. The MDLs in the ranges of detection were as follows: MDL = 0.009 μmol L^{-1} for PO_4^{3-} in the range 0 - 3 μmol L^{-1}, MDL = 0.09 μmol L^{-1} for $Si(OH)_4$ in the range 0 - 40

μmol L^{-1}, MDL = 0.06 μmol L^{-1} for NO_2^- + NO_3^- in the range 0 - 4 μmol L^{-1}, and MDL = 0.132 μmol L^{-1} for NO_2^- + NO_3^- in the range 0 - 43 μmol L^{-1}, and MDL = 0.42 μmol L^{-1} for NH_4^+ in the range 0 - 42 μmol L^{-1}. Volume normalized ammonia uptake rates by the sponge from this experiment was calculated as the product of its pumping rate and ΔNH_4^+ concentration between ambient seawater and the sponge excurrent samples, and ammonia oxidation rates were calculated normalizing to sponge volume and weight by using sponge density and dry and wet mass conversions determined for *M. grandis* in this study.

Results

Pumping rates

M. grandis was determined to pump at 114.9 ± 15.1 (mean ± 1 SD; n = 10) times its own volume per day, or a mean of 0.0027 L seawater $s^{-1}L^{-1}$ sponge. *M. grandis* individuals did not show significantly different average excurrent flow rates over the measure period (signed-rank test, p = 0.06). The pumping rate of seawater by the sponge ranged from 0.0025 to 0.0028 L seawater s^{-1} L^{-1} sponge (Figure 3.3), or 0.015 to 0.016 L seawater s^{-1} kg^{-1} sponge (dry mass) (Figure 3.4). A Wilcoxon signed-rank test showed that the pumping rates did not differ significantly from each other (z = -1.84, p = .07). Although attempts to measure flow rate in the field were unsuccessful due to excessive surface water movement disrupting the excurrent plume, the rate of uptake of Fluorescein dye as determined by the time it took to appear in oscula were similar in the field as those observed in the tank experiments.

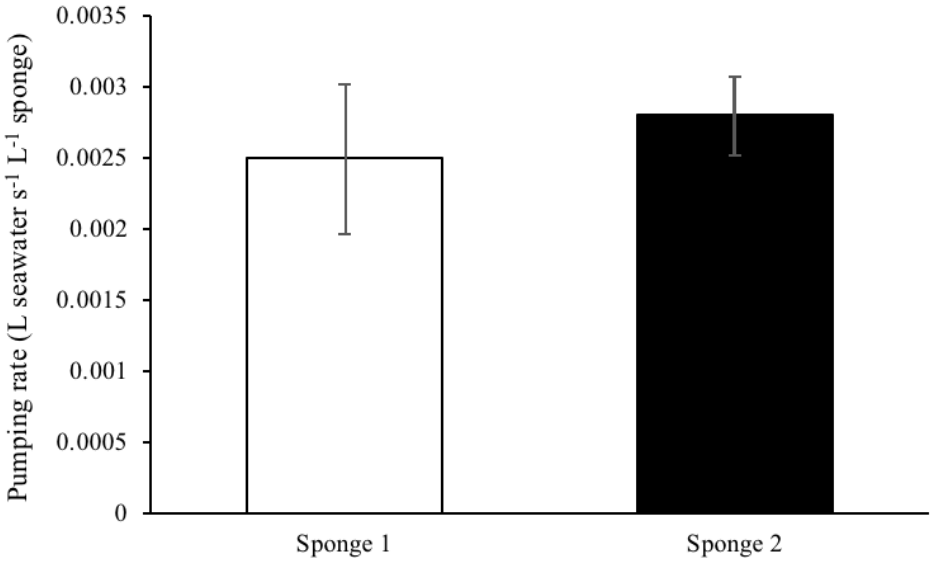

Figure 3.3a: Pumping rate per volume of sponge (reported in L seawater s^{-1} L^{-1} sponge) determined for *M. grandis* (mean ± 1 SD, *n* = 10) for *M. grandis* individual #1 (clear) and *M. grandis* individual #2 (filled).

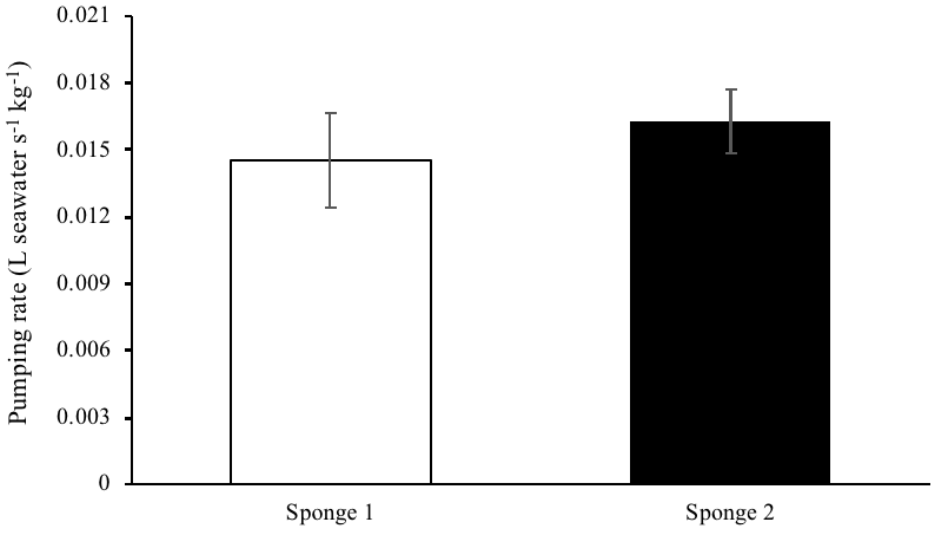

Figure 3.3b: Pumping rate by dry weight of sponge (L seawater s^{-1} kg^{-1} dry weight sponge) determined for *M. grandis* (mean ± 1 SD, *n* = 10) for *M. grandis* individual #1 (clear) and *M. grandis* individual #2 (filled).

Ammonia Oxidation Rates

The volume and mass normalized rates of $^{15}NH_4^+$ oxidation ranged from 3.9 to 75.1 nmol $g^{-1}h^{-1}$ (dry weight) (see Appendix Table A.2) and averaged 21.2 nmol $g^{-1}h^{-1}$ over all incubations. All incubations for the three different concentrations of $^{15}NH_4^+$ added showed active and sustained rates of ammonia oxidation, with no indication of rates declining over the course of the incubation. At the 0.1 μM concentration of added $^{15}NH_4^+$ (*n* = 10 measurements), the average ammonia oxidation rate was 23.5 nmol $g^{-1}h^{-1}$ for all sites; at the concentration of 1.0 μM $^{15}NH_4^+$ added (*n* = 7 measurements), the average ammonia oxidation rate was 60.2 nmol $g^{-1}h^{-1}$ (Table 3.1); and at the concentration of 5.0 μM added (*n* = 15 measurements), the average ammonia oxidation rate was 8.4 nmol $g^{-1}h$ (Table 3.2). Ammonia oxidation by site from where the sponge was collected is reported in Table 3.2.

The rates determined from each 1.0 μM incubation was significantly different from each 1.0 μM and 5.0 μM incubation outside of two standard deviations. Neither 0.1 μM incubation was statistically different from either 5.0 μM incubations outside of two standard deviations. All 0.1 μM, 1.0 μM and 5.0 μM incubations were not statistically different from the other incubation performed at the same concentration. For all incubations performed at 0.1 μM, 1.0 μM and 5.0 μM, rates were lowest at the 5.0 μM concentration. Although only two rate measurements from the experiments performed in the presence of 10 μM $^{15}NH_4^+$ are considered to be reliable because of excessive incorporation of the label into the $NO_3^- + NO_2^-$ pool in the remaining samples, rates at 10 μM were lowest of all and comparable to rates measured at 5 μM. Rates peaked at the intermediate 1.0 μM incubations, which also matches typical concentrations of NH_4^+ in Kāneʻohe Bay most closely. Ammonia oxidation rates for each time interval of all incubations are reported in the Appendix in Table A.2.

Sponge	$^{15}NH_4^+$ added	$^{15}NH_4^+$ ox. rate (nmol h^{-1} g^{-1}) accumulation in $^{15}NO_3^- + ^{15}NO_2^-$ pool	NH_4^+ ox. rate (nmol h^{-1} g^{-1}) increase in peak area in masses 44+45
A	0.1 µM	14.9	26.38
B	0.1 µM	28.6	21.25
Average	0.1 µM	**23.5**	**23.82**
C	1.0 µM	75.11	22.95
D	1.0 µM	55.25	17.5
Average	1.0 µM	**60.22**	**20.23**

Table 3.1: Ammonia oxidation rates of *M. grandis* determined using accumulation of ^{15}N in the N+N pool and using increase in peak area of masses 44 ($^{14}N^{14}N^{16}O$) and 45 ($^{15}N^{14}N^{16}O$ or $^{14}N^{15}N^{16}O$) as a function of time in $^{15}NH_4$ incubation experiments performed at 0.1 µM and 1.0 µM. Rates are reported in nmol h^{-1} g^{-1} sponge (dry weight).

	Concentration $^{15}NH_4^+$ added		
	0.1 µM	**1.0 µM**	**5.0 µM**
Reef 2	14.9	75.1	
Lilipuna Pier	28.6	55.3	8.4

Table 3.2: Average ammonia oxidation rates by collection site and by concentration of $^{15}NH_4^+$ added reported in nmol $g^{-1}h^{-1}$ determined from $^{15}NH_4^+$ incubations of *M. grandis.* All ammonia oxidation rates are reported in Table A.2 in the Appendix.

Volumetric ammonia oxidation rates were converted into flux rate estimates on the reef by assuming an average thickness of 10 cm to 20 cm of *M. grandis*. Sponge thickness ranged from <1 cm to up to 50 cm on the reef in assessments performed for this study, however the

overwhelming population of *M. grandis* on the reef was between 10 and 20 cm thick and so this assumed best range was chosen to calculate flux. On Reef 2, average *M. grandis* coverage was 4.6% whereas coverage in the Lilipuna fringing reef averaged 2.9%, and coverage averaged 32.3% in the mangroves on the northern edge of Moku o Loʻe (see Chapter 2, this volume). The calculated benthic flux of DIN from *M. grandis* nitrification (per m^2 of projected reef area) for Reef 2 is 1.92 to 3.84 mmol m^{-2} d^{-1}, 1.21 to 2.42 mmol m^{-2} d^{-1} on Lilipuna Pier fringing reefs, and 13.5 to 26.9 mmol m^{-2} d^{-1} within mangroves (See Table 3.7).

Five out of six of the $^{15}NH_4^+$ incubations of *M. grandis* showed a steady linear accumulation of ^{15}N in the NO_3^- + NO_2^- pool over the four hour period indicating oxidation of $^{15}NH_4^+$ added in concentrations representative of a typical range of NH_4^+ levels found in Kāneʻohe Bay. Control incubations containing no sponge showed no detectable ^{15}N enrichment in the NO_x pool.

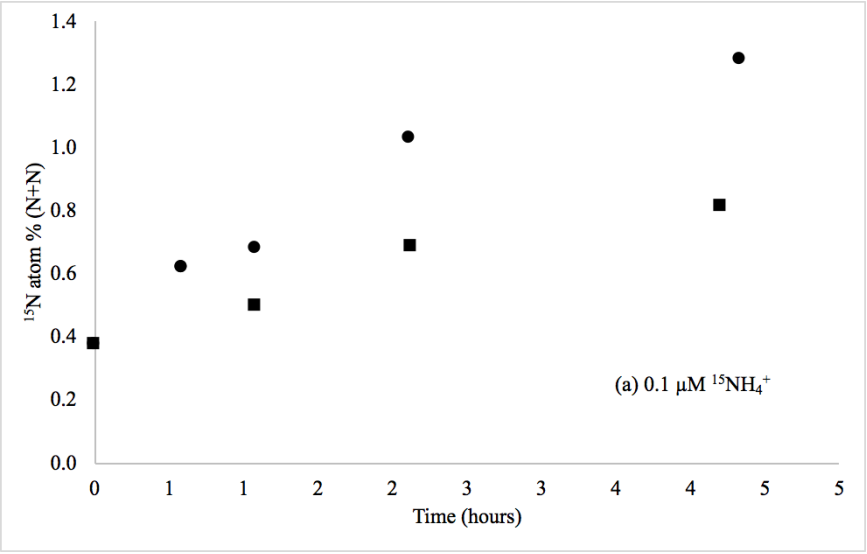

(a.)

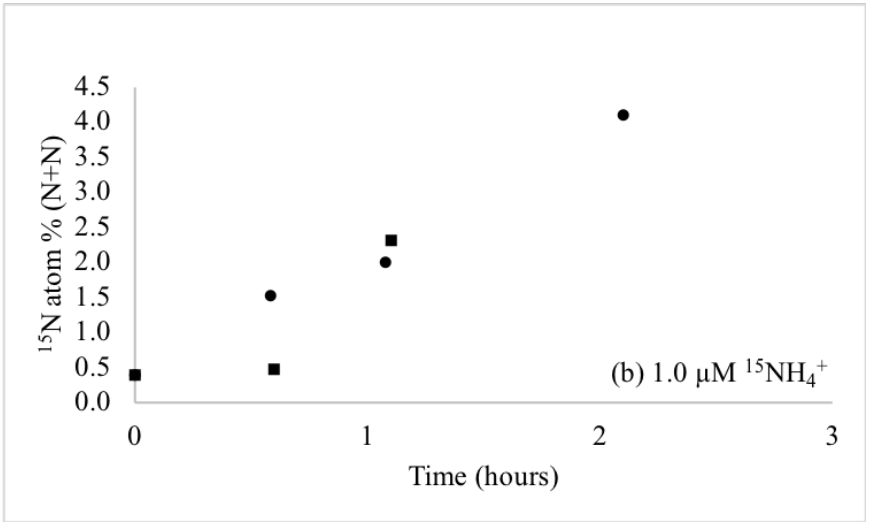

(b.)

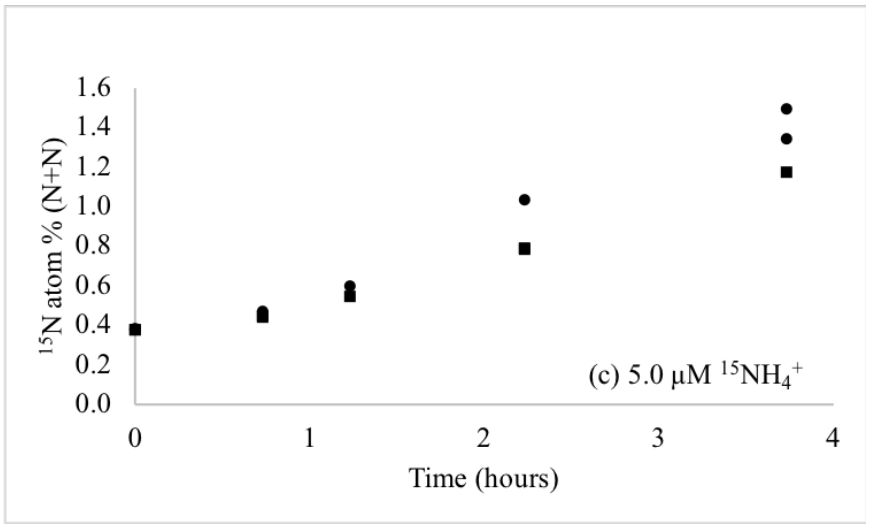

(c.)

Figure 3.4: Accumulated atom % ^{15}N in the NO_3^- + NO_2^- (N+N) pool over a four hour $^{15}NH_4^+$ incubation of *Mycale grandis* at 0.1 µM (a.), 1.0 µM (b.), and 5.0 µM (c.). Each figure includes two independent sponge incubations at the same concentration. In (a.) both sponges were collected from under the Lilipuna Pier. For incubations (b.) and (c.) sponges indicated by filled circles were collected from Lilipuna Pier and sponges indicated by filled squares were collected from Coconut Island Reef 2. For (b.) (the 1.0 µM incubation) water samples drawn beyond the two hour time stop maxed out the detector on the ThermoFinnigan MAT 252.

Rates of NO_3^- + NO_2^- production determined from the increase in peak area of masses 44 and 45 from incubation experiments in the presence of 0.1 µM $^{15}NH_4$ averaged 23.8 nmol day^{-1} g^{1} sponge (dry weight) (SD = 3.6) and ranged from 21.3 to 26.4 nmol day^{-1} g^{-1} (Table 3.1). In results from incubation experiments in the presence of 1.0 $^{15}NH_4^+$, the average rate of NO_3^- + NO_2^- production was 20.2 nmol day^{-1} g^{-1} sponge (dry weight) (SD = 3.9), and ranged from 17.5 to 23.0 nmol day^{-1} g^{-1} sponge (Table 3.1).

Change in nutrient concentration in excurrent versus ambient reef water

The concentration of nutrients, [NH_4^+], [N+N] ([NO_3^- + NO_2^-]), [TN] (total nitrogen), [TP] (total phosphorus, [PO_4^{3-}] (phosphate), and [$Si(OH)_4$] (silicate) was measured in the sponge excurrent relative to ambient concentrations. Δ[analyte] indicates the change in nutrient concentration (in µmol L^{-1}) from the ambient to exhalent sample (A-E). In four of the five sponges sampled, there was a drawdown in [NH_4^+] in seawater that had passed through the sponge (see Table 3.4). In the four sponges that showed a drawdown of [NH_4^+], the average Δ[NH_4^+] was 2.97 µmol L^{-1}, which is a drop by one third (33.6%) of the ambient [NH_4^+] in these samples (average of 8.85. µmol L^{-1}). For all 5 sponges, the average Δ[NH_4^+] was 2.12 µmol L^{-1}, which is over one third (36.7%) of the average ambient level of ammonium measured in Kāneʻohe Bay (5.78 µmol L^{-1}) in conjunction with these experiments. Average Δ[N+N] (A-E) was 0.06 µmol L^{-1} (ranging from -0.05 to 0.18 µmol L^{-1}), 2.23 µmol L^{-1} for Δ[TN] (-1.05 to 5.51 µmol L^{-1}), 0.08 µmol L^{-1} for Δ[TP] (-0.13 to 0.28 µmol L^{-1}), -0.02 µmol L^{-1} for Δ[PO_4^{3-}] (-0.09 to 0.04 µmol L^{-1}), and 0.5 µmol L^{-1} for Δ[$Si(OH)_4$] (-2.76 to 3.99 µmol L^{-1}). Individual measurements for the excurrent and ambient reef water samples are reported in the Appendix in Table A.3. Due to the small number of samples (*n* = 5), the non-parametric Wilcoxon signed-rank test was used to test for significant differences in nutrient concentrations in sponge excurrent and ambient seawater samples. Table

3.4 shows that [NH_4^+] in the excurrent were lower than the ambient concentrations, though the difference in rank sums was marginally significant ($p < 0.08$). [TN] in the sponges' excurrent were also marginally significantly lower than in the ambient seawater samples ($p < 0.08$). Exhalent [TP] and [PO_4^{3-}] concentrations were greater than ambient [TP] and [PO_4^{3-}] in 3 of the 5 sponges samples, whereas 4 out of 5 samples of exhalent concentrations were lower than the ambient concentrations for all other nutrients. Changes in [NH_4^+], [$NO_3^- + NO_2^-$], and [TN] (total nitrogen) were more significant than changes in [PO_4^{3-}] and [$Si(OH)_4$]. Table 3.4 also presents the mean differences in the ambient and exhalent concentrations together with 95% confidence intervals for the differences in scores. Volume normalized ammonia oxidation rates based on the drawdown in NH_4^+ between the ambient seawater and sponge excurrent samples range from 14.6 to 58.6 μmol h^{-1} L^{-1} of sponge or 84.5 to 339.1 nmol $g^{-1}h^{-1}$ (dry weight) which are approximately 5x higher than ammonia oxidation rates determined in the $^{15}NH_4^+$ oxidation incubations (Table 3.3). Flux rates of ammonium uptake calculated from the drawdown of NH_4^+ by *M. grandis* (per m^2 of projected reef area) for Reef 2 is 10.1 to 80.9 mmol m^{-2} d^{-1}, 6.4 to 51.0 mmol m^{-2} d^{-1} on Lilipuna Pier fringing reefs, and 70.7 to 567.8 mmol m^{-2} d^{-1} within mangroves, although it is important to note that these values serve as a proxy for ammonia oxidation/ammonia uptake rates rather than net flux of N+N as a product of nitrification, as the Δ[N+N] between ambient and excurrent samples were insignificant.

	Vol. normalized flux (μmol h^{-1} L^{-1})	NH_4^+ oxidation rate (nmol g^{-1} h^{-1})
$^{15}NH_4^+$ tracer experiments	0.7 - 8.0	3.9 - 46.4
NH_4^+ uptake excurrent v. ambient	14.6 - 58.6	84.4 - 339.1

Table 3.3: Range of volume normalized ammonia oxidation rates in µmol h^{-1} L^{-1} and ammonia oxidation rate by mass in nmol g^{-1} h^{-1} (dry weight) determined from $^{15}NH_4^+$ incubations compared to rates determined from $\Delta[NH_4^+]$ in sponge excurrent versus ambient seawater samples.

	Samples	Ambient (A)		Exhalent (E)		A>E	A<E			Mean difference
Nutrient	***n***	**Mean (µmol L^{-1})**	***SD***	**Mean (µmol L^{-1})**	***SD***	***n***	***n***	***z***	***p***	**A-E (95% *CI*)**
NH_4^+	5	7.9	3.61	5.78	1.31	4	1	1.75	0.08	2.12 (-1.05, 5.28)
Sum ranks						14	1			
Expected						7.5	7.5			
N+N	5	0.41	0.25	0.34	0.16	4	1	1.48	0.14	0.06 (-0.05, 0.18)
Sum ranks						13	2			
Expected						7.5	7.5			
TN	5	10.4	2.28	8.17	0.53	4	1	1.75	0.08	2.23 (-1.05, 5.51)
Sum ranks						14	1			
Expected						7.5	7.5			
TP	5	0.8	0.56	0.72	0.52	2	3	0.41	0.69	0.08 (-0.13, 0.28)
Sum ranks						9	6			
Expected						7.5	7.5			
PO_4^{3-}	5	0.1	0.04	0.12	0.01	2	3	-0.94	0.35	-0.02 (-0.09, 0.04)
Sum ranks						4	11			
Expected						7.5	7.5			
$Si(OH)_4$	5	8.79	0.93	8.17	2.18	4	1	0.67	0.5	0.62 (-2.76, 3.99)
Sum ranks						10	5			
Expected						7.5	7.5			

Table 3.4: Mean sponge exhalent versus ambient seawater nutrient concentrations in µmol L^{-1} reported with signed-rank comparisons for sponge exhalent (E) and ambient (A) seawater nutrient concentrations. A>E is number of samples in the sample set with a higher nutrient concentration in the ambient sample than in the exhalent sample and A<E is the number of samples with a lower nutrient concentration in the ambient sample than in the exhalent sample. A

value of $p < 0.10$ is considered as indicative of a marginally significant difference the between mean ambient concentration and mean exhalent concentration.

Discussion

The sponge *M. grandis* competes spatially with other benthic organisms in Kāneʻohe Bay as an alien and invasive species that does not provide the same habitat as native reef-building stony coral. Furthermore, the results of this study support the main hypotheses that *M. grandis* alters the nitrogen balance on reefs based on the measured seawater pumping rates by the sponge and its ability to facilitate microbially-mediated ammonia oxidation. The effects of altered nutrient concentrations found in sponge excurrent is retained on the localized reefs because of long residence times and sluggish circulation within Kāneʻohe Bay. Though the pumping rates of *M. grandis* are on the low end compared to rates reported for other sponges and the nitrification rates are moderate compared to other sponges, *M. grandis* plays an important role in biogeochemical cycling within the N limited, shallow habitats of Kāneʻohe Bay where this sponge is found. The DIN flux from *M. grandis* is higher than other non-sponge sources reported in other coral reef environments and compared to other benthic fluxes previously measured in Kāneʻohe Bay (Table 3.7).

Pumping rates

The pumping rate of *M. grandis* (0.0027 L s^{-1} L^{-1}) was comparable to the low end of rates measured for various Caribbean and Floridian sponge species and was an order of magnitude lower than some Caribbean sponges (Table 3.5). Weisz et al. (2008) measured rates for sponges on the Florida Keys ranging from 0.005 to 0.578 L s^{-1} L^{-1} for 25 species of LMA, HMA, and unclassified sponges. Volume normalized pumping rates for other sponges fell within this range

as well (Gerrodette and Flechsig 1979, Fiore et al. 2013, McMurray et al. 2014, Fiore et al. 2017) (see Table 3.5).

Species	Pumping rate (L seawater s^{-1} L^{-1} sponge)	
M. grandis	**0.0027**	**This study**
25 assorted FL Keys *spp.*	0.005 - 0.578	Weisz et al. 2008
X. muta	0.028 - 0.056	Fiore et al. 2013
S. vesparium	0.17 ± 0.11	Fiore et al. 2017
I. campana	0.08	Fiore et al. 2017

Table 3.5: Seawater pumping rate of *M. grandis* compared to seawater pumping rates measured in a variety of other tropical Caribbean and Floridian sponges, in liters of seawater pumped per second per liter of sponge.

Despite the relatively low pumping rate of *M. grandis* compared to some Caribbean sponges, it can significantly influence the nutrient balance on these reefs because of the shallow depth of its habitat and the long residence time of seawater (>30 days) in south Kāneʻohe Bay (Lowe et al. 2009). Pumping rates measured for *M. grandis* may be low compared to some other sponges for several reasons. The low pumping rate is consistent with *M. grandis* being classified as an HMA (high microbial abundance) sponge, as HMA sponges exhibit lower pumping rates (Weisz et al. 2008) although this is only one parameter of HMA/LMA classifications. Sponges are able to adjust their pumping rates and flow patterns based on their nutritional needs or stop pumping altogether. Sponges under stress may also reduce or suspend their pumping (Reiswig 1974). The pumping rates determined in these experiments were measured from initially cut but visually healed sponge fragments that had been transferred from one tank to another and may or may not have resumed their maximum pumping activity. Unfortunately, the small size of the oscula on *M.*

grandis was not conducive to measuring rates *in situ*. Initial attempts to use the Fluorescein dye method on sponges *in situ* did not result in coherent or sustained visible streams of dye in the sponge excurrent because of wave surge even on very calm days, necessitating that Fluorescein dye experiments be conducted in the more controlled environment of an aquarium tank with seawater flow temporarily halted. However, the time it took for Fluorescein dye to be taken up by the sponge and appear in the oscula was similar in the field as that in the aquarium suggesting the pumping rates in the field are similar to those measured in the laboratory.

Influence on reefs in south Kāneʻohe Bay

Biomass assessments in three different environments were performed within south Kāneʻohe Bay, the region found by Coles et al. (2007) to have the highest abundances of *M. grandis*. Findings from Coles et al. (2007) on 18 reefs throughout Kāneʻohe Bay indicated that the sponge had its greatest surface area coverage in the south bay near the Hawaiʻi Institute of Marine Biology (HIMB) pier and Coconut Island. Furthermore, coverage on other reefs decreased to less than 1% on reefs at 1-3 km from this area of maximum abundance. Therefore, I found it most productive to focus on these data rich areas of high abundance. The exact contribution to biogeochemical cycling on the reef cannot be fully quantified without a comprehensive survey of the coverage of *M. grandis* on all reefs in south Kāneʻohe Bay, including regions that were not surveyed here nor in previous studies, but the degree of impact over these studied areas can be extended to reasonably represent potential impacts on and in similar shallow reef environments where *M. grandis* is present.

M. grandis coverage on the reef was determined for three distinct environments in these areas of high abundance near HIMB: On a reef crest, on a fringing reef, and within mangrove roots. For

each region, the degree of influence of *M. grandis* can be described by the amount of time it takes *M. grandis* to overturn the overlying water column for each zone. Using the average biomass found in each zone and the corresponding water depth, the amount of time for all of the overlying water to circulate through the sponge is remarkably short due to the shallow water depths. As seawater is filtered through *M. grandis*, it comes into contact with the sponge's biogeochemically active microbiome. Over Coconut Island Reef 2, the volume of the entire overlying water column is pumped through *M. grandis* in 1.9 days, using the average water depth of 1.0 m over the reef crest as determined from a composite bathymetric map (Figure 3.5). Equivalently, this is the entire volume of the overlying water column circulating through *M. grandis* 16 times in a 30 day period, which is approximately the seawater residence time in this region. It requires just 3 days for the overlying water column to be circulated through *M. grandis* on the Lilipuna Pier fringing (average depth ~1m) or approximately 10 times per 30 day period. Within the mangrove root habitat with an average depth of ~0.5m, it takes merely 3.25 hours for seawater to be circulated through the *M. grandis* community, or 223 times per 30 day period. Due to the long residence of seawater in these habitats, the biogeochemical byproducts of the sponge are not expected to be immediately flushed or mixed away but rather retained within the system.

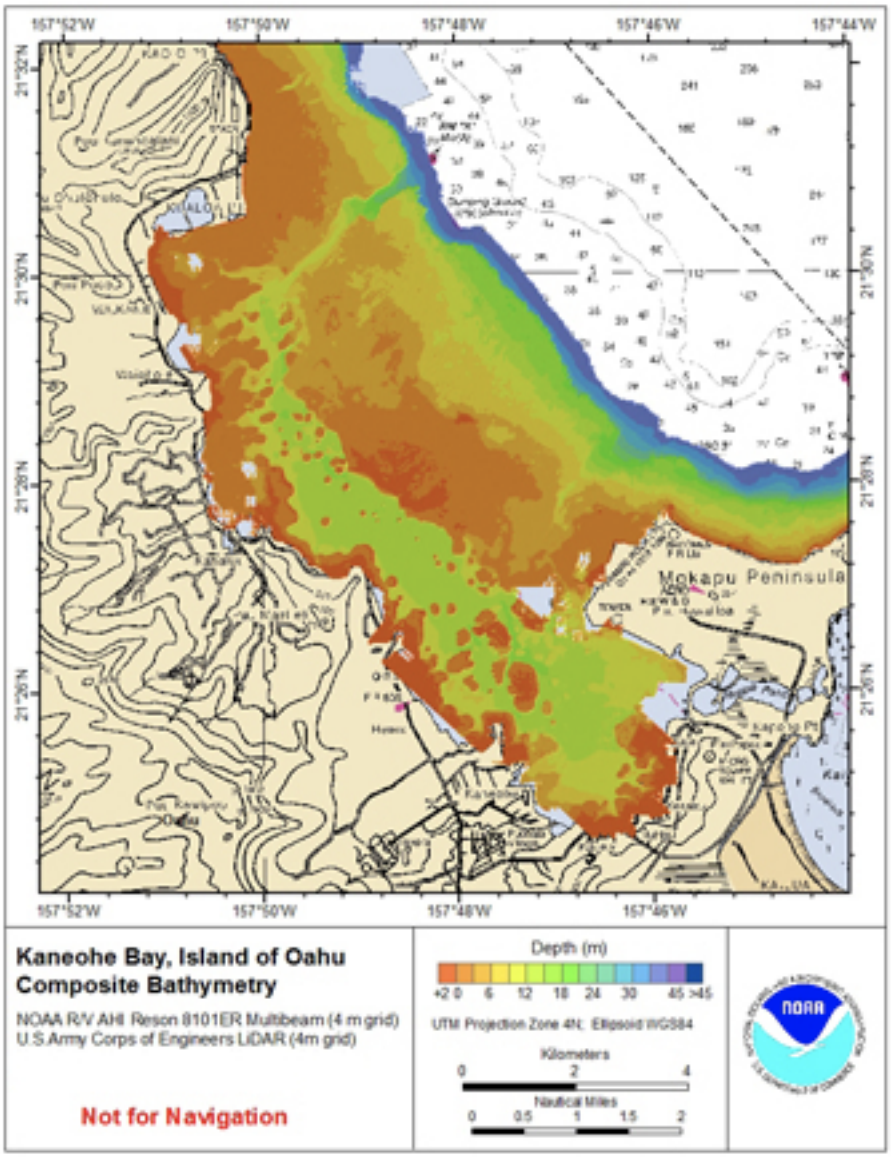

Figure 3.5: Bathymetric map of Kāne‘ohe Bay from NOAA/Army Corps of Engineers LIDAR showing depths used to calculate seawater turnover times of seawater filtered through *M. grandis*.

South Kāneʻohe Bay is characterized by extremely slow circulation with a residence time spanning two weeks to two months depending on wind forcing and to a much lesser extent on tidal forcing. Wind stress can slightly decrease the residence time of otherwise sluggish southern lagoon waters. The effect of tides is minimized by the negligible phase difference in the tides along the entrance of the bay and its relatively short extent (~8 km) (Lowe et al. 2009). The overall residence time is broadly considered to be *ca.* 30 days, with a minimum of 20.9 days and a maximum of 49.2 days (Lowe et al. 2009). This region is only weakly connected to the open ocean because the geographically isolated region is largely enclosed by Mokapu Peninsula and its connectivity with the rest of Kāneʻohe Bay is limited to just two narrow channels on either side of Coconut Island. The net slow movement of water in the bay is typically driven by the predominant trade winds, generating a clockwise circulation in the southern sector of Kāneʻohe Bay, resulting in the slow flow of riverine inputs along the shore northwards. Under "Kona", or southwesterly wind conditions, stream inputs are advected more directly northwards towards the sea from the Kāneʻohe Stream mouth (Ostrander et al. 2008).

Diffusion, rather than turbulent mixing, dominates the transport of dissolved organic materials within and through the boundary layer. Consequently, nutrients may accumulate near the sediment and are slow to mix into the overlying water column. For example, in Kāneʻohe Bay when nutrients are released from the sediments at higher rates than the rate of mixing into the water column, a nutrient-enriched zone develops from which benthic algae may acquire nutrients (Stimon and Larned 2000). A similar phenomenon of nutrients hotspots may occur through sponge-released DIN.

Nitrification

The rates of ammonia oxidation by *Mycale grandis* fall within the ranges reported for other sponges (Table 3.6). Nitrification rates of 14.7 and 8.8 nmol cm^{-3} day^{-1} (equiv. to 0.61 and 0.37 nmol $cm^{-3}h^{-1}$) were found for Mediterranean sponges *D. avara* and *C. reniformis*, respectively (Schlappy et al. 2010), 566 nmol N cm^{-3} day^{-1} for the Atlantic sponge *G. barretti* (Hoffman et al. 2009), and 3 to 13 nmol N g (dry weight)$^{-1}$ min^{-1} for six common sponges widely distributed in Mediterranean sublittoral rocky bottom habitats (*A. oroides*, *D. avara*, *C. reniformis*, *A. polypoides*, *I. oros*, and *A. aerophoba)* (Jiménez and Ribes 2007). Among tropical sponges, Diaz and Ward (1997) found that NO_2^- accumulated during all the experiments with *0. violacea* (170 to 580 nmol g^{-1} h^{-1}), while NO_3^-, accumulated with *P. zeai* (0 to 1033 nmol g^{-1} h^{-1}), *C. nucula* (360 to 2650 nmol g^{-1} h^{-1}), and *P. halichondroides* (0 to 320 nmol g^{-1} h^{-1}). Nitrification rates as high as 1μmol g^{-1} h^{-1} in *X. muta* were reported by Southwell (2007) though later studies observed a negative flux of N+N indicating either denitrification or anammox processes were taking place (Fiore et al. 2013). For further comparison, *M. grandis* nitrification exceeds other known benthic environments where nitrification rate was measured, such as in consolidated coral reef carbonate sediments on the Great Barrier Reef that produce at a maximum measured nitrification rate of 3.8 nmol g^{-1} of dry sediment per hour.

Source	Nitrification rate	Study
M. grandis	**3.9 - 46.4 nmol $g^{-1}h^{-1}$**	**This study**
Mediterranean sponges (6 *spp.*)	180 - 780 nmol $g^{-1}h^{-1}$	Jimenez and Ribes 2007
O. violacea	170 - 580 nmol $g^{-1}h^{-1}$	Diaz and Ward 1997
P. halichondroides	0 - 320 nmol $g^{-1}h^{-1}$	Diaz and Ward 1997
G. barretti	56.6 nmol $g^{-1}h^{-1}$	Hoffman et al. 2009
X. muta	0 - 1 µmol $g^{-1}h^{-1}$	Southwell et al. 2008, Fiore et al. 2013
Consolidated reef sediments	3.8 nmol g-1 h-1	Capone et al. 1992

Table 3.6: Ammonia oxidation rates in *M. grandis* compared to rates measured in a selection of Caribbean and Mediterranean sponges. Rates of ammonia oxidation are comparably low but fall within order of magnitude range compared to other sponges.

The flux of DIN from *M. grandis* on the Reef 2 reef crest and Lilipuna Pier fringing reef are comparable to flux rates from other coral reef sponge nitrification rates measured in the Caribbean (12 mmol m^2 d^{-1} NO_3^- DIN for *C. nucula and A. varians* (Corredor et al. 1988), 5.8 to 10.9 mmol m^2 d^{-1} NO_3^- + NO_2^- for *P. zeai* (Diaz and Ward 1997), and 13 ± 2.8 mmol m^2 d^{-1} for 14 specific sponge species on Conch Reef in Florida (Southwell et al. 2008b) and 15 ± 3.0 mmol m^2 d^{-1} for the extrapolated total nonencrusting sponge community (>23 species) on Conch Reef. The flux rate calculated for the mangrove is high compared to other sponge flux rates due to the exceptionally high biomass (32.3% coverage) of *M. grandis* in mangrove roots.

M .grandis flux rates of N+N exceed all other benthic N+N flux rates previously measured in Kāneʻohe Bay by one to two orders of magnitude (see Table 3.7). The Kāneʻohe Bay reef flats had a negative efflux of -490.7 µmol m^{-2} d^{-1} N+N, while the reef slope had an average positive flux rate of 122.7 µmol m^{-2} d^{-1}, which is one order or magnitude below *M. grandis* N+N flux

rates measured on the reef. The south bay bottom was measured to have a flux rate of 295 µmol m^{-2} d^{-1}, while the mid bay had a flux rate of 3 µmol m^{-2} d^{-1}, and the north bay had a flux rate of 194 µmol m^{-2} d^{-1} (Stimson and Larned 2000). There are no known reports of DIN flux from coral cavities in Kāneʻohe Bay, but *M. grandis* flux rates exceed those measured from coral cavities in the Red Sea (22.3 mmol m^2 d^{-1} (Richter et al. 2001)) and in the Caribbean (5.4 ± 9.8 mmol m^2 d^{-1} (Scheffers et al. 2004)). Although coral cavities are space limited habitats, they may contain cryptic sponges that are responsible for some of the DIN flux measured in cryptic habitats (de Goeij et al. 2013, Hoer et al. 2017).

Source	Flux rate	Study
Kāneʻohe Bay fringing reef	**6.4-51.0 mmol m^2 d^{-1}**	**This study**
Kāneʻohe Bay Reef 2	**10.1-80.9 mmol m^2 d^{-1}**	**This study**
Kāneʻohe Bay mangroves	**70.7-567.8 mmol m^2 d^{-1}**	**This study**
Kāneʻohe Bay reef flat	-490.7 µmol m^{-2} d^{-1}	Stimson and Larned 2000
Kāneʻohe Bay reef slope	122.7 µmol m^{-2} d^{-1}	Stimson and Larned 2000
South Kāneʻohe Bay bottom	295 µmol m^{-2} d^{-1}	Stimson and Larned 2000
Mid Kāneʻohe Bay	3 µmol m^{-2} d^{-1}	Stimson and Larned 2000
North Kāneʻohe Bay	194 µmol m^{-2} d^{-1}	Stimson and Larned 2000
Shallow marine sediments	0.613 mmol m^2 d^{-1}	Stimson and Larned 2000
GW seepage (North K. bay)	4 µmol m^{-2} d^{-1}	McGowan Thesis 2004
Red Sea coral cavities	22.3 mmol m^2 d^{-1}	Richter et al. 2001
Caribben coral cavities	5.4 ± 9.8 mmol m^2 d^{-1}	Scheffers et al. 2004
Microbial mats (France)	~1 mmol m^2 d^{-1}	Bonin and Michetoy 2006
Coral reef sediment (Puerto Rico)	0.018-0.033 mmol m^2 d^{-1}	Corredor and Morell 1985

Table 3.7: *M. grandis* DIN flux rates from this study compared to other benthic environments in Kāneʻohe Bay and other coral reef substrates.

Finally, flux rates of DIN from *M. grandis* exceeded all reported flux rates of DIN of other benthic habitats such as microbial mats in southeastern France (~1 mmol m^2 d^{-1} NO_3^-) (Bonin and Michetoy 2006), coral reef sediment (0.018 - 0.033 mmol m^2 d^{-1}) (Corredor and Morell 1985), and shallow water marine sediments in Hawai‘i (0.613 mmol m^2 d^{-1}) (Stimson and Larned 2000). These data suggest *M. grandis* is the most important source of DIN flux to the reef within Kāne‘ohe Bay.

There are no known measured water column nitrification rates in south Kāne‘ohe Bay but it is presumed to be negligible compared to *M. grandis* hosted nitrification. Water column ammonia oxidation rates have been measured in the open ocean at Station ALOHA within the broad nitrite maximum at the base of the euphotic zone, with reports of rates ranging from 1 to 137 nmol $L^{-1}d^{-1}$ during three HOT cruises (Dore and Karl 1996), a maximum oxidation rate of 1 nmol $L^{-1}d^{-1}$ at Station ALOHA by Sutka et al. (2004), and 2.89 to 10.3 nmol $L^{-1}d^{-1}$ also at Station ALOHA by Beman et al. (2011). While rates of water column ammonia oxidation at Station ALOHA are already substantially lower than rates of sponge-hosted ammonia oxidation (16.8 µmol $L^{-1}d^{-1}$ to 1.4 mmol $L^{-1}d^{-1}$), water column nitrification rates in Kāne‘ohe Bay are most certainly lower than nitrification rates measured at the base of the euphotic zone at Station ALOHA due to light inhibition of ammonia oxidizers. Photoinhibition in *Thaumaracheaota* and AOB have been described (Merbt et al. 2012), while evidence of sensitivity of ammonia oxidizing species to ROS (reactive oxygen species) rather than direct photoinhibition has been described by Tolar et al (2016). ROS such as H_2O_2 is produced by abiotic and biotic processes in all sunlit marine waters where it can enter and damage cells that do not have detoxifying

enzymes, although this effect was found to be more pronounced in polar waters than in temperate waters (Tolar et al. 2016).

Although the appearance of ^{15}N in the $NO_3^- + NO_2^-$ pool as a function of time in incubation experiments with added $^{15}NH_4^+$ is a quantitative measure of ammonia oxidation, results may not indicate complete nitrification. Sponges can harbor microorganisms capable of N_2 production from anaerobic ammonia oxidation (Mohamed et al. 2010) and presumably denitrification (Fiore et al. 2013). In addition, nitrite oxidation can be decoupled from ammonia oxidation in the open ocean (Beman et al. 2013). Increases in the concentration of N_2O produced during the denitrification method and quantified by the mass spectrometer as a function of time in incubation experiments in the presence of 0.1 and 1.0 μM $^{15}NH_4^+$ provide unequivocal evidence of the production of $NO_3^- + NO_2^-$. The net rate of $NO_3^- + NO_2^-$ production in these experiments can provide insight into the coupling of ammonia oxidation and nitrite oxidation as well as nitrogen loss mechanisms.

Rates of $NO_3^- + NO_2^-$ production calculated from the increases in masses 44 and 45 as a function of time in samples from incubation experiments with $^{15}NH_4^+$ added may overestimate or underestimate rates. In our measurements, mass 45 was not corrected for contribution of ^{17}O ($^{14}N^{14}N^{17}O$). Although most of the oxygen atoms in N_2O produced from NO_2^- and NO_3^- using *Pseudomonas aureofaciens* originates from NO_2^- and NO_3^-, there is up to 10% exchange with water (Casciotti et al. 2002). Consequently, the origins of ^{17}O in mass 45 may be uncertain. In addition, mass 46, which frequently includes doubly ^{15}N-labeled N_2O ($^{15}N^{15}N^{16}O$), which would form predominantly from the oxidation products of the added $^{15}NH_4^+$, was not included in our calculation. In incubation experiments in the presence of 1.0 μM $^{15}NH_4^+$ mass 46 was not

quantifiable at incubation times exceeding 1 hour because this mass saturated the detector. However, the contribution of ^{17}O to mass 45 and the lack of quantification of mass 46 probably did not change our rates markedly since ^{17}O contributes less than 0.04% to the isotopes of oxygen and the signal of mass 46 in the mass spectrometer is highly amplified because of its low abundance in nature. With these caveats in mind, however, it is possible to compare rates of ammonia oxidation from $^{15}NH_4^+$ with rates of NO_2^- and NO_3^- production quantified using masses 44 and 45.

Rates of ammonia oxidation agree well with rates of $NO_3^- + NO_2^-$ production in incubation experiments in the presence of 0.1 μM $^{15}NH_4^+$ but not in experiments in the presence of 1.0 μM $^{15}NH_4^+$ (Table 3.1). The agreement between rates of ammonia oxidation and $NO_3^- + NO_2^-$ production in incubation experiments in the presence of 0.1 μM $^{15}NH_4^+$ suggest that these processes were tightly coupled and that there was no appreciable N_2 production. However, rates of $NO_3^- + NO_2^-$ production in incubation experiments in the presence of 1.0 μM $^{15}NH_4^+$ were three times lower than the rate of ammonia oxidation suggesting that either nitrite oxidation was decoupled from ammonia oxidation or that anammox or denitrification occurred under the conditions of this experiment and led to loss of nitrogen as N_2. Although it is impossible to distinguish these processes from these results, sponges are known to modulate their pumping rates in response to environmental conditions (Reiswig 1971). Anoxic zones within sponges can temporarily form in sponges (Fiore et al. 2010), potentially facilitating denitrification or decreasing rates of nitrite oxidation mediated by their aerobic symbiotic prokaryotes. Nitrogen cycling in sponges is likely complex. I speculate that the lower NH_4^+ concentrations in excurrent water relative to ambient with little change in $NO_3^- + NO_2^-$ concentrations in the same samples

(see below) reflects this complexity. The lack of change in $NO_3^- + NO_2^-$ concentrations in excurrent versus ambient samples where there was a clear decrease in ammonium concentrations is most likely due to ammonia assimilation (Kirchman 1994, Kirchman et al. 1998) by associated bacteria or may also partially reflect a decoupling of ammonia and nitrite oxidation (e.g., Beman et al. 2013) or could indicate N_2 formation from anaerobic processes (Mohamed et al. 2010, Fiore et al. 2013). Heterotrophic bacteria can account for a large fraction of ammonium uptake in marine environments (Kirchman 1994), although the rate of ammonium uptake varies with bacterial assemblages within an environment, substrate availability, and C:N ratios required to support bacterial production (Kirchman 1998). Further research including measuring rates of nitrite oxidation and N_2 formation would be helpful in distinguishing the importance of these processes.

Excurrent versus ambient reef water nutrient profile

Uptake of ammonium by the sponge microbiome was evidenced by the depletion of ammonium in the exhalent relative to the surrounding seawater concentrations. The change in DIN across the samples along with the $^{15}NH_4^+$ incubation experiments indicate that the sponge serves as a sink for NH_4^+, supporting the hypothesis that the sponge holobiont is removing reduced N and adding oxidized N to seawater as it passes through the sponge. Kāneʻohe Bay is characterized by high ammonia levels for a coral reef (up to 4.38 μM) (Drupp et al. 2011) and averaged 3.9 μM in south Kāneʻohe Bay measured at the time of the experiments. Sponges likely pump water as much for food and substrate acquisition as for removing metabolic wastes. Observed ammonia oxidation rates suggest that an efficient coupling between ammonia waste production by the sponge and subsequent ammonia and nitrite oxidation could exist, a mechanism by which

harmful ammonia is converted to NO_2^- (slightly less toxic than NH_3) and NO_3^- (mildly toxic) that can be further used as microbial substrates or subsequently pumped away.

The wide variety of microbial symbionts found in sponges benefit the host in an array of ways including maintaining favorable nutrition, metabolic waste removal, and other functions such as the exchange of primary metabolites contributing to nutrition, and the production of secondary metabolites for chemical defense purposes. Indeed sponges use both vertical (Schmitt et al. 2007, Sharp et al. 2007) and horizontal transmission strategies (Taylor et al. 2007, Schmitt et al. 2008, Webster et al. 2010) to maintain their complex and diverse microbial communities.

Microbial phylotypes found in *M. grandis* are related to eight phyla: *Proteobacteria* (classes *Alpha-, Beta-, Delta- and Gammaproteobacteria*), *Bacteroidetes*, *Actinobacteria*, *Cyanobacteria*, *Firmicutes*, *Chloroflexi*, *Acidobacteria,* and *Crenarchaeota* (Wang et al. 2009). *Thaumarchaeota* (previously *Crenarchaeota*) are recognized to be ammonia oxidizers in the marine environment (Francis et al. 2008), including the marine ammonia oxidizer *Nitrosopumilus maritimus*. The associated microbial community of sponges has been found to be quite stable through space and time, with minimal or no temporal variability (Taylor et al. 2007). The case for bacterially driven ammonia oxidation in sponges is supported by natural abundance isotopic fractionation observed for nitrification (Southwell et al. 2008a), although more recent research points to the significance of archaea as responsible for driving ammonia oxidation in the ocean (Beman et al. 2008, Santoro and Casciotti 2011). The proportion of bacteria relative to archaea-driven processes which otherwise produce the same biogeochemical products may be identified by differences in coupled biogeochemical transformations, carbon fixation

mechanisms, competitive availability, environmental sensitivity (e.g. light inhibition), and isotopic fractionation (Southwell et al. 2008a).

Volume-normalized flux ammonia oxidation rates calculated from NH_4^+ drawdown the in excurrent versus ambient samples (14.6 to 58.6 μmol h^{-1} L^{-1}) were much higher compared to volume-normalized ammonia oxidation rates determined from the conversion of $^{15}NH_4^+$ to $^{15}N+^{15}N$ in the $^{15}NH_4^+$ oxidation incubations (0.7 to 8.0 μmol h^{-1} L^{-1}). The higher rate determined from the drawdown of NH_4^+ in the excurrent versus ambient samples supported by the lack of significant difference in N+N in the excurrent versus ambient samples suggests that ammonia assimilation by chemolithoautotrophs (Zerh and Ward 2002) within the sponge is occurring, and that some N+N resulting from nitrification may also undergo N loss processes through coupling of nitrification to denitrification processes in the sponge. The presence of *P. denitrificans*-like phylotypes were identified in *M. grandis* (Wang et al. 2009) and merits the investigation of whether *M. grandis* hosts microbially-mediated nitrogen loss processes. This could also partially explain the lower rate of ammonia oxidation measured in the $^{15}NH_4^+$ incubations if some of the label is further incorporated into N loss processes, although this effect would likely be insignificant. If denitrification were occurring during the $^{15}NH_4^+$ incubations, it would not have been observed because of the high ^{15}N activity in NH_4^+ even though the isotope fractionation observed for denitrification is reasonably high (ε = 28.6‰ in *P. denitrificans)* (Barford et al. 1999), but that isotope fractionation is small relative to the amount of ^{15}N label in the experiments. Therefore the atom % ^{15}N of NO_3^- + NO_2^- throughout the time series is likely representative of the rate of ammonia oxidation.

The lower rates observed in the $^{15}NH_4^+$ incubations may have been in part due to isotope dilution effect. Isotope dilution effect is due to the *in vitro* regeneration of the substrate (in this case, regenerated ammonium by the sponge) being measured and could increase the unlabeled NH_4^+ pool (Harrison and Harris 1986, Kanda et al. 1987). In $^{15}NH_4^+$ tracer experiments, the isotope enrichment of ammonium can change significantly as the incubation proceeds, confounding the precise determination of ^{15}N content in the substrate. While isotope dilution effect can be corrected for or minimized by increasing the ^{15}N activity of the substrate, regeneration rates from the sponge would be difficult to ascertain due to coupled nitrogen cycling processes. Conventional calculations that do not take isotope dilution into account would result in an underestimate of the true ammonia oxidation rates. However, effects are strongest in longer incubations and lower substrate concentrations (Harrison and Harris 1986, Kanda et al. 1987). These incubations were kept to four hours and did not exhibit a drop-off in the accumulation of ^{15}N in the N+N pool. Paradoxically, incubations using higher concentrations of $^{15}NH_4^+$ (5 μM $^{15}NH_4^+$ added incubations) resulted in lower ammonia oxidation rates compared to incubations in the presence of 1 μM $^{15}NH_4^+$, which yielded the highest ammonia oxidation rates, which does not align with this rationale. It is possible that NH_4^+ concentrations of 5 μM were slightly toxic to the microbes. Variable concentrations of ammonium in the Kāneʻohe Bay on the different days these incubations were performed may also lead to different ammonium oxidation rates, i.e. if ambient [NH_4^+] was 1 μM, an addition of 5 μM $^{15}NH_4^+$ would make the total [NH_4^+] ($^{14}NH_4^+$ + $^{15}NH_4^+$) 6 μM, which is still within the range of typical ammonium concentrations found in the bay. However, if ambient [NH_4^+] on the day of incubations was 10 μM, an addition of 5 μM $^{15}NH_4^+$ would drive the total [NH_4^+] to 15 μM which could approach toxic levels for the sponge organism. Indeed some incubations with 5 μM $^{15}NH_4^+$ added yielded good results, while other

incubations at the same added concentration repeated on different days did not yield viable data. The samples at the beginning of those experiments (t_0 and t = 30 min) yielded peaks that were too small for reliable isotope measurement, but the later time incorporated too much label and greatly exceeded the linear range of the detector of the mass spectrometer used, indicating that a higher rate of ammonia oxidation could be occurring during these incubations. Differences in ammonia oxidation rates may also be due to temporal variations of ammonia oxidation performed by the sponge in response to nutrient concentrations or metabolic needs which could also explain the discrepancy in ammonia oxidation rates determined from $^{15}NH_4^+$ incubations versus the higher rates determined from the difference in $[NH_4^+]$ in ambient versus excurrent samples. Also, while $^{15}NH_4^+$ incubations are incontrovertible evidence that ammonia oxidation is occurring, the ambient versus excurrent samples were drawn from unperturbed sponges under natural nutrient concentrations albeit growing under non-natural conditions in an aquarium with flowing seawater.

In previous studies, sponges that belong to the HMA group were observed to excrete NO_3^- whereas sponges of the LMA group do not excrete N+N, or excretions were at much reduced rates (Jiménez and Ribes 2007, Yahel et al. 2007, Bayer et al. 2007), supporting the hypothesis that *M. grandis* is an LMA. However, the low pumping rates and active oxidation of ammonia imply that *M. grandis* may be an HMA sponge, though the density of associated microbes would have to be confirmed through enumeration methods such as through cell counts using electron microscopy.

Conclusion

Sponges rely on their ability to regulate seawater pumping and to facilitate biogeochemical processes in response to environmental variables, such as to changes in nutrient loads and metabolic needs. Despite lower pumping rates and less significant biomass compared to large barrel sponges on reefs in the Caribbean, *M. grandis* plays a proportionally significant biogeochemical role within Kāneʻohe Bay and potentially other Hawaiʻi coral reef ecosystems because of its shallow water habitat. *M. grandis* has also proven to be a pervasive and adaptable alien invasive species. These are the first measurements of pumping rates and ammonia oxidation in the sponge *Mycale grandis*. Ammonia oxidation rates calculated using $^{15}NH_4^+$ tracer experiments were commonly lower than in the comparison of $[NH_4^+]$ in excurrent water versus ambient seawater suggesting either that ammonia oxidation was decoupled from nitrite oxidation or there was loss of nitrogen as N_2 either through denitrification or anammox or there was ammonia assimilation. Regardless, the flux of $NO_3^- + NO_2^-$ from *M. grandis* was the most significant benthic source of biologically available nitrogen in the environments studied.

The vulnerability to invasive reef species in Hawaiʻi coupled with the threats of increased anthropogenic activity, ocean acidification, and ocean warming have growing implications for the native ecosystem within Kāneʻohe Bay. It is evident that where sponges are abundant members of the reef community, they can play an important role in organic matter recycling and altering nutrient profiles within the water column. A further increase in the abundance of invasive sponges such as *M. grandis* could result in concomitant changes to delicate balances on Hawaiian reefs, leading to or strengthening phase shifts. *M. grandis* may further directly or indirectly shape community structure through its feeding behaviors and relationship to other

organisms within the environment. These first results indicate that *M. grandis* has the potential to impact ecosystem balance through biogeochemical cycling on coral reefs in the Pacific.

CHAPTER 4:

Trophic estimates and insights into the dietary strategy between the tropical Pacific sponge Mycale grandis *and its microbial symbionts using compound specific isotopic analysis*

Abstract

Many sponges host abundant and active microbial communities and are known to rely on them for nutrition. An increasing number of sponges have been identified to feed on dissolved organic matter (DOM), in particular of algal and coral origin, although the mechanism of DOM uptake in sponges is not well described. Bulk and compound specific isotopic analysis of whole sponge, isolated sponge cell, and isolated symbiotic microbial cells of the shallow water tropical Pacific sponge *Mycale grandis* were used to elucidate the dietary relationship between the host sponge and its associated microbial community. δ^{15}N and δ^{13}C values of the majority of amino acids in *M. grandis* isolated sponge cells are not different from those of its bacterial symbionts, and hence there is no difference in trophic position calculated from the difference in the δ^{15}N values of glutamic acid and phenylalanine or from the differences in the average or weighted average δ^{15}N values of trophic and source amino acids, which are a proxy of trophic position. These observations indicate that *M. grandis* sponge cell isolates do not display amino acid isotopic characteristics typical of metazoan feeding but rather are consistent with some phagotrophic protists. Furthermore, both the isolated microbial and sponge cell fractions were characterized by a similarly high ΣV value, calculated from the sum of variance among individual δ^{15}N values of trophic amino acids and is a measure of bacterial resynthesis of organic matter. These high ΣV values observed in the sponge suggests that *M. grandis* is not reliant on nutrition from photosymbionts nor through feeding on water column phytoplankton but through uptake of amino acids of bacterial origin. Presently, the specific fraction(s) of DOM utilized by sponges have not been identified. These results suggest that direct assimilation of bacterially-synthesized amino acids from its symbionts either in a manner similar to translocation observed in the coral

holobiont or through phagotrophic feeding is an important if not primary pathway of amino acid acquisition for *M. grandis*. Sponge-associated bacteria may also serve as an intermediary for the assimilation of photosynthates of photosymbionts and algae and for DOM of coral origin that are then passed on from bacterial symbiont to sponge.

Introduction

Sponges are ubiquitous members of benthic coral reef communities and many species are known to host diverse and active symbiotic microbial communities. Sponges are essential to sustaining high productivity on oligotrophic coral reefs through their rapid uptake of dissolved organic matter (DOM) and subsequent shedding of particulate organic matter, driving an efficient transfer of DOM to higher trophic levels (de Goeij et al. 2013). The mechanisms by which DOM is assimilated and transferred by the sponge is not well known but is thought to be facilitated by a close symbiosis between sponges and their microbial communities (Hoer et al. 2017). This symbiosis is amongst the most ancient of metazoan symbioses (Wilkinson 1984) and is likely often of mutualistic and fundamental importance as even distantly related sponges from geographically disparate regions share a common set of associated microbes, some of which are unique to sponges and cannot be acquired from the surrounding environment (Hentschel 2002, 2006).

Many of these sponge-microbial associations are assumed to be mutually beneficial in which the symbiont is provided with a substrate-rich sheltered environment and in exchange the sponge is provided with products of microbial metabolism. On coral reefs, the essential mutualism between corals and their dinoflagellate *Symbiodinium* has been extensively studied and it has been shown

that some reef building coral cannot grow or compete for substrates on the reef in the extended absence of their symbionts (Muscatine 1969 and 1989). Some of the symbioses in marine sponges may serve a similar function. Sponges often host microbial communities that are capable of photo- and chemoautotrophic carbon fixation and nitrogen transformation processes such as nitrification, nitrogen fixation, denitrification, and anammox (Wilkinson 1979, Hoffmann et al. 2006, 2009, Southwell et al. 2008a and b, Mohamed et al. 2010, Fiore et al. 2013). Microbially-mediated nitrification is confirmed in the invasive sponge *Mycale grandis* (Shih, this volume, Chapter 3), which is found in Kāneʻohe Bay and other partially degraded coral reef habitats around the main Hawaiian Islands, and there is evidence to suggest that other microbially-mediated processes such as denitrification may also occur in the sponge. Sponge associated symbionts most likely also contribute to sponge nutrition (Weisz et al. 2007), and some sponge symbionts can produce secondary metabolites that are believed to be provided to their hosts that function as chemical defense (Kennedy et al. 2007, Siegl and Hentschel 2010, Thomas et al. 2010).

Though sponges are known to acquire carbon through heterotrophic filter feeding, some sponges can obtain half of the energy budget and more than half of their carbon budget from their photosymbionts (Wilkinson 1983). It is proposed that symbiont supplied nutrition is essential to some Caribbean sponge hosts (Erwin and Thacker 2008) and widely in Indo-Pacific sponges (Wilkinson 1987). Several studies have established that a transfer of carbon and nitrogen from microbial symbionts to sponge hosts occurs (de Goeij et al. 2008b, Freeman and Thacker 2011, Freeman et al. 2013, Rix et al. 2016, Rix et al. 2017, Hoer et al. 2017), although the exact mechanism by which these nutrients are transferred is not currently known and direct evidence of

such nutrient transfer is yet to be confirmed. An increasing number of sponges have been identified to feed on dissolved organic matter (DOM), with DOM accounting for up to 90% of the diet of some sponges (Mueller et al. 2014, de Goeij et al. 2008b, Hoer et al. 2017). In fact, while Caribbean sponge species are primarily observed to derive much of their required metabolic C through heterotrophic feeding, Indo-Pacific species have been observed to rely heavily on photoautotrophy (Wilkinson 1983, Wilkinson 1987).

On reefs, sponges are primarily responsible for total DOM uptake and remove the same amount of DOM from the water column in 30 minutes as free-living bacteria take up in 30 days (de Goeij et al. 2007, de Goeij et al. 2009). Sponges subsequently transform a substantial fraction of this DOM into particulate organic matter (POM), primarily as rapidly shedding choanocyte cells. This sponge detritus is then available to a variety of benthic detritivores. Therefore, sponges retain organic matter within the reef community and thereby prevent energy and nutrient losses to the open ocean (de Goeij et al. 2013).

The underlying mechanisms of DOM uptake and rapid cell turnover in sponges are not yet fully understood. The close associations between sponges and their microorganisms form a so-called holobiont, and studies using ^{13}C labeled DOM have shown ^{13}C uptake by sponge cells and microbes (Rix et al. 2017), although the pathways of acquisition of DOM and their relative contributions remain largely unknown and are expected to vary across species. Sponge cells are likely predominantly capable of taking up larger colloidal material in DOM such as viruses and free amino acids while bacteria can assimilate the smaller, truly dissolved fraction of DOM (Yahel et al. 2003, de Goeij et al. 2008a, b).

Here I suggest that the means of transferring nutrition from microbial symbiont to sponge is through uptake of amino acids synthesized by its symbiotic bacteria, and that specifically, bacterially-produced amino acids are a major substrate by which carbon and nitrogen is transferred from microbial symbiont to the sponge. This efficiency of the mechanism of transfer is benefitted by the high concentrations of microbial communities hosted within their mesohyl.

Studies on the Caribbean sponge *Xestospongia muta* have been performed using uptake rates of dissolved oxygen (respiration demand) and rates of removal of dissolved organic carbon (DOC), showing that DOC from the water column is used by the entire sponge holobiont to fuel respiration (Hoer et al. 2017). Other studies sought to investigate specific sources of DOM to the sponge. De Goeij et al. (2008b) used ^{13}C enriched diatom DOM and POM to positively demonstrate that algae derived DOM was assimilated by the sponge and furthermore shed as sponge cells as POM that was then consumed by other reef fauna at higher trophic levels. Rix et al. (2016) used ^{13}C and ^{15}N labeled warm and cold water coral mucus DOM as food sources for a warm water Red Sea sponge and a North Atlantic cold water sponge respectively, and demonstrated assimilation of coral mucus into sponge tissue and subsequent sponge-derived POM. Through observing the assimilation of coral mucus C into sponge phospholipid-derived fatty acids (PLFAs) synthesized *de novo* or by modification of coral-derived PLFAs, they demonstrated that sponges actively process coral mucus similarly to algal and bacterial food sources, confirming its viability as a nutritional source. Rix et al. (2017) used ^{13}C and ^{15}N enriched coral and algal derived DOM to compare uptake by Red Sea coral reef sponges of the two sources and demonstrated that both coral and algal derived DOM were assimilated. However, the two DOM sources were processed differently, with algal derived DOM being

incorporated into bacteria-specific PLFAs at a higher rate while coral derived DOM was preferentially incorporated into sponge-specific PLFAs. Both DOC and DON from the two sources were shown to be assimilated by the sponge and subsequently released as sponge-derived POM, however, algal-derived DOM was released as sponge cell detritus as a higher rate.

The main producers of DOM on coral reefs are primary producers, particularly the algal symbionts in scleractinian corals and macroalgae, which release a substantial fraction of their excess photosynthates into the water column（Wild et al. 2004). However, since some sponges can harbor concentrations of bacteria over 10^9 microbial cells g^{-1} of sponge wet weight (Hentschel et al. 2006), I hypothesize that bacterially-derived DOM is also a significant source of dissolved organic matter to sponges.

The study of a diverse and complex consortia of symbionts within sponges is challenging because multiple functions and interactions can take place simultaneously and it is difficult to resolve the specific roles and contribution of these symbionts. Here I use stable carbon and nitrogen isotope analyses of whole sponge, sponge cell and microbial cell fractions as well as isotopic analyses of individual amino acids in the cell fractions to elucidate the dietary pathways of *M. grandis* nutrition.

Stable N isotopic composition (δ^{15}N values) has been widely used in ecosystem research based on the consistent increase in $^{15}N/^{14}N$ ratios from food source to consumer. Bulk sample δ^{15}N measurements have been used in earlier studies of marine food webs as an indicator of relative trophic position (Peterson and Fry 1987, Lajtha and Michener 1994), however key dietary details

can be limited due to multiple factors influencing bulk tissue δ^{15}N values including mainly differences in baseline values and questions regarding trophic levels of organisms. Compound specific isotopic measurements can be used to address some of these challenges. δ^{15}N values of individual amino acids allows for determination of trophic positions (TP) based on the differential fractionation of amino acids during trophic transfer. In samples of consumer tissues, "source" amino acids retain the isotopic composition of nitrogen sources at the base of the food web, whereas "trophic" amino acids are greatly enriched in ^{15}N with each trophic transfer (Chikaraishi et al. 2009, McClelland and Montoya 2002, Popp et al. 2007, Bradley et al. 2014). The amino acid compound specific isotopic analysis (AA-CSIA) approach can generally be attributed to the fact that the nitrogen isotopic composition of an individual AA reflects the degree of isotopic fractionation associated with various biochemical reactions that involve C-N bond breakage (i.e. deamination and transamination) in individual AA involved in nitrogen metabolism, although the exact mechanisms are complex (O'Connell 2017, Fuller and Petzke 2017). The δ^{15}N value of an organism also inherently reflects the isotopic composition of inorganic nitrogen sources (e.g. nitrate, nitrite, ammonia, and urea) assimilated by primary producers at the base of the food web, but since source amino acids retain δ^{15}N values at the base of the food web, results of AA-CSIA can provide information about nitrogen metabolism, constrain trophic position, identify the source and transformation of dissolved and detrital organic matter in marine waters and sediments (McCarthy et al. 2007, Calleja et al. 2013, Hannides et al. 2013), and can provide location and migration patterns of a consumer (Dale et al. 2011).

The mechanisms of organic matter assimilation by sponges are still not well known but is thought to involve the close symbiosis between sponges and the microbial communities they host. While the suite of functional roles of the microbial community of *M. grandis* is not known, *M. grandis* has been shown to host active autotrophic nitrifying microorganisms. Previous studies on *M. grandis* show it hosts a wide variety of other associated microbial phylotypes (Wang et al. 2009). One central question is whether *M. grandis* obtains carbon and nitrogen from their microbial symbionts in addition to or instead of through heterotrophic filter feeding. Bulk and compound specific isotopic analysis of nitrogen and carbon can reveal key dietary details of sponge nutrition and nutrient acquisition. To investigate possible transfer of carbon and nitrogen from microbes to *M. grandis*, microbial cells and sponge cells were isolated from whole sponge samples prior to isotopic analysis.

I propose that *M. grandis* derives a major part of its nutrition directly from amino acids produced by its microbial symbionts. *M. grandis* hosts a diverse microbial community (Wang et al. 2009) and is demonstrated to at least host microbially-mediated nitrogen cycling. The results of this work provide support for the hypothesis that the means of transferring carbon and nitrogen of symbiont-driven nutrition to *M. grandis* is through direct assimilation of amino acids derived from their associated microbial communities.

Methods

Sampling locations

Kāneʻohe Bay on the northeast coast of Oʻahu is characterized by an extensive system of stony coral fringing reefs, patch reefs, and a large barrier reef. Sponge samples for bulk tissue isotopic

analysis were collected from two patch reefs just northwest of Coconut Island (21°26'07.5"N 157°47'43.9"W) in the southern portion of Kāneʻohe Bay (n = 34), from a patch reef in mid Kāneʻohe Bay (21°27'37.5"N 157°49'19.7"W) (n = 10), and from a patch reef in the northern portion of Kāneʻohe Bay (21°28'37.6"N 157°49'54.7"W) (n = 10) in the spring of 2015. Sponge samples for bulk and compound specific isotopic analysis of isolated cell fractions (n = 8) were collected from approximately 1 m depth from the fringing reef located beneath the Lilipuna Pier in south Kāneʻohe Bay (21°25'46.0"N 157°47'31.2"W) in the spring of 2017. Sponge specimens were inclusive of surface pinacoderm, inner mesohyl, and choanocyte chambers. Visible debris and epiphytes were removed from the surface of the samples. Specimens from north, mid, and south Kāneʻohe Bay collected for bulk isotopic analysis were immediately frozen at -80°C and stored until analysis. Whole sponge samples for epi-fluorescence microscopy were collected from under the Lilipuna Pier, rinsed with filtered seawater, and preserved in 1% paraformaldehyde.

Separation of microbial cells and sponge cells from sponge tissue

Separate analyses of isolated sponge cell and symbiotic microbial cells can reveal information about the relationship and mechanism of nutrient transfer between symbionts and the sponge host. Sponge and microbial cells of *M. grandis* were separated through size fractionation using the methods described in Freeman and Thacker (2011 and 2013) with the following modifications: Samples were homogenized with mortar and pestle for 3 minutes to dissociate the sponge cells and vacuum filtered (Whatman No. 4 filter, 20-25 µm nominal pore size). The resulting filtrate was centrifuged (430 x *g*) for 6 minutes to form a sponge cell pellet for *M. grandis*. The supernatant containing microbial cells was decanted and stored at 4ºC. The pellet

was then resuspended and centrifuged (770 x g) for 5 minutes at 4ºC. The supernatant was discarded and this rinse step was repeated twice, resuspending the pellet between each rinse. The pellet was then resuspended, transferred into a microcentrifuge tube and centrifuged (3900 x g) for 2 minutes. This additional rinse step was repeated twice and the isolated sponge cell pellet was stored frozen at -20ºC for future analysis.

To isolate the microbial cell fraction, the previously frozen supernatant containing the microbial fraction was thawed and centrifuged (17,000 x g) for 17 minutes at 4ºC. The supernatant was decanted, the pellet was resuspended, and the centrifuge step was repeated. The pellet was resuspended and transferred to a 1.5 mL centrifuge tube and the microbial cell fraction centrifuged 12,800 x g for 2 minutes, and the supernatant was carefully removed and discarded. The resulting microbial pellet was rinsed twice using the same procedure and the remaining pellet was frozen at -20C until analysis. Good separation of the fractions was confirmed through flow cytometry and significant differences in bulk isotopic composition and C:N ratios, described in detail in the discussion sections below.

Flow cytometry

A small volume (40 µL) of the separated sponge cell and microbial cell fractions were fixed in paraformaldehyde to a final concentration of 1% in preparation for flow cytometry analysis (FCM). Frozen samples were transported to the University of Hawai‘i at Mānoa on ice and stored at -80°C until analysis. Samples were thawed and diluted with 800 µl of filtered seawater (FSW) and stained with Hoechst 33342 (to 1 µg/mL final concentration) for 1 hour in the dark and analyzed using the methods outlined in Selph et al. (2011). Microbial samples were run at

~700 V. The sponge cell fractions were run at low voltage settings (~400 V). Microbial cells were below the limit of detection for this instrument at this setting, indicating that smaller bacteria and phytoplankton were effectively removed by sample processing.

Cell abundances within samples were estimated using FCM enumeration. Aliquots of 100 µL were analyzed for *Synechococcus* (SYN), photosynthentic eukaryotes (P-Euk), and non-pigmented bacterial (HBACT) abundances using a Beckman Coulter EPICS Altra flow cytometer with a Harvard Apparatus syringe pump for volumetric sample delivery. Simultaneous (co-linear) excitation of the plankton was provided by two water-cooled 5-W argon ion lasers, tuned to 488 nm (1 W) and the UV range (200 mW). Discrete populations were enumerated on the basis of chlorophyll *a* (red fluorescence, 680 nm), phycoerythrin (orange fluorescence, 575 nm), DNA (blue fluorescence, 450 nm), forward scatter, and right-angle scatter signatures. Calibration beads (0.5- and 1.0-mm yellow-green beads and 0.5-mm UV beads) were used as fluorescence standards. Listmode files were processed using the FlowJo software (Treestar Inc., www.flowjo.com).

Subtraction of picoplankton containing chl *a* from the total prokaryotes yielded the non-pigmented bacterial fraction of the community while cyanobacterial cells were identified by the presence of phycoerythrin fluorescence. Cell counts were converted to carbon contribution for each fraction assuming carbon cell quota of 30 fg cell^{-1} for bacteria (Fukuda et al. 1998), 200 fg cell^{-1} for *Synechococcus* and other picophytoplankton, 800 fg cell^{-1} for nanophytoplankton (Garrison et al. 2000), and 3 pg cell^{-1} for sponge cells (de Goeij et al. 2009).

Bulk sponge and cell isotope analysis

The $\delta^{13}C$ and $\delta^{15}N$ values of lyophilized bulk sponge tissue (1.7-2.1 mg), isolated sponge (0.2-0.3 mg) and microbial cells (0.3-0.4 mg) were determined using a Costech elemental combustion system (Model 4010) coupled to a ThermoFinnigan Delta Plus XP Isotope Ratio Mass Spectrometer (IRMS) through a Conflo IV interface, and are reported in standard δ-notation relative to V-PDB and atmospheric N_2, respectively. Accuracy and precision were <0.2‰, as determined from multiple laboratory reference materials extensively calibrated using National Institute of Science and Technology reference materials and analyzed every 10 samples.

Preparation of samples for amino acid isotope analysis

Isolated sponge and microbial cells were prepared for compound-specific amino acid (AA) $\delta^{13}C$ and $\delta^{15}N$ analysis (AA-CSIA). Due to insufficient materials, cell fractions isolated from separate sponges (8 starting in total) had to be grouped prior to analysis. Microbial fractions for sponges 1 and 3 were combined, as were the sponge cell fractions. For sponges 4, 6 and 7 sufficient materials were available for AA-CSIA of microbial cell fractions for each sponge, however these three sponge cell isolates were combined for $\delta^{13}C$ and $\delta^{15}N$ analysis.

Samples for AA-CSIA were hydrolyzed and trifluoroacetyl/isopropyl ester derivatives created according to the methods of Popp et al. (2007) and Hannides et al. (2009). For preparation of trifluoroacetyl/isopropyl ester derivatives, 4 - 11 mg were hydrolyzed using trace-metal grade 6M HCl and the hydrolysate purified using low protein-binding filters and cation exchange chromatography. Purified samples were esterified using 4:1 isopropanol:acetyl chloride and derivatized using 3:1 methylene chloride:trifluoroacetyl anhydride. Finally,

trifluoroacetyl/isopropyl ester derivatives were purified using solvent extraction (Ueda et al. 1989) and stored at -20°C for up to two weeks before analysis. Samples were prepared with an additional vial containing a mixture of 15 pure AAs purchased commercially (Sigma Scientific).

Nitrogen isotope analysis of amino acids

The $\delta^{15}N$ values of trifluoroacetyl/isopropyl ester derivatives of AAs were determined using gas chromatography combustion isotope ratio mass spectrometry (GC-C-IRMS, Hayes et al. 1990). Specifically, I used an isotope ratio mass spectrometer (IRMS; Thermo Scientific Delta V or MAT 253) interfaced to a gas chromatograph (GC; Thermo Scientific Trace) fitted with a 60 m BPX5 *forte* column (0.32 mm internal diameter with 1.0 μm film thickness; SGE, Inc.) through a GC-C III combustion furnace (980°C), reduction furnace (650°C), and liquid nitrogen cold trap. Helium (1.2 mL min^{-1}) was used as the carrier gas. Immediately before analysis, samples were dried and redissolved in an appropriate volume of ethyl acetate. The analysis consisted of at least 3 injections for each sample, with norleucine and aminoadipic acid internal reference compounds co-injected in each run. The suite of 15 pure amino acids was also analyzed every 3 injections to provide an additional measure of instrument accuracy. The isotopic composition of all pure amino acid reference compounds were previously measured using the bulk isotope technique described above. Nitrogen isotope values are reported in standard δ-notation relative to atmospheric N_2. For replicate injections of samples, amino acid $\delta^{15}N$ standard deviations averaged 0.46‰ and ranged from 0.12‰ to 0.99‰. Uncertainty in calculations of trophic position was determined using propagation of errors and include all analytical errors and the uncertainty in the constants used (Bradley et al. 2015, Jarman et al. 2017).

Carbon isotope analysis of amino acids

$\delta^{13}C$ values of individual amino acids were also determined using GC-C-IRMS. The $\delta^{13}C$ values of trifluoroacetyl/isopropyl ester derivatives were determined using an IRMS (MAT 253) interfaced with a Trace GC Ultra via a combustion furnace (1000°C) and ConFlo IV interface (Thermo Scientific). Samples were injected using a PTV (pressure/temperature/volume) injector, held at 40°C for three seconds, heated to 87°C (400°C min^{-1}), heated again to 200°C and transferred at 200°C using a 1:10 split. Helium (1 mL min^{-1}) was used as the carrier gas. Individual AAs were separated using a BPX5 *forte* capillary column (30 m x 0.32 mm internal diameter with 1.0 μm film thickness; SGE, Inc.). The oven temperature for the GC started at 40°C and was held for one minute before heating at 15°C min^{-1} to 120°C, then 3°C min^{-1} to 190°C, and finally 5°C min^{-1} to 300°C where it was held for an additional 10 min. Isotope values are reported in standard δ-notation relative to V-PDB. Analysis consisted of at least 3 injections per sample with a perdeuterated *n*-C_{20} alkane with a well-characterized $\delta^{13}C$ value co-injected as an internal reference. The 15 AA reference suite was analyzed every 3 injections, and sample $\delta^{13}C_{AA}$ values corrected relative to this AA suite following Silfer et al. (1991). For statistical analysis, I compared our $\delta^{13}C_{AA}$ values to those previously published by Larsen et al. (2009, 2012, 2013). To account for inter-laboratory differences, I used results of previous extensive inter-calibrations (see Arthur et al. 2014, Gómez et al. 2018).

Trophic proxy and trophic level

A proxy for trophic level was also determined using the difference in averaged $\delta^{15}N$ values between trophic (Ala, Leu, Glx) and source amino acids (Phe, Lys). A second trophic level proxy

was also calculated using weighted mean $\delta^{15}N$ values of trophic (Ala, Leu, Glx) and source amino acids (Phe, Lys) using:

$$\delta^{15}N_{\bar{x}_w} = \frac{\sum \frac{\delta^{15}N_x}{\sigma_x^2}}{\sum \frac{1}{\sigma_x^2}}, \quad \text{(Equation 4.1)}$$

(Hayes et al. 1990, Bradley et al. 2015),

where $\delta^{15}N_x$ is the nitrogen isotopic composition of a specified AA within the grouping and σ_x is the standard deviation in $\delta^{15}N$ value of that specific AA determined by triplicate isotopic measurements (Equation 4.1) (Hayes et al. 1990). Errors for proxy trophic level calculations were propagated using the measured reproducibility of individual AA in at least triplicate.

Trophic level was estimated using the difference in $\delta^{15}N$ values between the trophic amino acid glutamic acid (Glx) and the source amino acid phenylalanine (Phe), assuming a β value of 3.4‰ for the difference in $\delta^{15}N$ values between Glx and Phe in primary producers and assuming that Glx was enriched in ^{15}N relative to Phe (Δ value) of 7.6‰ with each trophic transfer, e.g.: TP = (($\delta^{15}N_{glx}$ - $\delta^{15}N_{phe}$ - 3.4) / 7.6) + 1 (Chikaraishi et al. 2009). The error in this TP calculation was propagated assuming the uncertainty in β value is ±0.9‰ and the error in Δ is ±1.1‰ and using the measured analytical uncertainty in $\delta^{15}N_{Glx}$ and $\delta^{15}N_{Phe}$ based on at least triplicate analyses (see equations in Jarman et al. 2017).

Summed variance in $\delta^{15}N$ values of trophic amino acids (ΣV)

McCarthy et al. (2007) introduced an index for microbial resynthesis of amino acids: ΣV, which is the sum of variance among individual $\delta^{15}N$ values of trophic amino acids (Equation 4.2). I

calculated ΣV for isolated sponge cell and microbial cell fractions using $\delta^{15}N$ values of alanine, leucine, proline, aspartic acid and glutamic acid using

$$\Sigma V = \frac{1}{n} \Sigma \text{ Abs } |\chi i| \quad \text{(Equation 4.2)}$$

where χ_i is the deviation of $\delta^{15}N$ values of each individual amino acid from the average value of all of the trophic amino acids in a sample = [$\delta^{15}N_i$ - AVG $\delta^{15}N_i$], and *n* is the number of amino acids used in the calculation.

Results

Flow cytometry

The population abundances of cell types found within the separated sponge (host) and microbial (symbiont) fractions are reported in Tables 4.1 and 4.2. All flow cytometry count event images for isolated sponge cell and microbial cell fractions can be found in the Appendix (Figure A.1). There were substantially more (*ca.* 8x) sponge cells present than residual phytoplankton or bacterial cells in the sponge cell fractions. "HiDNA" cells within the sponge fraction are sponge cells containing very high chlorophyll signature and high phycoerythrin signal (PMT 3) and are most likely sponge cells with phytoplankton prey within them. "LowChl" cells indicate sponge cells without prey in them.

Sponge cell fractions contained a mean of 6 x 10^3 sponge cells per gram wet weight of starting sample (range 1.4 x 10^3 to 1.2 x 10^5 cells g^{-1}, *n*=8) (Table 4.1.). Of the sponge cells, hiDNA cell

counts ranged between 4 x 10^2 and 3.9 x 10^3 cells g^{-1} and lowChl cell counts ranged from 1.0 x 10^3 and 8.2 x 10^3 cells g^{-1}. Possible residual microbial sample cell count contained a mean of 9.8 x 10^2 cells g^{-1} wet weight starting sample, (range 2.5 x 10^2 to 2.1 x 10^3 cells g^{-1}), with subsets of "lowChl/LowSS" (smaller phytoplankton and bacterial cells) counts ranging from 49 to 1.2 x 10^3 cells g^{-1} and "lowDNA" (photosynthetic eukaryotes) cell counts ranging from 1.9 x 10^2 to 1 x 10^3 cells g^{-1}. Using carbon per cell contributions for sponge cells (de Goeij et al. 2009) and for picophytoplankton, nanoplankton, and microplankton (Verity et al. 1992, Garrison et al. 2000, Menden-Deuer and Lessard 2000), the carbon contribution of sponge cells carbon to the "sponge" fraction ranged from 85% to 98% and averaged 94 ± 4%, and residual microbial cells carbon contribution to the "sponge" fraction ranged from 1.8% to 15% and averaged 6.3 ± 4% (See Figure 4.1).

Sample	hiDNA g^{-1}	lowChl g^{-1}	Tot. sponge cells g^{-1}	lowChl/LowSS g^{-1}	lowDNA g^{-1}	Residual microbial cells
1	1124	1762	2887	242	453	695
2	409	995	1404	49	199	249
3	871	2201	3072	429	1005	1435
4	3238	4037	7275	492	189	681
5	1045	2969	4014	442	531	973
6	3908	8147	12055	1218	868	2086
7	2970	5594	8564	316	401	717
8	1999	6395	8394	518	510	1028
Mean	1946	4013	5958	463	520	983
Stdev	1203	2340	3426	320	271	525

Table 4.1: FCM cell count per gram for sponge cell fraction samples, *n* = 8. Total sponge cells per gram is the sum of "hiDNA" and "lowChl". Residual microbial cells are the sum of "lowChl/LowSS" and "lowDNA".

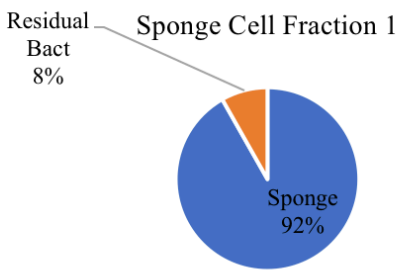
Sponge Cell Fraction 1
Residual Bact 8%
Sponge 92%

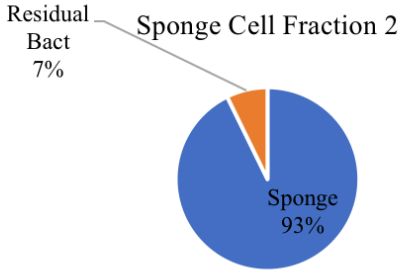
Sponge Cell Fraction 2
Residual Bact 7%
Sponge 93%

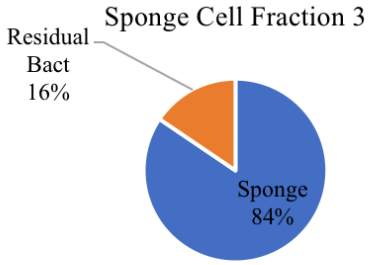
Sponge Cell Fraction 3
Residual Bact 16%
Sponge 84%

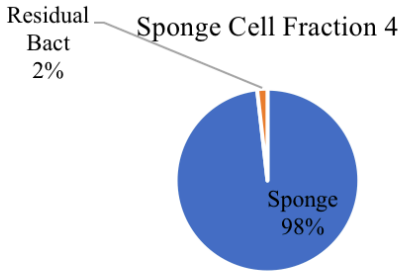
Sponge Cell Fraction 4
Residual Bact 2%
Sponge 98%

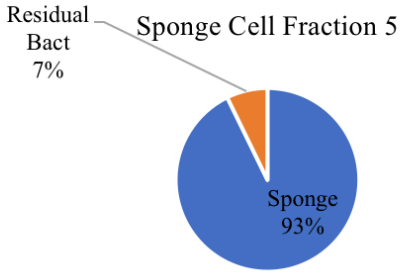
Sponge Cell Fraction 5
Residual Bact 7%
Sponge 93%

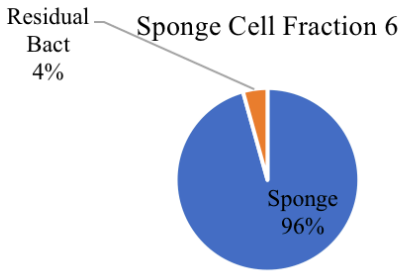
Sponge Cell Fraction 6
Residual Bact 4%
Sponge 96%

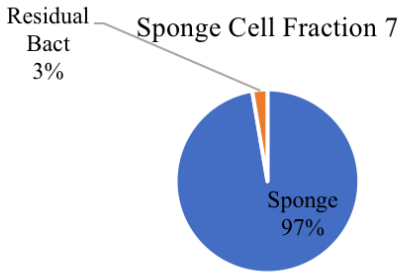
Sponge Cell Fraction 7
Residual Bact 3%
Sponge 97%

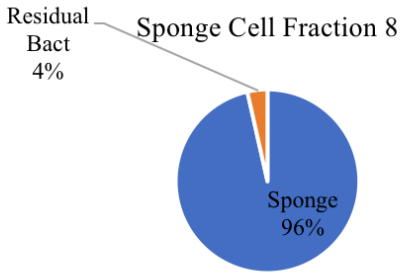
Sponge Cell Fraction 8
Residual Bact 4%
Sponge 96%

Figure 4.1. Composition of sponge cell fractions by carbon contribution based on C $cell^{-1}$ contributions for sponge cells from de Goeij et al. (2009) and picophytoplankton, nanoplankton, and microplankton from Verity et al. (1992), Garrison et al. (2000), and Menden-Deuer and Lessard (2000). Sponge cells include cells with high DNA ("hiDNA") and low chlorophyll ("lowChl"). "HiDNA" are sponge cells containing high chlorophyll and high phycoerythrin (PMT 3) signals and are sponge cells with phytoplankton prey within them. "LowChl" cells indicate sponge cells without prey in them. Residual bacterial cells include "LowChl/lowSS" cells that are likely residual bacteria and "lowDNA" cells are likely residual phytoplankton.

The microbial fraction samples were run using Chl and DNA detectors and contained high counts of bacteria and phytoplankton (Table 4.2). No cells larger than 5 μm diameter were detected in the microbial fraction. Microbial cell samples contained between 3.8×10^6 and 2.9×10^7 non-pigmented heterotrophic bacterial cells ("HBACT") g^{-1} starting wet weight. High DNA heterotrophic bacteria ("HiDNA BACT") and low DNA heterotrophic bacteria ("LowDNA BACT") cell counts are subsets of "HBACT" and ranged from 3×10^6 to 1.2×10^7 cells g^{-1} and 8.1×10^5 and 2.2×10^7 cells g^{-1} respectively. Counts of *Synechococcus* ranged from 4.1×10^3 to 2.4×10^4, and counts of "hiChl" eukaryotes (likely larger nanophytoplankton or smaller microphytoplankton) ranged from 3.1×10^3 to 1.6×10^4. "LowChl" eukaryotes (likely smaller nanophytoplankton) ranged from 4.9×10^4 to 3.1×10^5 cells per gram starting wet weight. The carbon contribution of heterotrophic bacterial cells carbon to the microbial fraction ranged from 33% to 84% and averaged 69 ± 20%, the carbon contribution of Synechococcus to the microbial fraction ranged from 0% to 1% and averaged 1 ± 0.4%, and the carbon contribution of

nanophytoplankton to the microbial fraction ranged from 16% to 66% and averaged 30 ± 20% (see Figure 4.2).

Sample	HBACT g^{-1}	HiDNA BACT g-1	LowDNA BACT g^{-1}	SYN g^{-1}	hiChl g^{-1}	lowChl g^{-1}
1	23283951	11135802	12148148	13565	11946	219072
2	8327622	6958868	1301166	5665	3081	90250
3	4343524	3503816	813761	24263	15647	306312
4	7858732	3027416	4907431	4090	7582	48781
5	3888216	3036261	830422	17010	13667	193005
6	29018265	6962043	22465753	18253	9548	220820
7	15132641	5244879	10403691	6148	13998	104983
8	13965937	11970803	2362637	23642	8679	177068
Mean	13227361	6479986	6904126	14080	10518	170036
Stdev	8467844	3287285	7175466	7541	3851	78607

Table 4.2: FCM cell counts per gram wet weight for microbial cell fraction samples $n = 8$. "HiDNA BACT" and "LowDNA BACT" are subsets of "HBACT". "SYN" represents *Synechococcus*. "HiChl" and "lowChl" cells are likely large and small nanophytoplankton, respectively.

A one-tailed t test was used to test for differences in "HiDNA" and "LowChl" between samples S1 through S5 and samples S6 through S8, as the sponges for samples 6 through 8 contained sponge eggs in the mesohyl. The sponge cell fraction samples S6 through S8 contained significantly more "HiDNA" cells ($p = 0.04$) and "LowChl" cells ($p = 0.00$) than samples S1 through S5. The standard deviations do not differ significantly, and there were no significant differences for the other FCM parameters for cell type in either the remaining sponge fractions samples or the microbial fraction samples.

Microbial Cell Fraction 1

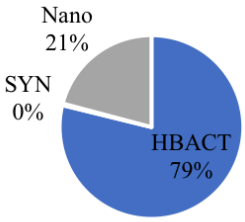

Microbial Cell Fraction 2

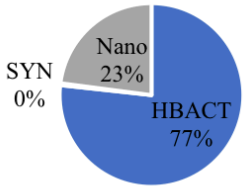

Microbial Cell Fraction 3

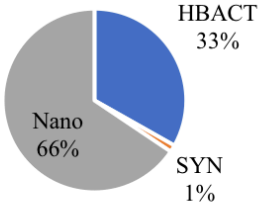

Microbial Cell Fraction 4

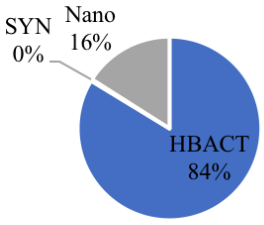

Microbial Cell Fraction 5

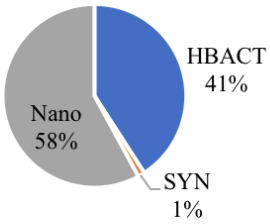

Microbial Cell Fraction 6

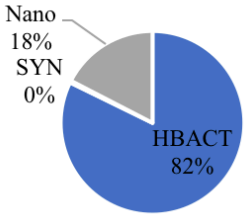

Microbial Cell Fraction 7

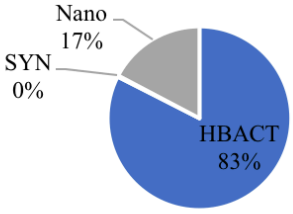

Microbial Cell Fraction 8

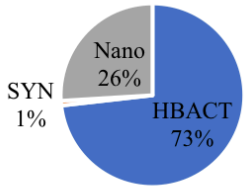

Figure 4.2: Composition of microbial cell fractions by carbon contribution. "HBACT" is composed of "HiDNA BACT" (actively growing and dividing) and "LowDNA BACT" (likely dormant) bacteria. "SYN" represents *Synechococcus*. "Nano" is composed of "HiChl" and "lowChl" cells are likely large and small nanophytoplankton respectively. C cell^{-1} values of 30 fg cell^{-1} for bacteria (Fukuda et al. 1998), 200 fg cell^{-1} for *Synechococcus* other picophytoplankton, and 800 fg cell^{-1} for nanophytoplankton (Garrison et al. 2000) were used for conversion.

C:N molar ratios of whole sponge and isolated sponge and microbial cell fractions

C:N molar ratios for whole sponge samples averaged 4.5 and ranged from 4.0 to 5.4 but varied with geographic location (Table 4.3). Mean C:N ratio of the isolated sponge cell fraction was 6.0 ± 0.2 (Table 4.4) and the mean C:N ratio of the isolated microbial cell fraction was 7.3 ± 1.3 (see Table 4.5). The sponge cell and microbial cell fraction C:N ratios were significantly different in one-tailed ($p = 0.006$) and two-tailed t tests ($p = 0.0124$). Whole sponge samples in the north bay had significantly higher C:N than samples from mid bay (one-tailed $p = 0.005$ and two-tailed $p = 0.009$ t tests) as well as from the south bay (one-tailed ($p = 0.003$) and two-tailed ($p = 0.006$) t tests). C:N ratios of whole sponge samples collected from the mid bay were not statistically different than C:N ratios of whole sponge samples collected from the south bay ($p = 0.25$, one-tailed t test). The C:N of both the sponge cell fraction and the microbial cell fraction were significantly higher than the C:N all of the whole sponge samples from all locations ($p = 0.000$ for all in one- and two-tailed t tests).

Bulk $\delta^{15}N$ and $\delta^{13}C$

Bulk tissue δ^{15}N and δ^{13}C values of whole sponge samples averaged 5.1‰ and -18.0‰, respectively, but varied by geographic location within Kāneʻohe Bay (Table 4.3). The mean bulk δ^{15}N values of whole sponge samples from the north bay were significantly higher than the mean δ^{15}N values of whole sponge samples from the mid bay (p = 0.001, one-tailed t test; p = 0.003, two-tailed t test) and the mean δ^{15}N values of whole sponge samples from the south bay (p = 0.005, one-tailed t test; p = 0.008, two-tailed t test). However, δ^{15}N values of sponges from the mid bay and south bay were not significantly different (p = 0.25, one-tailed t test; p = 0.51 two-tailed t test). The mean bulk δ^{13}C value of sponges for the north bay were significantly higher than the mean δ^{13}C values of sponges from the mid bay (p = 0.04, one-tailed t test) and the mean δ^{13}C values of sponges from the south bay (p = 0.000, one-tailed t test, p = 0.000, two-tailed t test). The mean δ^{13}C values of sponges from the mid bay were also significantly higher than the mean δ^{13}C values of sponges from the south bay (p = 0.02, one-tailed t test; p = 0.04, two-tailed t test). Average bulk δ^{15}N value of the isolated sponge cell fraction was 8.1‰ ± 0.3‰ (n = 7) and average δ^{13}C value was -22.4‰ ± 0.4‰ (n = 7). Average bulk δ^{15}N value of the isolated microbial cell fraction was 7.9‰ ± 0.4‰ (n = 8) and average δ^{13}C was -26.0‰ ± 3.4‰ (n = 8) (See Tables 4.4 and 4.5). The mean δ^{15}N values of the sponge cell and microbial cell fractions were not significantly different (p = 0.1, one-tailed t test; p = 0.2, two-tailed t test). However, the mean δ^{13}C value of the sponge cell fraction was significantly higher than the δ^{13}C values of the microbial cell fraction (p = 0.01, one-tailed t test; p = 0.02, two-tailed t test). The δ^{15}N value of both the sponge cell and the microbial cell fractions were significantly higher than the δ^{15}N value of whole sponges collected from all locations (p = 0.000 in one- and two-tailed t tests for all), and the δ^{13}C value of both the sponge cell and microbial cell fractions were significantly lower

than the $\delta^{13}C$ values of whole sponges collected from all locations ($p = 0.000$ in one- and two-tailed t tests for all).

$\delta^{13}C$ values of the microbial cell fractions were significantly and positively correlated with C:N molar ratios (Figure 4.3, $F < 0.001$, $R^2 = 0.97$). In addition, $\delta^{15}N$ values of whole sponge samples and sponge cell fraction are significantly and positively correlated with C:N molar ratios (Figure 4.4, $C:N = 0.4244\delta^{15}N + 2.3506$, $R^2=0.825$).

Location	Sample	$\delta^{15}N$ ‰ vs. AIR	$\delta^{13}C$ ‰ vs. V-PDB	C:N
North Bay				
n=10	NB1	6.4	-17.4	4.9
	NB2	5.5	-16.9	4.8
	NB3	5.7	-18.1	4.3
	NB4	6.9	-17.7	5.4
	NB5	5.8	-17.8	4.7
	NB6	6.0	-17.9	4.3
	NB7	5.9	-17.7	5.4
	NB8	5.8	-16.2	4.9
	NB9	5.2	-17.3	4.3
	NB10	5.4	-17.6	4.8
	Mean (NB)	5.9 ± 0.5	-17.5 ± 0.6	4.8 ± 0.4
Mid bay				
n=10	MB1	6.1	-18.0	4.6
	MB2	4.5	-18.3	4.3
	MB3	4.5	-18.0	4.1
	MB4	4	-18	4.6
	MB5	5.2	-17.7	4.6
	MB6	4.5	-17.6	4.5
	MB7	5.5	-17.4	4.3
	MB8	4.8	-18.5	4.1
	MB9	5.1	-18.1	4.2
	MB10	4	-18.1	4.3
	Mean (MB)	4.8 ± 0.7	-18.0 ± 0.3	4.4 ± 0.2
South bay				
n=10	SB1	2.5	-19.8	4.0
	SB2	4.7	-18.5	4.2
	SB3	4.3	-18.5	4.0
	SB4	4.7	-19.1	4.2
	SB5	3.9	-19	4.1
	SB6	6.1	-18.5	4.6
	SB7	4.8	-19	4.5
	SB8	4.9	-17.2	4.3
	SB9	4.1	-17.8	4.2
	SB10	6	-19.6	4.7
	Mean (SB)	4.6 ± 1.0	-18.7 ± 0.8	4.3 ± 0.2

Table 4.3: Bulk $\delta^{15}N$, bulk $\delta^{13}C$, and C:N (mol:mol) values for whole sponge samples collected from north (NB), mid (MB), and south (SB) Kāneʻohe Bay, with mean values ± SD reported by location.

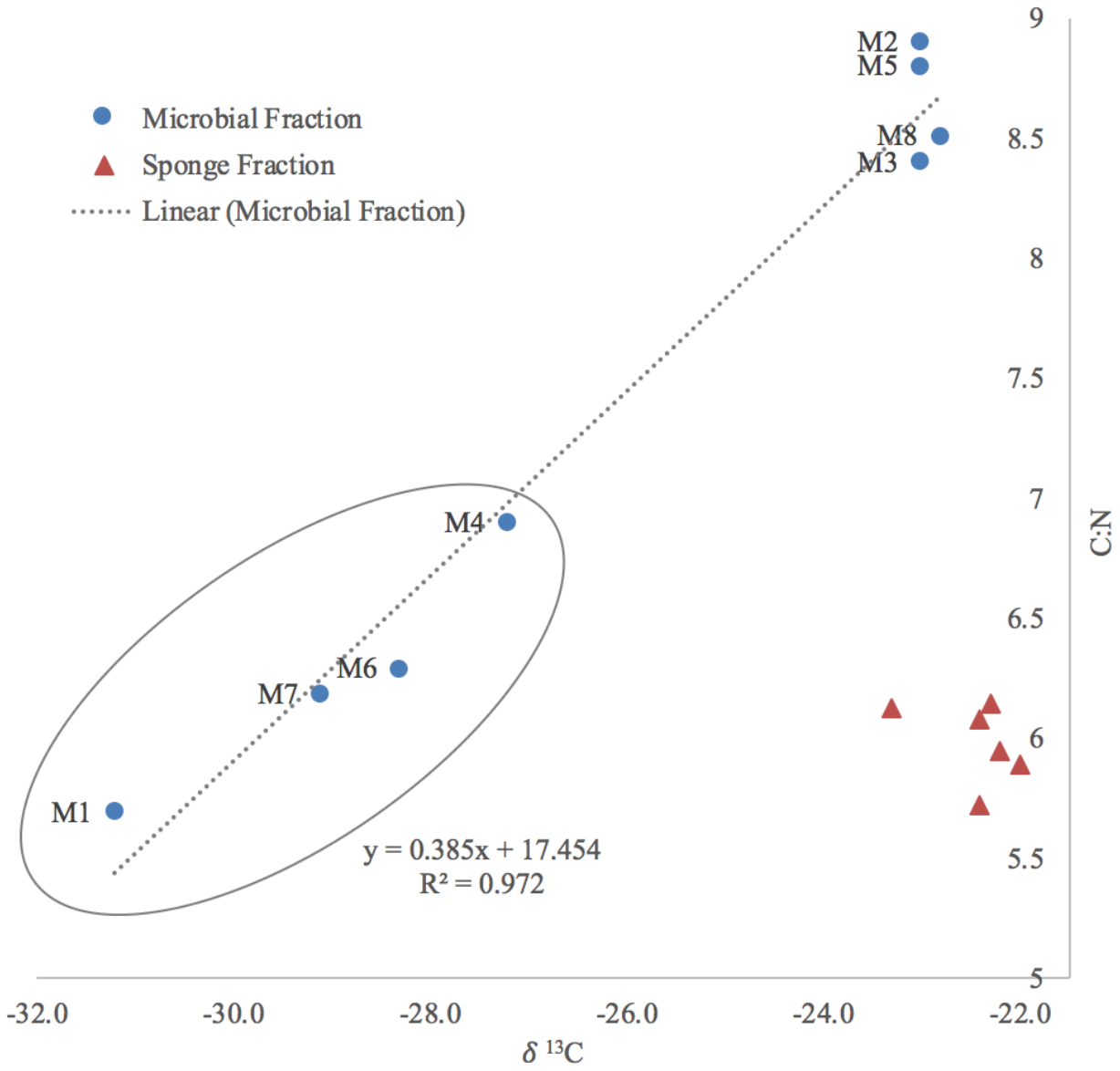

Figure 4.3: Relationship between C:N (mol:mol) ratio and bulk $\delta^{13}C$ in the microbial fraction showing that when $\delta^{13}C$ values are corrected for high C:N (circled samples), the microbial cells have a much lower bulk $\delta^{13}C$ value than the sponge cells.

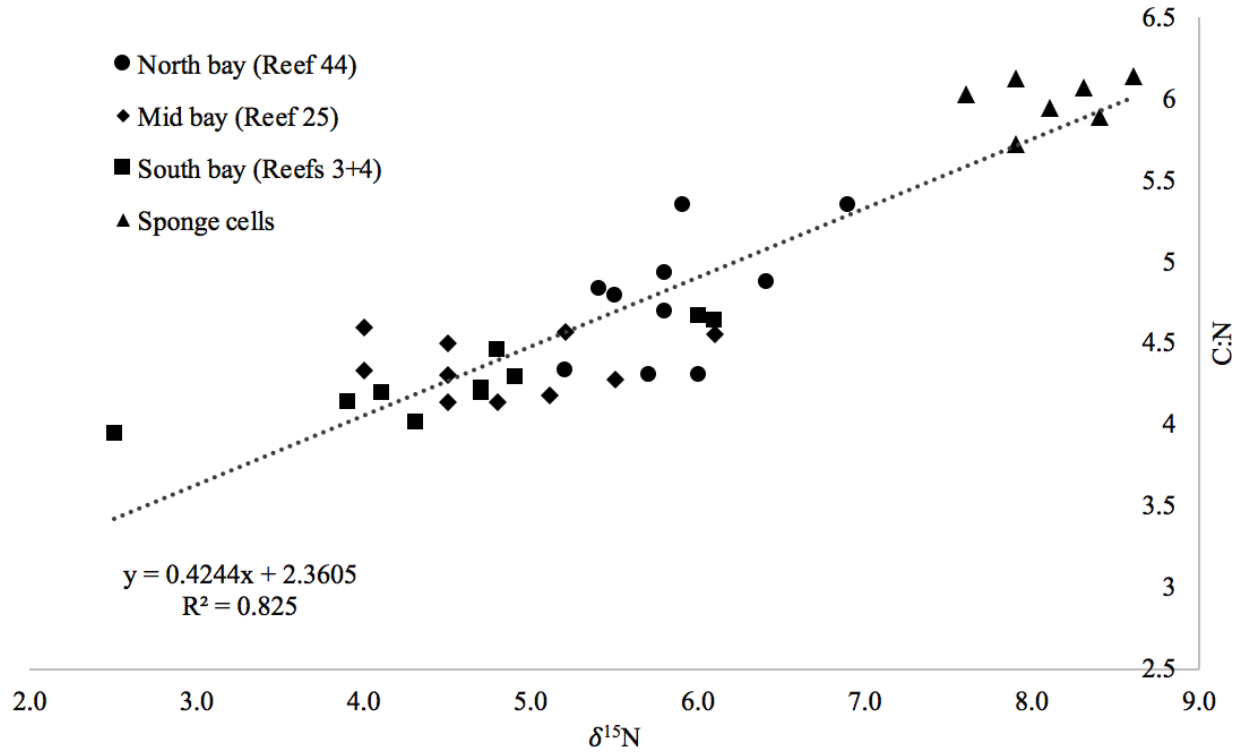

Figure 4.4: Bulk $\delta^{15}N$ versus C:N (mol:mol) of whole sponge samples and sponge cell fraction samples. Regression through all sample data points: C:N = 0.4244$\delta^{15}N$ + 2.3506, R^2=0.825. The bulk $\delta^{15}N$ values and C:N ratios of whole sponges reflect variation by site of collection.

Compound specific amino acid analysis

Carbon isotopic composition of individual amino acids were determined on six samples, however some fractions were combined in order to have sufficient material for analyses (Table 4.4). Microbial cell fractions M1 and M3 as well as sponge cell fractions S1 and S3 were combined into a single microbial and a single sponge sample, respectively for AA CSIA. Three microbial cell fractions M4, M6 and M7 were analyzed individually, however their equivalent sponge fractions had to be combined into a single sample (S4 + S6 + S7). Although 14 amino acids were detected, the $\delta^{13}C$ values of 12 were reliably measured in all samples (Table 4.5). I

was unable to measure the carbon isotopic composition of isoleucine and methionine in all samples. The $\delta^{13}C$ values of amino acids ranged from -27.0 to 4.5‰. The essential amino acid (Thr, Val, Leu, Phe and Lys) $\delta^{13}C$ values of microbial cell fraction M1 + M3 were not significantly different from those of sponge cell fraction S1 + S3 ($p = 0.446$, one-tailed and $p = 0.892$, two-tailed t tests). In addition, the essential amino acid $\delta^{13}C$ values of microbial cell fractions M4, M6 and M7 were not significantly different from those of sponge cell fraction S4 + S6 + S7 ($p = 0.461$, one-tailed and $p = 0.922$, two-tailed t tests).

Recovery limited nitrogen isotope analyses even more than carbon isotope analysis and only five samples had sufficient material for analysis. In addition, only eight amino acids were reliably measured in all samples (Table 4.5). $\delta^{15}N$ values ranged from 2.3 to 16.4‰ and trophic amino acid (Ala, Leu, Pro, Asx, Glx) $\delta^{15}N$ values were higher (10.6 ± 3.3‰) than those of source amino acids (Lys, Phe, 4.1 ± 1.3‰). Direct comparison of nitrogen isotopic compositions between microbial and sponge cell fractions could only be made for M4, M6 and M7 and S4 + S6 + S7. The source amino acid $\delta^{15}N$ values of microbial cell fractions M4, M6 and M7 were not significantly different from those of sponge cell fraction S4 + S6 + S7 (t test, one-tailed $p = 0.144$ and two-tailed $p = 0.288$). In addition, the trophic amino acid $\delta^{15}N$ values of microbial cell fractions M4, M6 and M7 were not significantly different from those of sponge cell fraction S4 + S6 + S7 (t test, one-tailed $p = 0.133$ and two-tailed $p = 0.267$).

Trophic level calculated from the difference in $\delta^{15}N$ values of Glx and Phe ($TL_{Glx\text{-}Phe}$) for the combined sponge sample (S4 + S6 + S7) is 2.1 (propagated SD=0.2) and the average trophic level for samples M4, M6, and M7 is 1.9 (propagated SD=0.3) (see Table 4.6). $TL_{Glx\text{-}Phe}$ of these

sponge cell and microbial cell fractions were not significantly different (t test, one-tailed p = 0.311 and two-tailed p = 0.622).

The difference in the average $\delta^{15}N$ values of trophic and source amino acids of the sponge cell fraction (sample S4 + S6 + S7) was 6.9 ± 1.3‰ and that of the microbial cell fractions (samples M4, M6, and M7) was 5.9 ± 1.2‰. These proxy measurements of trophic level of the microbial and sponge cell fractions were not significantly different (t test, one-tailed p = 0.270 and two-tailed p = 0.540).

The difference in the weighted mean $\delta^{15}N$ values of trophic and source amino acids of the sponge cell fraction (sample S4+S6+S7) was 9.4 (propagated SD = 0.4) and 8.9 (propagated SD = 0.3) for the microbial cell fractions (samples M4, M6, and M7). This trophic proxy of the microbial and sponge cell fractions was also not significantly different (t test, one-tailed p = 0.143 and two-tailed p = 0.286).

				Trophic AAs					Source AAs		
		Bulk		Ala	Glx	Leu	Pro	Asx	Phe	Tyr	Lys
Sample	Fraction	δ^{15}N (‰)	C:N	δ^{15}N (‰)	δ^{15}N (‰)	δ^{15}N (‰)	δ^{15}N (‰)	δ^{15}N (‰)	δ^{15}N (‰)	δ^{15}N (‰)	δ^{15}N (‰)
M1	microbial	8.1	5.7								
M2	microbial	8.3	8.9								
M3	microbial	8.0	8.4								
M1+M3	microbial			5.9±0.14	16.1±0.14	10.9±0.44	9.9±0.33	13.7±0.24	2.7±0.23	2.5±0.48	4.40.35
M4	microbial	7.8	6.9	5.7±0.21	15.2±0.01	9.8±0.07	8.6±0.4	11.8±0.09	5.1±0.25	4.2±1.3	3.4±0.19
M5	microbial	8.1	8.8								
M6	microbial	7.3	6.3	6.5±0.99	14.3±0.41	9.6±0.67	9.3±1.12	10.9±0.18	6.50±0.47	-	3.6±0.32
M7	microbial	7.3	6.2	5.3±0.37*	14±0.29	9.1±0.53	7.8±0.56	10.8±0.38	2.3±0.46	1.1±0.26	3.4±0.47
M8	microbial	8.0	7.5								
S1	sponge cell	7.6	6.0								
S3	sponge cell	8.1	6.0								
S4	sponge cell	8.4	5.9								
S5	sponge cell	8.3	6.1								
S6	sponge cell	7.9	6.1								
S7	sponge cell	7.9	5.7								
S4+S6+S7	sponge cell			6.4±0.15	16.4±0.08	12.2±0.26	9.71.05	14.1±0.16	4.6±0.31	2.4±0.31	5.2±0.66
S8	sponge cell	8.6	6.2								

Table 4.4. Bulk and amino acid δ^{15}N values for Ala, Glx, Leu, Pro, Asx (trophic AAs) and Phe, Tyr, Lys (source AAs) for isolated sponge cell and microbial cell fractions. Samples were run in triplicate. The isotope value of a combined Glu + Gln is measured (termed Glx), and the isotope value of a combined Asn + Asp is measured (termed Asx). Values are reported with SD. Value marked with * did not have an optimal peak shape.

			Nonessential amino acids							Essential amino acids				
Sample	Fraction	Bulk δ^{13C} (‰)	Ala δ^{13C} (‰)	Gly δ^{13C} (‰)	Ser δ^{13C} (‰)	Pro δ^{13C} (‰)	Asx δ^{13C} (‰)	Glx δ^{13C} (‰)	Tyr δ^{13C} (‰)	Leu δ^{13C} (‰)	Phe δ^{13C} (‰)	Lys δ^{13C} (‰)	Val δ^{13C} (‰)	Thr δ^{13C} (‰)
M1	microbial	-31.2												
M1+M3	microbial		-18.3	-11.3	4	-19.8	-15.9	-14.6	-19.9	-26.6	-24.4	-16.2	-25.1	-13.5
M2	microbial	-23.0												
M3	microbial	-23.0												
M1+M3	microbial													
M4	microbial	-27.2	-17.5	-8.5	-0.5	-20	-16.8	-14.9	-24.6	-26.5	-23.5	-17.6	-24.5	-15.3
M5	microbial	-23.0												
M6	microbial	-28.3	-17.2	-7	-2.9	-20.2	-17.2	-15.4	-25.2	-25.7	-23.4	-17.4	-24.8	-15.6
M7	microbial	-29.1	-21	-9.4	-0.5	-19.9	-16.6	-15.9	-22.6	-26.5	-24.4	-18.5	-24.1	-15.2
M8	microbial	-22.8												
S1	sponge cell	-22.4												
S1+S3	sponge cell		-19	-12.4	-17.3	-19.5	-19.1	-15.8	-26.3	-27	-24.2	-18.2	-23.9	-14.9
S3	sponge cell	-22.2												
S4	sponge cell	-21.9												
S5	sponge cell	-22.4												
S6	sponge cell	-23.3												
S7	sponge cell	-22.4												
S4+S6+S7	sponge cell		-17.3	-13.4	4.5	-19.6	-17.2	-14.6	-23.3	-26.3	-23.8	-17.9	-25.3	-13.8
S8	sponge cell	-22.3												

Table 4.5. Bulk and amino acid $\delta^{13}C$ values for Ala, Gly, Ser, Pro, Asx, Glx, and Tyr (nonessential AAs) and Leu, Phe, Lys, Val, and Thr (essential AAs) for isolated sponge cell and microbial cell fractions. The isotope value of a combined Glu + Gln is measured (termed Glx), and the isotope value of a combined Asn + Asp is measured (termed Asx). Samples were run in triplicate.

Sample	TL	TP using average δ15N	TP using weighted mean δ15N
S4 + S6 + S7	2.1 ± 0.2	6.9 ± 1.3	9.4 ± 0.3
M4	1.9 ± 0.2	6 ± 1.0	11.1 ± 0.2
M6	1.6 ± 0.2	5.1 ± 1.4	7.9 ± 0.4
M7	2.1 ± 0.2	6.6 ± 1.1	7.7 ± 0.4
Average M4 + M6 + M7	1.9 ± 0.3	5.9 ± 1.2	8.9 ± 0.3

Table 4.6: Trophic level, trophic proxy calculated using average of δ^{15}N values of trophic and source amino acids, and trophic proxy using weighted mean δ^{15}N values of trophic and source amino acids, reported with propagated standard deviations.

Summed variance in δ^{15}N values of trophic amino acids (ΣV)

ΣV values ranged from 2.0 to 3.0 (Table 4.7). ΣV values of microbial cell fractions M4, M6 and M7 were not significantly different from those of sponge cell fraction S4 + S6 +S7 (t test, one-tailed $p = 0.115$ and two-tailed $p = 0.230$). The ΣV values in microbial and sponge cell fractions are similar to those found in cultures of heterotrophic bacteria and microbially reworked particles in the ocean (McCarthy et al. 2007, Calleja et al. 2013, Hannides et al. 2013) and are higher than values found in phytoplankton and zooplankton (McCarthy et al. 2007).

Sample	ΣV
M1 + M3	2.9
S4 + S6 + S7	3.0
M4	2.6
M6	2.0
M7	2.4
Average Microbial	2.5
Average M4 + M6 + M7	2.3

Table 4.7: Summed variance in the $\delta^{15}N$ values of select trophic amino acids (ΣV) of isolated sponge (S) cell and microbial (M) cell fractions of *Mycale grandis*. See text for details.

Discussion

Sponge associated microbial symbionts play an important role in sponge nutrition. Separate analysis of sponge and symbiotic microbial cells can reveal details about the relationship and mechanism of nutrient transfer from symbiont to sponge. While the sponge holobiont has been shown to be capable of DOM uptake and ultimately incorporation, the exact mechanisms and the role(s) microbes may play in this process has not been well described. The separated sponge cell and microbial cells fractions contained distinct cell compositions from each other, with the sponge fraction dominated by sponge cells and the microbial cell predominantly composed of heterotrophic bacteria. Despite variation of $\delta^{15}N$ and $\delta^{13}C$ values in sponge samples by location throughout Kāneʻohe Bay, the $\delta^{13}C$ values of the essential amino acids and $\delta^{15}N$ values of the source amino acids are not statistically different between the two fractions. The indistinguishable amino acid compositions and high ΣV values raise questions about the nature of transfer of carbon and nitrogen and suggest that the sponge is primarily if not exclusively acquiring carbon

and nitrogen through direct transfer of bacterially-synthesized amino acids, and not from feeding on their associated microbes or through filtration of plankton in the water column.

Separation of sponge and microbial cell fractions

Our results indicated good separation of the sponge and microbial cells. Flow cytometry revealed fractions distinguished by size, pigment (chl and PMT 3), and DNA content. Epi-fluorescence microscopy at 200x and 400x identified that large (~5 micron nuclei) cells within the sponge tissue samples were largely devoid of fluorescence and hence were composed of only sponge cells.

The distinct composition of the two fractions confirmed good separation of sponge cell and microbial cell fractions containing profiles of cells distinct from each other, with the sponge fraction containing predominantly sponge cells and the microbial fraction containing smaller prokaryotic cells. The sponge cell fraction contained on average 84.0% sponge cells by count for *M. grandis* identified through FCM in this study, consistent with Fiore et al.'s (2013) finding that their sponge fraction for *X. muta* contained ~85% sponge cells revealed through epi-fluorescence microscopy. The cell separation method has also been shown to be effective for other Caribbean sponge species (Freeman and Thacker 2011). While efforts were made to fully dissociate and homogenize the sponge tissue samples to allow for separation of the sponge cells from the prokaryotic cells, it is possible that some prokaryotes remained intracellularly in some sponge cell fraction samples. Overall, the sponge cell fraction resulting from the Freeman and Thacker (2011) protocol produces a representative mix of sponge cells of ~10 micron size and may contain small remnants of structural materials such as broken spicules or spongin fibers.

Sponge cell fraction S6 had the highest "HiDNA" and "LowChl" counts, and sponge cell fractions containing eggs within the mesohyl (S6, S7, and S8) all had significantly higher counts of "HiDNA" and "LowChl" than samples S1 through S5, which did not contain visible egg clusters. As expected, the presence of gametes in samples S6, S7, and S8 resulted in greater "HiDNA" cell counts. Samples S6, S7, and S8 also exhibited lower chlorophyll. Unlike other sponge tissue cell types, sponge gamete cells would not contain prey cells within them nor contain directly integrated chlorophyll from food sources.

Theoretically, all planktonic microbes have the potential to populate the mesohyl of a sponge provided they can survive the digestion and immune response in sponges and are capable of growing in the microenvironment within the sponge (Zhu et al. 2008). *Synechococcus* is the dominant cyanobacteria taxon in Kāneʻohe Bay and contributes ≥ 35% of phytoplankton biomass (Selph et al. 2018). At 200x and 400x magnification using epi-fluorescence microscopy, *Synechococcus* was the most abundant sponge-associated microbe in *M. grandis,* ranging in 0.5 to 1.5 micron in size as indicated by phycoerythrin (PMT 3).

In Kāneʻohe Bay, abundances of *Synechococcus* (primary producer) and heterotrophic bacteria (decomposer) are tightly coupled to each other. Rapid growth of *Synechococcus* and larger heterotrophic consumers are thought to augment the number of trophic pathways by which carbon moves from the microbial community to metazoan consumers and thereby supports higher transfer of production to metazoans (Azam at al. 1983, Selph et al. 2018).

Among cyanobacteria, the *Synechococcus/Prochlorococcus* clade is the single most dominant group in most of the world's oceans and have been found in at least 26 Demospongiae families (Hentschel et al. 2006). A monophyletic "*S. spongiarum*" clade that is phylogenetically distinct from the nearest free-living *Synechococcus* relative has been reported to be present in a total of 18 sponge species from various geographic locations (Steindler et al. 2005). "HiDNA" cells within the sponge fraction are sponge cells containing very a high chlorophyll signature and high phycoerythrin signal (PMT 3) and may be sponge cells with phytoplankton prey within them or residual phytoplankton cells in the sponge cell fraction. Some sponges have been shown to prey on *Synechococcus* in feeding clearance studies (Pile et al. 1997, Pile et al. 2003). It is unknown whether *M. grandis* can consume *Synechococcus* prey directly as a dietary strategy. To determine whether *M. grandis* consumes *Synechococcus*, future studies could include *Synechococcus* clearance feeding experiments, or alternatively, repeat comparative measurements of PMT 3 in sponge cell samples following starvation experiments. Disappearance of the phycoerythrin signal would suggest that ingestion of *Synechococcus* is the source of PMT 3 measured in sponge cell samples.

Bulk $\delta^{15}N$ and $\delta^{13}C$ values in the whole sponge, sponge cell, and microbial cell fractions also indicated good separation of the fractions (Figure 4.5). Although there is overlap in $\delta^{13}C$ values between the microbial and some sponge cell fractions, the average difference between these two fractions is quite large (3.5‰) and the mean C:N values of sponge cell and microbial cell fractions are statistically different indicating distinct compositions between the two fractions. Some microbial cell fractions (M2, M3, M5, and M8) were found to have unexpectedly high C:N ratios. In addition, $\delta^{13}C$ values of the microbial cell fractions are significantly and positively

correlated with C:N ratios (Figure 4.3) suggesting that some microbial cell fractions potentially contained a small amount of carbonate that would increase both C:N ratios and $\delta^{13}C$ values. An isotope mass balance based on the $\delta^{13}C$ value of microbial cell samples and carbon contribution and estimated $\delta^{13}C$ values of heterotrophic bacteria ($\delta^{13}C \sim -33.5‰$) and nanophytoplankton ($\delta^{13}C \sim -22‰$) within each sample was performed to calculate the estimated amount of residual carbonate (with $\delta^{13}C$ value of 0‰) in each sample. The contribution of *Synechococcus* was ignored because all fractions contained < 1% *Synechococcus* contribution to carbon. Isotope mass balance confirmed that samples with the highest $\delta^{13}C$ values also contained the high amounts of residual carbonate (samples M2 (26%), M3 (11%), M5 (14%), and M8 (25%)) (See Figure 4.3). While sample M4 and M6 also contained appreciable amounts of carbonate (14% and 10%), these two samples had the lowest contribution of nanophytoplankton and highest amounts of heterotrophic bacteria within the fractions which would drive $\delta^{13}C$ values lower (See Figure 4.3).

Greater nanophytoplankton contribution in some of the microbial cell fractions would have the effect of driving up $\delta^{13}C$ values. Nanophytoplankton carbon contribution was especially high in samples M3 (66%), M5 (58%), and M8 (26%) (see Figure 4.2). These samples were amongst those that exhibited the lowest $\delta^{13}C$ values. While different species of phytoplankton vary in ability to take up HCO_3^- versus CO_2 and exhibit a range in fractionation (Keller and Morel 1999, Laws et al. 2001), the overall effect of greater nanophytoplankton to heterotrophic bacteria counts would be higher $\delta^{13}C$ values compared to samples with greater heterotrophic bacteria to nanophytoplankton counts. Thus, the fractions with higher C:N values are not considered to be representative of the true microbial fraction, while the lower C:N values found in samples M1,

M4, M6 and M7 are considered to be more representative. The average microbial cell $\delta^{13}C$ values of M1, M4, M6 and M7 is -29.0 ± 1.6‰, which is significantly lower (one-tailed t test, $p < 0.001$) than the average sponge cell fractions $\delta^{13}C$ value of -22.4 ± 0.4‰.

Lastly, there is a significant negative linear relationship (F = 0.044) between the $\delta^{13}C$ values of bulk microbial cells and the abundance of bacteria (HiDNA BACT + LowDNA BACT). A plot of $\delta^{13}C$ versus 1/Sum BACT yields an intercept of -29‰ as the predicted value of a "pure" bacterial fraction, which closely resembles samples M1, M4, M6 and M7. Based on this relationship I suggest that a greater separation in $\delta^{13}C$ values is found in the microbial cell fractions with higher numbers of bacteria. From the composition of the sponge cell fraction and the relationship between $\delta^{13}C$ values and C:N ratios, I conclude these microbial cell samples are distinct from sponge cell fractions and are representative of sponge microbial cells.

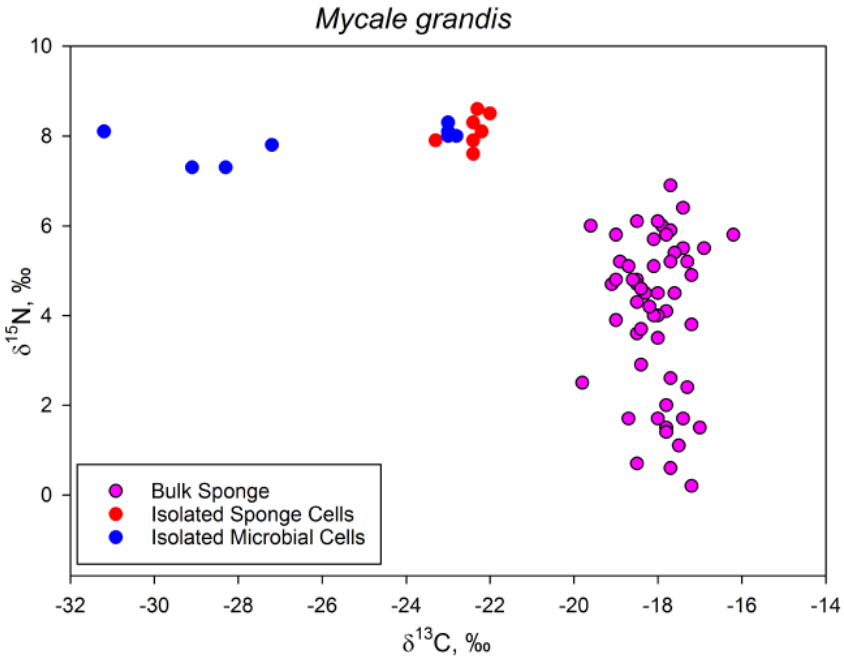

Figure 4.5: Relationship between the $\delta^{13}C$ and $\delta^{15}N$ values of whole sponges and the sponge and microbial cell isolates. The whole sponge carbon and nitrogen isotopic composition of the sponges that the cells were isolated from was not measured. Note: Sum of isolated sponge cell + microbial cell isolates ≠ whole sponge. Whole sponge samples include structural material not present in either fraction.

Isolated sponge cell and microbial cell fractions differ significantly from whole sponge tissue samples in C:N, $\delta^{15}N$ and $\delta^{13}C$ values. The internal sponge matrix is dominated by gelatinous collagen-rich mesohyl reinforced by a dense network of fibrous spongin. Spongin is a modified collagen protein found in demospongiae and provides structure and flexibility. Spongin fibers are secreted by collagen producing sponge cells found within the mesohyl. Bulk sponge tissue samples are predominantly composed of spongin and mesohyl. As observed in these samples, protein-rich spongin drives down the C:N ratio in bulk sponge. Diet-to-collagen isotope fractionation in bone collagen is known to result in ^{13}C enrichment in bone collagen of about 5‰

relative to other biomolecules from plants and animals (e.g., see Fernandes et al. 2012 and references therein). I speculate that similar carbon isotope fractionation can explain the ~5‰ difference between whole sponge and sponge cell fraction $\delta^{13}C$ values although certainly more work is required to confirm this hypothesis.

The C:N of the sponge cell fraction (average of S4 + S6 + S7) is significantly lower relative the C:N of the microbial fraction (average of M4 + M6 + M7), indicating fundamental differences in the composition of the two fractions. In addition, the microbial cell fraction also exhibits lower average bulk $\delta^{13}C$ values compared to the bulk $\delta^{13}C$ values of sponge cells. Higher lipid-to-biomass content drives $\delta^{13}C$ values lower and increases C:N ratio (Hayes 2001, Post et al. 2007). Higher lipid content in microbial cells may in part contribute to observed $\delta^{13}C$ values and C:N ratios. While the C:N ratio and the relative carbohydrate-lipid-protein composition of sponge associated bacteria are not known, the sponge cell fraction is expected to contain relatively higher protein and carbohydrate composition relative to the microbial samples, which may be reflected in the observed C:N ratios. While lipid content partially explains some of the observed C:N and $\delta^{13}C$ differences, the fraction of interest is the protein fraction that contains dietary information about the transfer of amino acids in the fractionation between trophic and source amino acids in nitrogen and non-essential and essential amino acids in carbon.

Although the $\delta^{15}N$ values of the sponge cell fraction is significantly different from those of whole sponge, I suggest that this difference is derived from the varying nitrogen isotopic composition of nutrients in different regions of Kāneʻohe Bay (Figure 4.4). Nitrogen inputs vary with seasonal patterns and weather (e.g. heavy rainfall and wind). Stream runoff and

anthropogenic inputs from urban developments such as coastal residential housing, He‘eia Harbor, and commercial developments are also sources of $\delta^{15}N$ variability across the bay. The higher $\delta^{15}N$ values measured in samples from the north bay may indicate input from higher concentrations of cesspools in the northern portion of the bay, as NO_3^- associated with sewage input is typically more enriched in ^{15}N (Kendall et al. 2001, Richardson et al. 2016). Additionally, submarine fresh groundwater discharge sources (Hunter and Evans 1995) would also result in higher $\delta^{15}N$ (McClelland and Valiela 1998, Vizzini et al. 2005). Indication of variations in nitrogen isotopic compositions by capture location of across the bay have also been observed the brown stingray *Dasyatis lata* (Dale et al. 2011). Brown stingrays captured in the southern part of Kane‘ohe Bay were consistently depleted in ^{13}C and enriched in ^{15}N compared with stingrays caught in the mid and north bay. While $\delta^{15}N$ trends for *D. lata* have opposite correlation by location compared to *M. grandis* samples, Dale et al. (2011) similarly attributes high $\delta^{15}N$ values measured in brown stingrays to high levels of human population in the south bay, high rates of nutrients, and residual effects of sewage discharge in the south bay from 1951-1978 (Hunter and Evans 1995). These differences are most likely due to seasonal variability and fluctuating inputs of nitrogen sources.

Average C:N in north Kāne‘ohe Bay was significantly different from average C:N in both mid and south Kāne‘ohe Bay, while the mid bay and south did not differ significantly from each other. Bulk $\delta^{15}N$ values of both sponge cell and microbial cells were significantly higher than the $\delta^{15}N$ of whole sponge samples. Despite these differences, the high correlation between C:N ratios and $\delta^{15}N$ values of whole sponge and sponge cell fractions (Figure 4.5) is consistent with our suggestions for the observed variation in $\delta^{15}N$ values across samples.

Although the flow cytometric and epifluorescence characteristics and the C:N ratios and carbon isotopic compositions of microbial and sponge cell fractions are distinctly different, the carbon and nitrogen isotopic compositions of amino acids in these fractions are remarkably similar (Tables 4.4 and 4.5). The compound specific amino acid isotopic data of the bacterial and sponge cell fractions strongly suggest that *M. grandis* is acquiring amino acids directly from its heterotrophic bacterial symbionts and not through *Synechococcus spp.* or other marine photoautotrophs. It is unlikely that *Synechococcus* would synthesize amino acids with a carbon and nitrogen isotopic composition identical to the pattern found in heterotrophic microbial cells that dominate the microbial cell fractions as identified through FCM.

Indo-Pacific sponges have long been considered to be phototrophic (Wilkinson 1983, Thacker 2005). Characteristics of *M. grandis* suggest that it can acquire nutrients from photoautotrophs, for example, it is found in well-lit shallow reef habitat and has bright orange coloration suggestive of photosymbionts such as the *Synechococcus spp.* that provide similar coloration to the Caribbean sponge *X. muta*. Furthermore, *M. grandis* (formerly *Mycale armata*) was revealed to host cyanobacterial phylotypes (Wang et al. 2009). One explanation for the lack of growth measured in *M. grandis* samples kept in flow through water tables at HIMB was a decrease in light levels (Shih, this volume, Chapter 2). Sponges that are classified to be extremely dependent on cyanobacterial photosynthesis lost mass under shaded conditions (Thacker 2005). *M. grandis* kept in water tables were exposed to natural light cycles but were partially shaded from direct sunlight. However, samples of sponge analyzed for FCM and CSIA were collected directly from the sunlit reef and revealed heterotrophic bacterial rather than cyanobacterial dominance in the microbial fraction. Although cyanobacterial symbionts can comprise 25 to 50% of a sponge's

cellular volume (Rützler 1990), relatively little is known about the metabolic exchanges and ecological interactions between sponges and their microbial symbionts. The unicellular cyanobacterium *Synechococcus spongiarum* is the most prevalent photosynthetic symbiont present in marine sponges (Erwin and Thacker 2007). In *M. grandis*, *Synechococcus spp*. represents less than 1% of the carbon contribution within the microbial cell fraction, although *Synechococcus* cells, which are larger than most bacterial cells, may have been lost in the efficiency of the separation by size fractionation.

Phylogenetic analyses of *S. spongiarum* 16S rRNA sequences from sponge host species revealed a genetically distinct symbiont clade from free living cyanobacteria but are indistinguishable from symbiont populations within different species and from distant geographic locations (Thacker 2005). *S. spongiarum* appears to be a generalist symbiont capable of horizontal transmission among hosts and exhibits widespread dispersal across the oceans. *Synechococcus* symbionts may be commensals that exploit the resources provided by their sponge hosts without significantly affecting sponge mass but may be consumed by their hosts or may be able to disperse from their host sponge when unfavorable environments arise (Thacker 2005).

Summed variance in $\delta^{15}N$ values of trophic amino acids (ΣV)

ΣV is a proxy for heterotrophic bacterial resynthesis of organic matter, as partial resynthesis introduces isotopic variability among amino acids in bacterial cells (McCarthy et al. 2007, Calleja et al. 2013, Yamaguchi et al. 2017). Heterotrophic reworking of proteinaceous material occurs through a range of processes including extracellular hydrolysis (Hannides et al. 2013), *de novo* synthesis, salvage AA incorporation into new biomass, selected resynthesis, and strict

catabolism (McCarthy et al. 2007). The ΣV index is a measure of the relative change $\delta^{15}N$ values of select trophic amino acids due to microbial alteration against a backdrop of other $\delta^{15}N$ values that remain relatively unaltered (Yamaguchi and McCarthy 2018). This pattern can differentiate microbial processing from eukaryotic processing of amino acids. Values above ΣV = 2 are generally considered to be a threshold for organic matter resulting from a predominantly heterotrophic resynthesis of detrital materials, although consumption of particles by zooplankton can also result in a slight increase in ΣV values (McCarthy et al. 2007).

Both sponge cell and microbial cell fractions exhibited high ΣV values, indicative of heterotrophic microbial alteration of amino acids. McCarthy et al. (2007) observed typical values of ΣV range from ~0 to 1 for phytoplankton, 1 to 1.5 for zooplankton and up to ~3 for detrital POM in surface sediment traps along the equatorial Pacific. Yamaguchi and McCarthy (2018) also measured high values of ΣV (~2 to 4) in high molecular weight dissolved organic matter in the North Pacific Ocean north of Hawai‘i. Yamaguchi and McCarthy (2018) showed that ΣV values increased from surface waters (21 m, ΣV = ~2) to mesopelagic depths (ΣV = ~2.8 at 915 m and ~4 at 670 m). In comparison, Yamaguchi and McCarthy (2018) found particles ranging in size from 500 kDa to ~1 μm (collected in GF/F filters) from depths of 25 to 750 m had ΣV values less than ~2. Consequently, they suggested that high ΣV values are found in highly bacterially altered particulate organic matter in the deep ocean, high molecular weight dissolved organic matter and in bacterial cells which have partly resynthesized amino acids (McCarthy et al. 2007, Callega et al. 2013, Yamaguchi et al. 2017, Yamaguchi and McCarthy 2018).

The ΣV of the microbial and sponge cell fractions can reveal the origin of the small particles found in the sample. The high values observed in the sponge cell fractions (S4 + S6 + S7) suggest that amino acids are not acquired directly from the consumption of fresh phytoplankton as a ΣV closer to that of phytoplankton (~1.0 to 1.5) would be expected. Although higher ΣV values were observed in zooplankton relative to phytoplankton in the equatorial Pacific Ocean (McCarthy et al. 2007), those changes were small (increase from ~0.7 to 1.5). Sponges have been demonstrated to be capable of uptake and incorporation of dissolved organic matter (de Goeij et al. 2008b, Rix et al. 2016, Rix et al. 2017, Hoer et al. 2017). The high ΣV observed in microbial and sponge cell fractions may be evidence of uptake of DOM with high ΣV values. However, the lack of statistical difference between the ΣV of sponge cell and microbial cell fractions supports the hypothesis that the high ΣV observed in the sponge cell fraction were inherited from their microbial symbionts, rather than the sponge cells directly taking up DOM from the water column.

Heterotrophic bacteria are thought to transform labile components into increasingly refractory dissolved organic matter (e.g., Jiao et al. 2010). It is unclear if bacterial symbionts in sponges are responsible for the observed direct uptake of DOM by sponges. If bacteria in *M. grandis* play a significant role in DOM uptake, they could acquire at least some of their high ΣV values from dissolved organic matter and transfer those partially resynthesized amino acids to the host sponge cells.

Results from FCM, lack of significant difference in the ΣV index, and amino acid patterns show that photosymbionts are not a major direct source of amino acids to *M. grandis* and that their role

in sponge nutrition may be less important than previously thought. If *Synechococcus spp.* are providing nutrition to the sponge, it would not be a direct source to the sponge, but through an intermediary, such as *Synechococcus* photosynthates being utilized by heterotrophic bacteria that subsequently transfer amino acids to the sponge host. Although the role of *Synechococcus* in *M. grandis* nutrition appears to be small if any, they could provide an alternate source of nutrition under different environmental regimes similar to the alternative stable states observed in coral that undergo bleaching (Cunning et al. 2017).

Trophic position and trophic proxy

Compound specific isotopic analysis revealed that both sponge cell and microbial cell fractions contain statistically indistinguishable amino acid composition. While calculation of the trophic position has become standard in determining a relative position in studies within a food web, the values of β and Δ are made on assumptions about the base of the food web being studied and the degree of enrichment between amino acids for each trophic level shift, and can exhibit variation across primary producers and consumers (Chikaraishi et al. 2009, Bradley et al. 2015). Although the absolute values of β and Δ in all predator-prey situations are not known, they are assumed to remain reasonably constant, therefore the difference between the isotopic compositions of trophic and source amino acids drives the calculation of trophic position.

Trophic position proxy (TP) removes the reliance on assumed constants and is based only on the difference in trophic and source amino acids in symbiont and host to reveal a relationship through the trophic position between the organisms (Decima et al. 2013, Bradley et al. 2015). Metazoan consumption would result in the ^{15}N enrichment of trophic amino acids relative to

source amino acids (McClelland and Montoya 2002, Popp et al. 2007, Chikaraishi et al. 2009). The trophic position of sponge cells (S4 + S6 + S7) was not greater than the trophic position of the complementary microbial cell samples (M4, M6 and M7) when determined from average $\delta^{15}N$ values of amino acids. Trophic position using weighted $\delta^{15}N$ averages based on the uncertainty of the measurements also revealed no significant difference in TP between the sponge and its associated microbes.

One caveat is the observation that phagotrophic protists do not necessarily follow the systematic ^{15}N trophic enrichment that is well established for metazoan consumers. Salvage incorporation of AA was thought to be restricted only to bacteria, but the trophic amino acids in protistan consumers are generally not, in fact, significantly enriched in ^{15}N relative to their prey (Gutierrez-Rodrıguez et al. 2014) with the exception of alanine (Gutierrez-Rodrıguez et al. 2014, Decima et al. 2017). While a similar effect cannot currently be eliminated as a possibility for the lack of difference observed between sponge and microbial cell fractions amino acid patterns, all other evidence discussed indicates that it is a direct transfer and incorporation of amino acids from microbes to sponge, inclusive of nonessential amino acids indicating that neither bond breakage nor resynthesis are taking place.

No significant differences in trophic level between the sponge cell and microbial cell fractions are observed. In addition, the $\delta^{15}N$ values of source amino acids and the $\delta^{13}C$ values of essential amino acids are not statistically different in microbial and sponge cell fractions, providing additional evidence that AA in the sponge fraction are directly transferred from the sponge-associated microbes to its host without isotope fractionation. These measures of AA suggest that

amino acids are translocated from the microbial symbionts to the sponge cells rather than through classic trophic transfer found in more typical metazoan consumers.

Sponges acting as a typical metazoan by consuming bacterial cells would exhibit a difference in trophic position through obligate deamination and transamination in amino acids. It appears amino acids are transferred from symbiont to the host by translocation in a manner similar to those found in coral and its symbiont *Symbiodinium* in the transfer of nutrients (Muscatine and Porter 1997, Radecker et al. 2015). Corals similarly harbor a variety of symbiotic archaea and bacteria. Reshef et al. (2006) proposed in their 'coral probiotic hypothesis' that a dynamic relationship between symbiotic microorganisms and the coral host selects for the most advantageous composition of the coral holobiont under varying conditions. Additionally, the translocation of photosynthates to the host can help the symbionts to maintain a favorable C:N ratio (Dubinsky and Jokiel 1994). Sponges may likewise be able to undergo shifts between translocation-like nutrient acquisition and heterotrophic feeding as observed in coral (Houlbreque and Ferrier-Pages 2009) under different environmental regimes. The amino acid compositions of sponge and microbial cells suggest that *M. grandis* acquires carbon and nitrogen predominantly through translocation of AA or through some kind of direct assimilation. Translocation specifically would be a process that does not produce isotopic fractionation. It is not currently known if translocation of amino acids can occur in sponges however our results are consistent with some type of translocation mechanism in sponges. I observe that isotopic compositions of amino acids in sponge and microbes are nearly identical although the sponge cell and microbial cell fractions were composed of distinct cells. In addition, the high ΣV

observed in the sponge is not indicative of a typical metazoan consumer but rather of bacteria or of bacterially reworked organic matter.

Conclusion

Evidence of symbiont-provided nutrition has been well studied in phototrophic sponges (Erwin and Thacker 2008, Freeman and Thacker 2011) as has the ultimate incorporation of algal and coral derived DOM into sponge tissue (de Goeij et al 2008b, Rix et al. 2016, Rix et al. 2017). Microbial symbionts are purported to provide nutrition to the host sponge. While primary producers have been identified as the original source of carbon and nitrogen to reefs and the sponge holobiont, previous experiments did not directly demonstrate that carbon and nitrogen were transferred from photoautotrophs directly to the sponge. Instead, I propose an intermediate step in the transfer of carbon and nitrogen facilitated through bacterial symbionts. It would be unlikely to observe identical isotopic compositions of amino acids in sponge and microbial cells if the direct transfer of AA from photosymbiont to sponge cell was occurring, as photosymbionts and heterotrophic bacteria would not be expected to contain the same amino acid isotopic compositions. Rather, I propose that the bacteria are consuming DOM, resynthesizing the organic material, and passing on nutrition to the sponge in the form of amino acids through translocation. This translocation may be key to the observed efficient transfer of carbon and nitrogen during the DOM uptake segment of the sponge loop. No change in trophic position and absence of amino acid isotopic fractionation between the microbe and the host sponge cells implies that no amine bonds were broken in this transfer of carbon and nitrogen and that a direct translocation of amino acids from symbiont to host is occurring, inclusive of nonessential and "trophic" and "source" amino acids. It has been previously established that *M. grandis* hosts

active nitrifying communities (Shih, this volume, Chapter 3) and there may well be other active microbial communities within the sponge holobiont. I further propose that regenerated ammonia from the sponge may be coupled to ammonia assimilation by its symbiotic bacteria which then synthesize the amino acids translocated to the sponge. Indeed, nitrogen cycling within marine sponges is likely more complex than previously assumed. These data are evidence that the transfer of nutrients from primary producers to sponge are mediated by bacterial symbionts in a process similar to translocation observed in coral.

CHAPTER 5:

Summary of Findings, Conclusion, and Future Directions

This dissertation investigated the influence of the alien invasive sponge *Mycale grandis* and the role it plays in the cycling of nitrogen (N) in shallow coral reef habitats in Hawai‘i. In addition, abundances of the sponge *Mycale grandis* in Kāne‘ohe Bay and seawater pumping rates were ascertained, and life history and key dietary behavior and how their microbial symbionts relate to their nutrition are investigated and discussed. Although this sponge is native to the Indo-Australian south Pacific, no research had previously been done on the sponge in its native habitat. Therefore little was known about the impacts it would have as an alien invasive sponge in Hawai‘i and elsewhere. Anecdotally, the sponge has also spread to regions in Guam and Mexico. The appearance of *M. grandis* in Hawai‘i is of particular significance because Hawai‘i has one of the highest rates of endemism in the world. We owe these unique species to the fact that Hawaiian Archipelago is the most isolated and the largest tropical reef ecosystem on the planet (Coles and Eldredge 2002, Eldredge and Carlton 2002) and thus is extremely susceptible to the threat of invasive species. While research on sponges on tropical coral reefs in the Caribbean provides clues to the success of sponges as community benthic members and their ability to influence biogeochemical cycling on the reefs, we can only infer how some of those roles will manifest in analogous ways on Hawaiian coral reefs. This research focused on collecting data needed to test hypotheses about drivers of sponge biomass and success on the reef and their ability to cycle seawater. Through controlled experiments on live sponges, further hypotheses were addressed regarding the physiological behaviors of the sponge through measurements of pumping rates and through complementary methods of measuring change in dissolved inorganic nutrients (DIN) in seawater that is circulated by the sponge. How the sponge microbiome manipulates DIN levels was measured using incubation methods and comparison methods between sponge excurrent and ambient seawater. Underlying mechanisms of DOM

uptake by the sponge was investigated using compound specific isotope analyses of amino acids. Sponge nutrition appears to be intimately tied to its symbiotic microbial community in a way that is suggestive of direct assimilation of bacterially-produced amino acids rather than through typical metazoan feeding.

From these investigations we can slowly piece together the story of *M. grandis* and what led to its success on local reefs. We have a better understanding of the mechanisms that lead to the observed biomass and how it further shapes its habitat to compete with other benthic members as well as possibly indirectly benefiting other invasive species such as the invasive native macroalga *Dictyosphaeria cavernosa* and non-native macroalgae *Gracilaria salicornia* and *Kappaphycus striatum*. The sponge *M. grandis* grows on the same substrate as native reef building coral. The consequence of this spatial competition, besides the overgrowing of coral itself, is that sponge does not contribute to the creation of new stony substrate and alters the available habitat for other native reef species. Furthermore, sponge metabolic products and algal exudates may further harm coral health (Smith et al. 2006). Despite the lower seawater pumping rates measured in *M. grandis* compared to other sponges (Weisz et al. 2008, Fiore et al. 2013), *M. grandis* still impressively cycles over 100 times its own volume of seawater through its body each day, essentially putting this seawater into direct contact via filtration through its active microbiome. Sponges have been referred to as "microbial fermenters" (Hentschel et al. 2003) and the ability to affect seawater chemistry is a very deliberate strategy for the sponge's various physiological demands. Kāneʻohe Bay is a relatively shallow habitat and the semi-enclosed body of water in the south bay has extremely slow turnover and circulation with seawater residence times measured upwards of one month (Lowe et al. 2009). From pumping measurements and

known circulation information, the degree that *M. grandis* can assert its influence on seawater within the south bay was calculated, defined as the amount of time it takes *M. grandis* to overturn the overlying water column for each zone examined. The findings were compelling in that on Coconut Island Reef 2, which is similar to nearby Reefs 4, 5 and 7, the equivalent of the entire overlying volume is circulated in just 1.9 days. It requires just 3 days for the overlying water column to be circulated through *M. grandis* on the Lilipuna fringing reef. In nearby mangrove areas that were studied, it took merely 3.25 hours for seawater to be circulated through the *M. grandis* community. Whether the DIN produced by the sponge remains within generated nutrient hotspots (Shantz et al. 2015) or is gradually dispersed through diffusion or limited circulation, the local and broad chemistry within south Kāneʻohe bay certainly contains the contribution of sponge-produced DIN.

Previous sponge research especially in the Caribbean and the Mediterranean region have highlighted the importance of sponges on shaping ecosystems dynamics. It has been found that sponges are responsible for driving the high productivity found on coral reefs despite oligotrophic conditions due to their ability to take up dissolved organic matter (DOM) to fuel the rapid growth and shedding of active pumping sponge cells (choanocytes), therefore creating a continual source of POM available to higher trophic levels (de Goeij et al. 2013). The "rainforest of the sea" status of coral reefs can in a very meaningful way be credited to sponges' ability to move and recycle carbon efficiently and rapidly through the ecosystem. Sponges act as hosts for what is essentially a concentrated analogue of the microbial loop (Azam et al. 1938) within their bodies through their proactive pumping activity and dense and active microbial communities within their mesohyl.

Sponges have been found in this and other studies to be a greater source of DIN flux that other sources measured from a variety of habitats in the oceans, including high sources such as marine sediments (Stimson and Larned 2000) and microbial mats (Bonin and Michetoy 2006). I found that the rate of DIN flux from *M. grandis* greatly exceeds the known fluxes measured in coral reefs in other parts of the world as well as known fluxes within Kāne‘ohe Bay inclusive of sediments, reef flats, and reef slopes (Stimson and Larned 2000). As a major source of DIN, sponges can shape the structure of the community in situations where nutrient levels can tip dynamics in one direction or the other. Kāne‘ohe Bay itself is an N limited system except for very short periods after extreme rain events (De Carlo et al. 2007) and so a shift in the N balance due to sponges has the ability to alter ecological aspects within the bay. If the overall baseline N balance in the bay is shifted towards more bioavailable N, the degree of N limitation could be reduced and frequency of N relief could increase. The bay is not generally considered to become phosphorous (P) limited because P is never fully drawn down even by phytoplankton blooms following N input, potentially because P is slowly but steadily released by suspended soil particles following these heavy runoff events (De Carlo et al. 2007).

Chapter 2 assessed current biomass of the sponge on multiple sites within south Kāne‘ohe Bay using belt transects and photo quadrats as well as preliminary details about the life history of the sponge and controls on *M. grandis* in the bay. *M. grandis* currently averages 6.6% coverage over the habitats surveyed in south Kāne‘ohe Bay. While positive growth rates were not measured in specimens kept in aquaria, this does not rule out that *M. grandis* abundances can continue to persist. These are the first updated biomass assessments since those performed by Coles et al. (2006 and 2007) since the mid 2000s and served both as an update and current biomass

comparison to those records and for the purpose of determining the influence of *M. grandis* within the bay based on its abundance combined with its biogeochemical cycling activities. Findings from Coles et al. (2007) on 18 reefs throughout Kāneʻohe Bay indicated that the sponge had its greatest abundance in the south bay near the Hawaiʻi Institute of Marine Biology (HIMB) pier and Coconut Island. Coverage on other reefs decreased to less than 1% on reefs at 1 - 3 km from this area of maximum abundance in the south bay and thus this study was focused on these areas of maximum abundance and significance. There is no indication that *M. grandis* abundance has declined since the mid 2000s despite a recovery from algal dominance within the bay. The presence of *M. grandis* on coral reefs is of first order significance because it is an invasive species that has only been observed in Hawaiʻi since the late 1990s. Chapter 3 utilized Fluorescein dye pumping and videography methods modified from Weisz et al (2008) to determine a seawater pumping rate for *M. grandis*. Seawater filtration coupled to nutrient cycling is generally considered the most important functional role of sponges to reef communities. Ammonia oxidation rates were determined using $^{15}NH_4^+$ incubations of the sponge and DIN fluxes were constrained from analyses of sponge excurrent water compared to ambient seawater. In addition, DIN flux to the reef from *M. grandis* was also determined from biomass and these ammonia oxidation rates. The higher ammonium uptake rates determined from DIN flux measurements suggest that true ammonia oxidation rates are likely at the higher end of rates determined from these experiments because the lack of difference between $[NO_3^-+NO_2^-]$ in ambient and excurrent samples indicate that NO_3^- and NO_2^- may be subsequently lost to denitrification or anammox performed by the sponge microbiome. The implication of this process is that some bioavailable DIN may be removed from the system by the sponge. This raises questions about net DIN flux that must take into consideration both the sponge's own

generated ammonia and sponge-hosted nitrogen loss processes. Chapter 4 elucidated nutritional strategies and trophic relationship of the sponge to its microbial symbionts through bulk and compound specific isotopic analysis of whole sponge and isolated sponge cell and microbial cell fractions. A consortia of microbial types found associated with *M. grandis* was identified through flow cytometry methods (FCM). These broad microbial communities identified within the sponge were examined as a presumed food source for the sponge. No significant difference in amino acid $\delta^{15}N$ and $\delta^{13}C$ values between sponges and its bacterial symbionts was found suggesting that bacterial cells rather than phototrophic feeding is the major source of amino acids in these sponges. Furthermore, sponges may be indirectly rather than directly acquiring carbon and nitrogen from coral and algal derived DOM, although carbon and nitrogen, including labeled C from ^{13}C labeled coral or algal mucus feeding experiments (de Goeij et al. 2008, Rix et al. 2016, Rix et al. 2017) would be passed on to the sponge through its bacterial symbionts. Like the microbial cell fraction, the sponge cell fraction was characterized by high ΣV values, an index indicative of heterotrophic bacterial resynthesis of amino acids. Certainly, *M. grandis* is not feeding on host-associated or water column phytoplankton. Instead, results of amino acid carbon and nitrogen isotopic analyses indicate direct assimilation of bacterially-derived amino acids through either a translocative process or phagotrophic feeding.

Much of the approach to this research on *M. grandis* was based on our knowledge of Caribbean sponges on which the vast majority of previous tropical sponge research has been conducted. These results create a framework for further studies on this and other sponges in Hawai‘i and the Pacific. Although *M. grandis* is the most abundant and conspicuous invasive sponge in Hawai‘i, recent surveys continue to identify additional species of sponges in Hawai‘i, one third of which

are previously unknown species (https://marinegeo.si.edu/place/kane%CA%BBohe-bay-O‘ahu, see also Núñez Pons et al. 2017). In addition, one third of total alien marine species in Hawai‘i are sponges (Eldredge and Carlton 2002). These results established baseline measurements for future studies on *M. grandis* and other sponges in Hawai‘i. For example, how much can *M. grandis* vary its pumping rate? Would we see changes in pumping rate under different levels of particulate or dissolved matter? Do sponges pump more or less over the diel cycle, and can it be linked to primary production either in the water column or within the sponge itself? Perhaps most importantly, how many of the cryptic sponges that are just now being recognized in Kāne‘ohe Bay host microbial consortia similar to that of *M. grandis*, which can affect the biogeochemistry of ambient seawater?

The measurements in this study were performed on cut and transferred sponges that were placed in aquarium tanks for measurements. Though all care was taken to ensure that sponges were handled carefully and were fully healed before experiments, there are likely differences between undisturbed sponges left *in situ* and those raised in aquariums. Furthermore, the flow pattern within aquaria likely modified sponge morphology that adapted to the flow regime found in the water tables. Seawater residence times in aquaria are much shorter than in the environment and therefore sponges may expend less energy pumping to create water flow. I would hypothesize that true pumping rates would be closer to the higher end of rates measured in the aquaria and if future measurements could be made *in situ* we may measure even higher pumping rates. This of course would increase the significance of sponge influence already elucidated in this study. Pumping rates can be measured under known conditions of higher and lower POM and DOM as well to study sponge preference and potential shifts in dietary behavior. Previously *M. grandis*

was believed to reproduce asexually and predominantly by fragmentation (Eldredge and Smith 2001). The discovery of eggs within the mesohyl of samples collected in the month of May is indication of sexual reproduction. Sponge eggs in *M. grandis* have not been previously observed or reported and raise the question of spawning behavior and whether there are spawning seasons for *M. grandis*. This information would address questions about how *M. grandis* spreads to new areas on the reef and if perturbation or stressors to the animal induces spawning. *M. grandis* also spreads by fragmentation that can be facilitated through activities that mechanically break and propagate sponge pieces. Both fragmentation and possible stress-induced spawning necessitate care in sponge removal methods for both research and invasive species control.

While identification of phylotypes (Wang et al. 2009) and flow cytometry methods have helped to identify populations present in the sponge microbiome, they do not provide abundances of individual populations found within the sponge nor provide information about which populations are most biogeochemically active. The fraction of some of the dormant and active broad populations of associated microbes could be identified using flow cytometry methods, but whether those populations were active could not be ascertained. Functional genomics would identify which biogeochemical transformations are performed most actively by the microbial communities hosted within *M. grandis*. The differences in DIN measured in the sponge excurrent versus ambient seawater revealed that while the sponge was actively taking up ammonium as also confirmed through the $^{15}NH_4^+$ incubations, little change in $NO_3^- + NO_2^-$ was found in the excurrent, implying that there must be a further sink for $NO_3^- + NO_2^-$ created by sponge-mediated ammonia oxidation. The natural question to ask is whether *M. grandis* hosts N loss processes such as denitrification or anammox. ^{15}N labeled substrates can be used to distinguish

denitrification versus anammox mechanisms for N_2 production by sponge-hosted microbes using the modified isotope pairing technique (IPT) (Trimmer et al. 2006) in experiments conducted in sealed *in situ* incubation chambers of the sponge. The modified IPT method uses ^{15}N-labeling of N_2O to determine the ratio of $^{14}NO_x^-$ to $^{15}NO_x^-$, which distinguishes between N_2 production via anammox and denitrification (Risgaard-Petersen et al. 2003, Trimmer et al. 2006). Interpretation of ^{15}N tracer results is complicated because NH_4^+ and $NO_3^- + NO_2^-$ with natural abundance ^{15}N contents are always present in incubations due to respiration and nitrification (e.g., Corredor et al. 1988, Southwell et al. 2008b). Isotopic labeling using $^{15}NH_4^+$ and $^{15}NO_3^-$ could be used to distinguish between major nitrogen loss processes. When $^{15}NH_4^+$ is added $^{29}N_2$ could be produced by coupled nitrification-denitrification ($^{15}NH_4^+ \rightarrow {}^{15}NO_2^-$ + ambient $^{14}NO_x^-$) or by anammox ($^{15}NH_4^+$ + ambient $^{14}NO_2^-$). Likewise, when $^{15}NO_3^-$ is added, $^{29}N_2$ could be produced by denitrification ($^{15}NO_3^-$ + ambient $^{14}NO_x^-$) or anammox ($^{15}NO_3^- \rightarrow {}^{15}NO_2^-$ + ambient $^{14}NH_4^+$).

As we work towards a more complete picture for the biogeochemical processes performed by *M. grandis*, we will be able to answer questions on the net contribution of *M. grandis* to the N pool within Kāne‘ohe Bay. How much net nitrification does *M. grandis* perform when taking into account regenerated ammonium? How much of this N+N is further lost through N loss processes? Does *M. grandis* serve as a net positive or negative flux of DIN to the reef? Is this flux involved in any kind of feedback cycle? Could there be a balance whereby conditions that allow for sponge growth then draws down local DIN and POM/DOM and creates a stable phase shift on the reef inclusive of sponges and coral, for example? Do macroalgae and sponges help or harm each other through similar processes?

Amino acid isotopic composition between sponge cell and microbial cell fractions imply that bacterially-produced amino acids, including nonessential and source amino acids, are directly assimilated into the sponge and that for *M. grandis* this may be the dominant if not sole source of carbon and nitrogen for the sponge. Can *M. grandis* switch to other feeding strategies? If so, it would necessarily be reflected in the amino acid isotopic composition, which were identical to bacterial amino acids in this study. Do symbiotic bacteria serve as an intermediary between other sources of carbon and nitrogen on the reef and the sponge, in other words, is the uptake of carbon and nitrogen from coral and algal derived DOM passed on to the sponge through its bacterial symbionts? If so, is this a process similar to -or identical to- translocation observed in coral between the coral animal and their *Symbiodinium*? Can the microbial communities found within sponge and coral holobionts on the same reef undergo horizontal transmission between the two hosts?

Preliminary and intriguing results of carbon and nitrogen contents and whole sponge nitrogen isotopic composition suggest a strong influence of corals on sponge nutrition. In a single experiment, sponges from Reef 4 were collected and whole sponge C:N molar ratio and $\delta^{15}N$ values were determined. A subset of these sponges was incubated for six weeks in aquaria with flow through seawater at HIMB. Some sponges were incubated in contact with coral (*Montipora capitata* and *Porites compressa*) whereas other sponges were incubated in tanks without corals. At the end of the experiment, whole sponge C:N molar ratio and $\delta^{15}N$ values were determined (Figure 5.1). These results indicate that when sponges are incubated in contact with coral for six weeks, C:N ratios and $\delta^{15}N$ values of *M. grandis* are lowered significantly (t test, $p < 0.001$) and there is a significant positive correlation between C:N ratios and $\delta^{15}N$ values for all specimens

analyzed ($R^2 = 0.87$, $F < 0.001$). Although the mechanism(s) responsible for change in C:N ratios and $\delta^{15}N$ values of *M. grandis* are unknown, they suggest that sponge nutrition may be derived from corals when the two are grown in contact with each other and perhaps sponge nutrition is derived from coral mucus as has been suggested for other sponges (Rix et al. 2016, Rix et al, 2017). It is unknown if these results indicate that only the sponge benefits from intimate contact with corals or if the relationship is beneficial to both sponges and corals. Since many of the previously unrecognized cryptic sponges in Kāneʻohe Bay are found in association with corals, it could be significant to further investigate other specimens of *M. grandis* as well as other sponges growing in association with corals in Kāneʻohe Bay (e.g., see Figure 2.2).

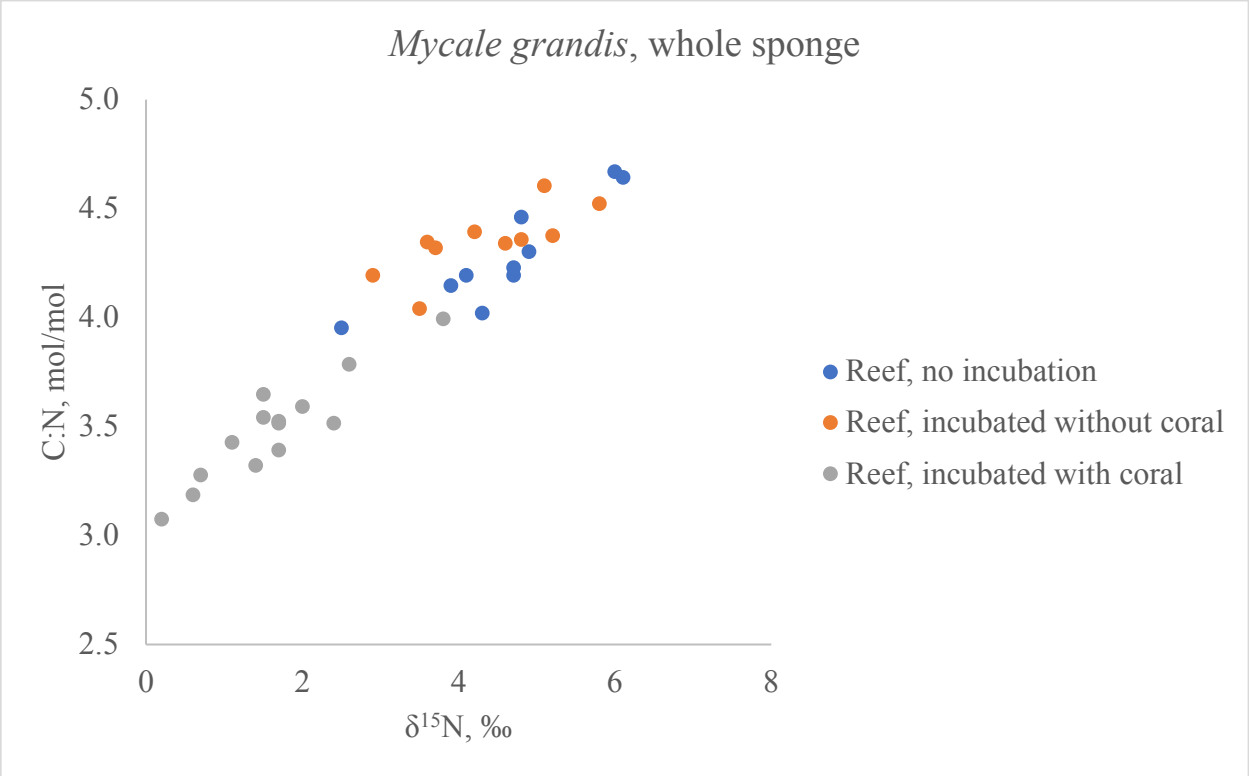

Figure 5.1: C:N molar ratios and $\delta^{15}N$ values of *M. grandis* from Reef 4 in Kāneʻohe Bay. Sponges incubated with corals in aquaria with flow-through seawater have significantly lower C:N ratios and $\delta^{15}N$ values compared with sponges collected from Reef 4 and analyzed as well as sponges that were collected from Reef 4 and incubated for six weeks without sponges (t test, $p < 0.001$).

The original contributions of this work contain several first descriptions of a Pacific sponge including ammonia oxidation rates, pumping rates, and its relationship with its microbial symbionts through the separation of *M. grandis* sponge cells from its microbial cells. These data complement similar research conducted in other ocean basins with the added component of examining the influence of the sponge in the context of a fairly new invasive species on its environment. Furthermore, I employ powerful compound specific isotopic analysis tools to examine sponge dietary sources relative to its bacterial symbionts. Thus far, minimal research using amino acid ^{13}C and ^{15}N tools has been applied to sponge dietary studies.

The broad implication of this research is that demosponges such as *M. grandis* have evolved exceptional life strategies through their well-established associations with its symbiotic microbes (Wilkinson 1984) that likely led to its success within new and degraded environments through competitive substrate acquisition and high adaptability. Ecological dynamics are driven and supported by microbially driven chemistry, and sponges are essentially prolific and deliberate hubs for biogeochemical activity. The most obvious application of this research is to use what we have learned about a highly successful invasive species for consideration of local invasive species management and as an incentive for and how to prevent the spread of invasive sponges to other reef habitats in Hawai‘i. In the context of research, these findings compel us to consider how increases in sponge biomass can be due to or cause the success or decline of other species and how it can enhance, influence, or drive nutrient dynamics within the observed phase shifts in Kāne‘ohe Bay. *M. grandis* certainly has the ability to directly impact the success of some species through spatial competition, but the more interesting questions revolve around how these sponges shape overall biogeochemistry on the reef and the implications of those findings. How

this sponge will affect coral reef resilience in the future grows in relevance throughout ecosystems in Hawai‘i and around the world as these valuable ecosystems respond to further changes to anthropogenic activity, ocean warming, and ocean acidification.

All sponge specimens were collected under the Special Activity Permits (SAP): SAP 2015–7, SAP 2016–55, and SAP 2018-3 issued by the Board of Land and Natural Resources Department, Division of Aquatic Resources, State of Hawai’i.

APPENDIX

Sponge	Initial mass (g)	mass (g) 4 weeks	mass (g) 10 weeks	% change in mass
1	56.56	49.77	45.25	20
2	49.75	35.82	37.3	25
3	77.22	72.6	64.1	17
4	64.89	51.26	46.45	28
5	39.08	32.05	25.4	35
			Average	24

Table A.1: Change in mass of *M. grandis* kept in aquaria to measure growth rates. Wet weight was measured in g on an analytical scale in the Wetlab at the Hawai‘i Institute of Marine Biology. All sponges exhibited a decline in mass averaging a loss of 24% and ranging from 17% to 35% loss from the initial weight over ten weeks.

Table A.2: $^{15}NH_4^+$ oxidation rates measured in 0.1 µM, 1.0 µM, 5.0 µM, and 10.0 µM added $^{15}NH_4^+$ incubations. Includes rate for each time interval, mean rate by concentration, and mean rate of all incubations.

Sponge	[$^{15}NH_4^+$] added	Incubation duration (hrs)	Vol. sponge (ml)	$^{15}NH_4^+$ ox. rate in nM/h/g for each interval (dry weight)
A	0.1	0.0	280	-
A	0.1	0.6	280	(289.3)
A	0.1	1.1	280	13.9
A	0.1	2.1	280	18.0
A	0.1	4.2	280	12.8
			Ave rate for Sponge A:	14.9
B	0.1	0.0	415	-
B	0.1	0.6	415	37.8
B	0.1	0.6	415	38.1
B	0.1	1.1	415	23.8
B	0.1	2.1	415	25.7
B	0.1	4.3	415	17.8
			Ave rate for Sponge B:	28.6
			Ave of 0.1µM incubations:	23.5
C	1	0.0	195	-
C◇	1	0.6	195	7.40
C	1	1.1	195	75.11
C*	1	2.1	195	63.88
C*	1	4.3	195	35.99
			Ave rate for Sponge C: 75.11	
D	1	0.0	250	-
D	1	0.6	250	69.90
D	1	1.1	250	49.27
D	1	2.1	250	46.58
D*	1	4.3	250	26.93
			Ave rate for Sponge D:	55.25
			Ave of 1.0µM incubations:	60.22

(continued on next page)

E	5	0.0	39	-
E	5	0.0	39	-
E	5	0.7	39	5.7
E	5	1.2	39	8.1
E	5	2.2	39	13.4
E	5	3.7	39	13.7
E	5	3.7	39	11.8
			Ave rate for Sponge E:	10.6
F	5	0.0	41	-
F	5	0.0	41	-
F	5	0.7	41	4.0
F	5	0.7	41	3.9
F	5	1.2	41	5.9
F	5	2.2	41	8.1
F	5	2.2	41	8.0
F	5	3.7	41	9.4
			Ave rate for Sponge F:	6.6
			Ave of 5.0μM incubations:	8.4
G	10	0.0	395	-
G	10	0.0	395	-
G◇	10	0.5	395	4.2
G	10	0.5	395	4.6
G◇	10	0.5	395	4.6
G*	10	1.1	395	4.6
G*	10	2.1	395	4.5
G*	10	3.7	395	3.0
			Ave rate for Sponge G:	4.6
H	10	0.0	375	-
H	10	0.0	375	-
H◇	10	0.5	375	4.8
H	10	0.5	375	5.0
H*	10	1.1	375	4.3
H*	10	2.1	375	3.8
H*	10	3.7	375	2.9
			Ave rate for Sponge H:	5.0
			Ave of 10.0μM incubations:	4.8
			Mean rate (all)	21.2
			Min rate (all)	3.9
			Max rate (all)	75.1

◇ sample peaks too small
* maxed out detector
() Outlier excluded from analyses (>2σ)

	NH_4^+ (µmol L^{-1})		NO_3^- + NO_2^- (µmol L^{-1})		TN (µmol L^{-1})		TP (µmol L^{-1})		PO_4^{3-} (µmol L^{-1})		$Si(OH)_4$ (µmol L^{-1})	
	Ambient	**Exhalent**	**Ambient**	**Exhalent**	**Ambient**	**Exhalent**	**Ambient**	**Exhalent**	**Ambient**	**Exhalent**	**Ambient**	**Exhalent**
Sponge 1	9.2	6.5	0.1	0.2	9.5	8.2	0.5	0.5	0.1	0.1	8.3	12.0
Sponge 2	6.7	5.1	0.3	0.2	11.8	7.8	0.9	0.5	0.1	0.1	8.0	7.8
Sponge 3	13.5	7.6	0.3	0.3	13.6	7.9	0.4	0.5	0.0	0.1	8.3	7.1
Sponge 4	6.1	4.3	0.6	0.5	9.1	7.8	0.5	0.5	0.1	0.1	9.1	7.0
Sponge 5	4.1	5.4	0.7	0.5	7.9	9.1	1.7	1.7	0.1	0.1	10.3	6.9

Table A.3: Nutrient concentrations measured in ambient seawater versus sponge exhalent samples. TN=total nitrogen, TP=total phosphorus. Concentrations are reported in µmol L^{-1}.

Figure A.1: Flow cytometry count event images. For microbial cell samples parameters for lowChl, hiChl, and HBACT were measured. For sponge cell samples parameters for HiDNA, lowChl, lowDNA, and lowChlLowSS were measured. Sponge samples (S) were run at a much lower voltage setting (~400 vs. 900 V) for Chl and DNA detectors indicating that the signals on those detectors are much higher than in the microbial (M) samples. This indicates there is more DNA per cell and more Chl per cell when present.

Sample M1

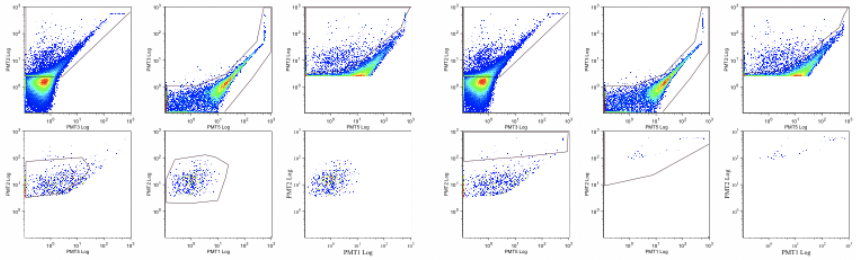

lowChl
00057736.LMD
Event Count: 2164

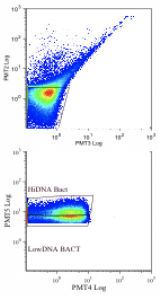

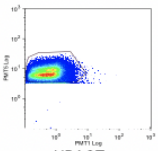

HBACT
00057736.LMD
Event Count: 228093
Frequency: 78

hiChl
00057736.LMD
Event Count: 118

Sample M2

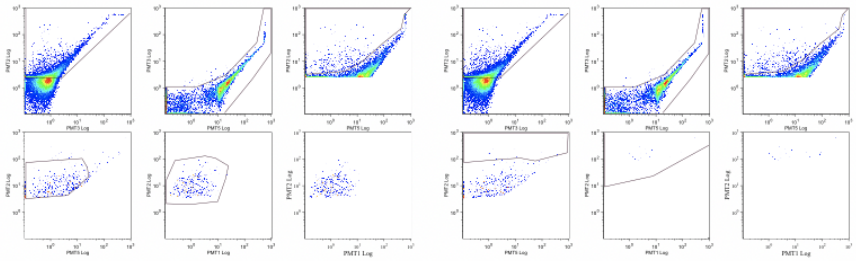

lowChl
00057737.LMD
Event Count: 908

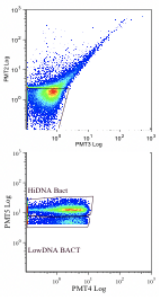

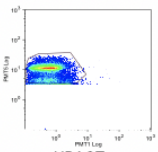

HBACT
00057737.LMD
Event Count: 83784
Frequency: 69

hiChl
00057737.LMD
Event Count: 31

Sample M3

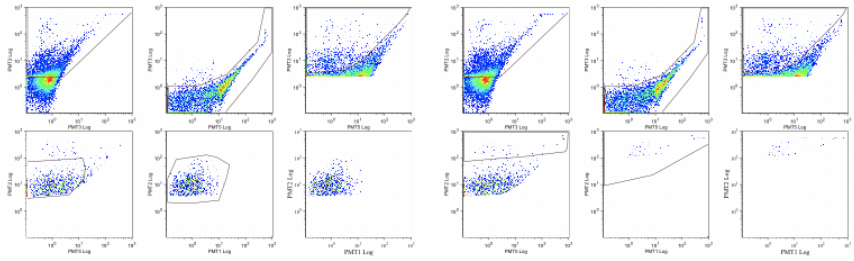

lowChl
00057738.LMD
Event Count: 3093

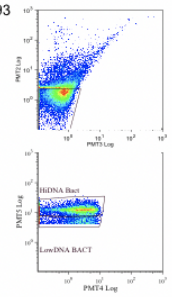

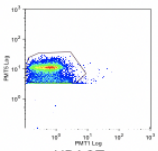

HBACT
00057738.LMD
Event Count: 43859
Frequency: 60

hiChl
00057738.LMD
Event Count: 158

Sample M4

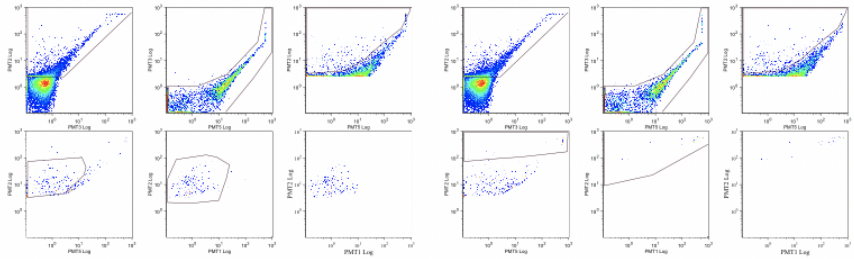

lowChl
00057739.LMD
Event Count: 489

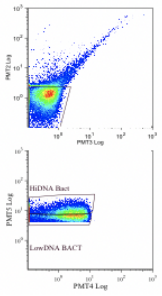

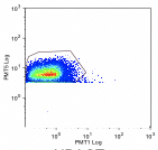

HBACT
00057739.LMD
Event Count: 78779
Frequency: 80

hiChl
00057739.LMD
Event Count: 76

Sample M5

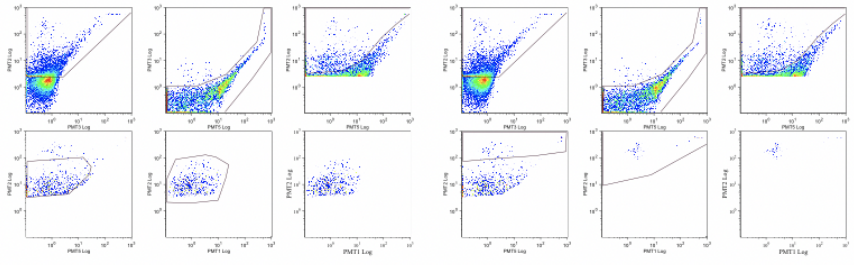

lowChl
00057740.LMD
Event Count: 1963

hiChl
00057740.LMD
Event Count: 139

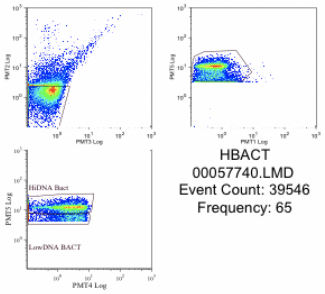

HBACT
00057740.LMD
Event Count: 39546
Frequency: 65

Sample M6

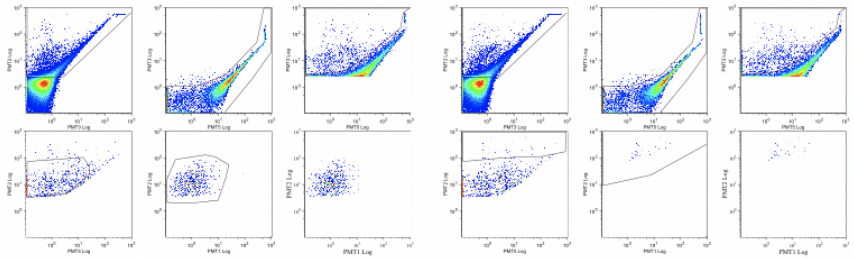

lowChl
00057741.LMD
Event Count: 2359

hiChl
00057741.LMD
Event Count: 102

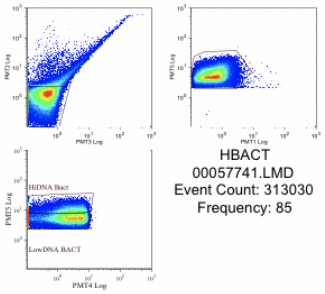

HBACT
00057741.LMD
Event Count: 313030
Frequency: 85

Sample M7

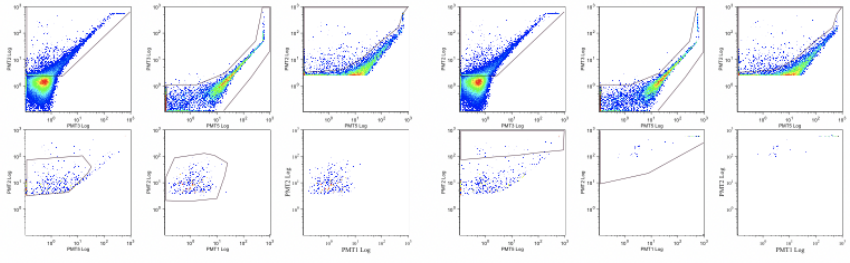

lowChl
00057742.LMD
Event Count: 1110

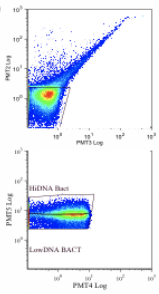

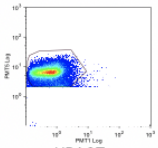

HBACT
00057742.LMD
Event Count: 155905
Frequency: 83

hiChl
00057742.LMD
Event Count: 148

Sample M8

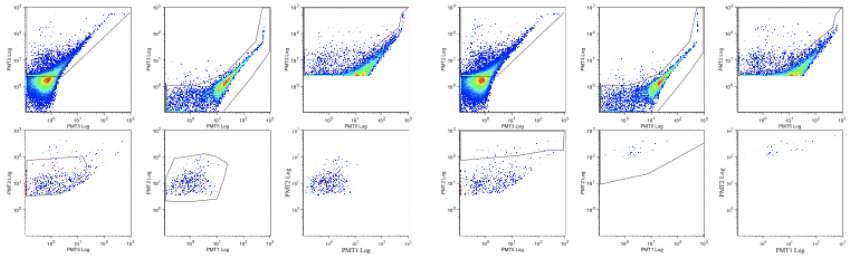

lowChl
00057743.LMD
Event Count: 1775

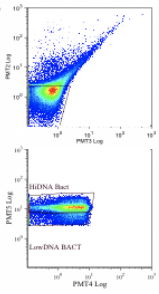

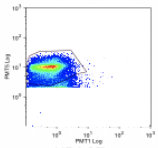

HBACT
00057743.LMD
Event Count: 138749
Frequency: 71

hiChl
00057743.LMD
Event Count: 87

Sample S1

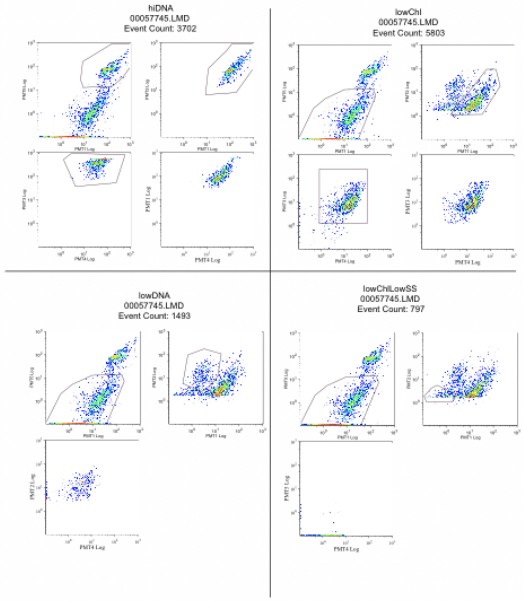

Sample S2

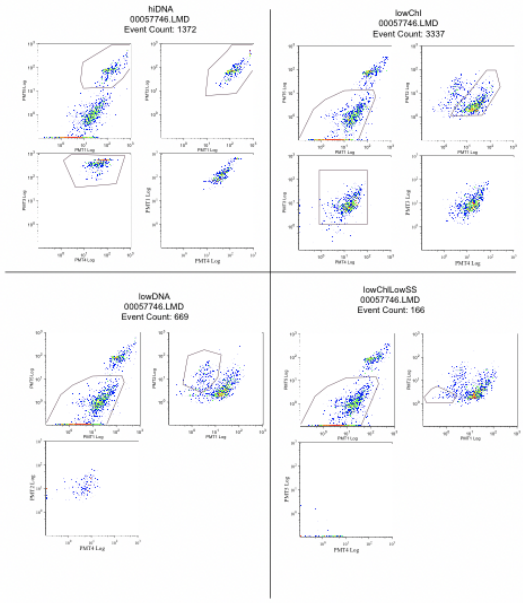

Sample S3

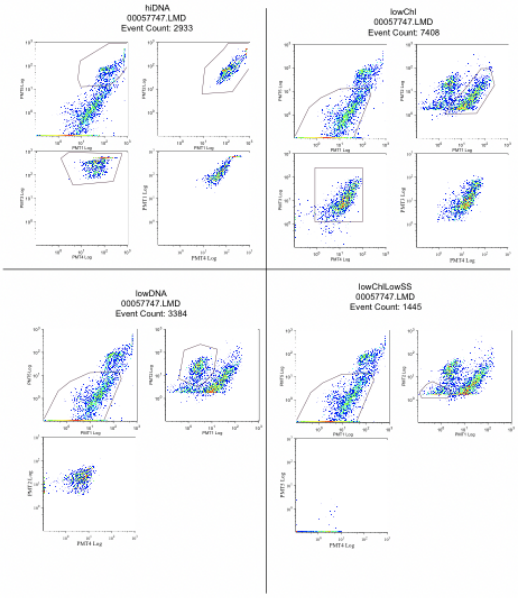

Sample S4

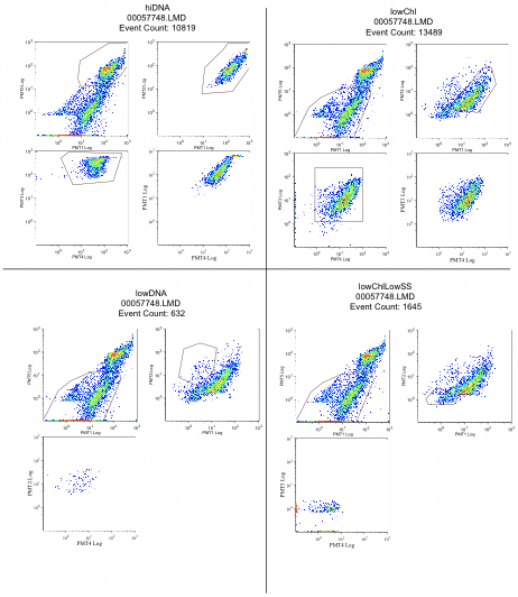

Sample S5

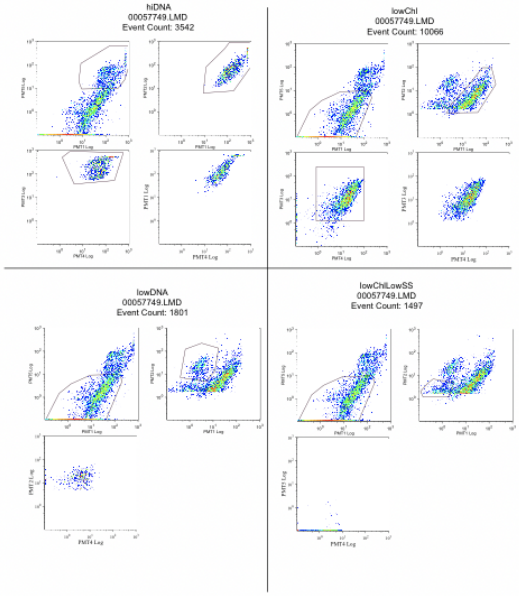

Sample S6

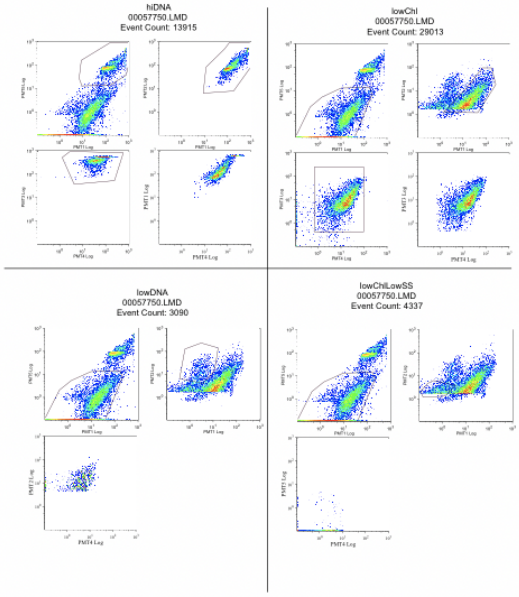

Sample S7

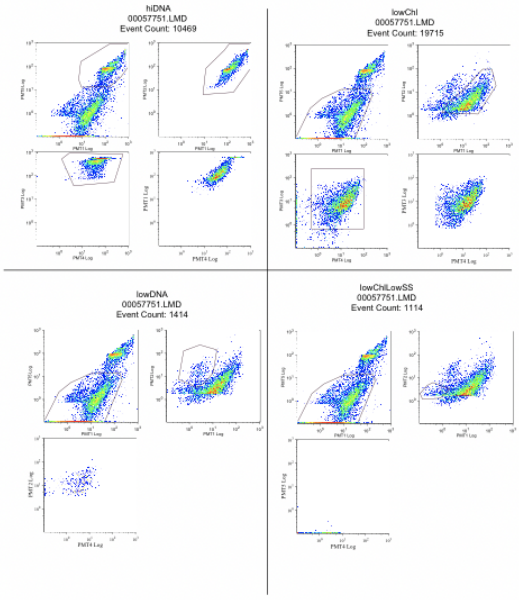

Sample S8

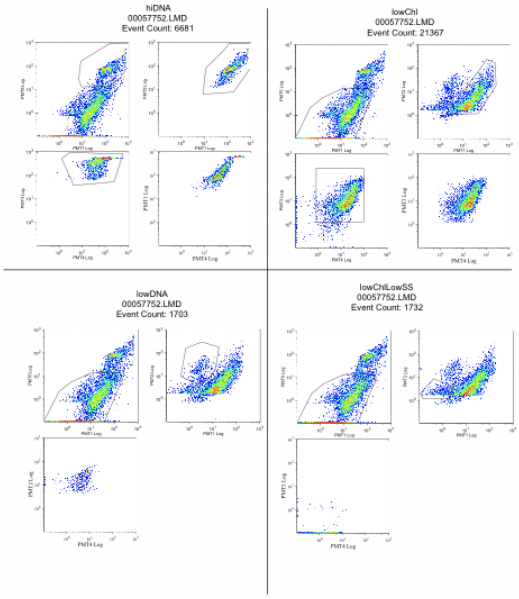

REFERENCES

Armstrong FAJ, Sterns CR, Strickland JDH. 1967. The measurement of upwelling and subsequent biological processes by means of the Technicon AutoAnalyzer and associated equipment. Deep-Sea Res. 14(3): 381-389.

Arthur KE, Kelez S, Larsen T, Choy CA, Popp BN. 2014. Tracing the biosynthetic source of essential amino acids in marine turtles using $\delta^{13}C$ fingerprints. Ecology. 95:1285-1293.

Atkinson, MJ. 1987. Rates of phosphate uptake by coral reef flat communities. Limnol Oceanogr. 32: 426–435.

Azam F, Field JG, Graf JS, Meyer-Rei LA, Thingstad F. 1983. The Ecological Role of Water-Column Microbes in the Sea*. Mar. Ecol. Prog. Ser. 10: 257–263.

Barford CC, Montoya JP, Altabet MA, Mitchell R. 1999. Steady-state nitrogen isotope effects of N_2 and N_2O production in *Paracoccus denitrificans*. Appl Environ Microbiol. 65(3):989–94.

Bathen K. 1968. A descriptive study of the physical oceanography of Kane'ohe Bay, O'ahu, Hawai'i. Department of Oceanography. Honolulu, University of Hawai'i at Manoa.

Bayer K, Schmitt S, Hentschel U. 2007. Microbial nitrification in Mediterranean sponges: possible involvement of ammonia-oxidizing *Betaproteobacteria*. Porifera Res Biodiversity, Innov Sustain. 2007: 165–71.

Bell JJ, Davy SK, Jones T, Taylor MW, Webster NS. 2013. Could some coral reefs become sponge reefs as our climate changes? Glob Chang Biol. 19(9):2613–24.

Beman JM, Popp BN, Francis CA. 2008. Molecular and biogeochemical evidence for ammonia oxidation by marine *Crenarchaeota* in the Gulf of California. ISME J. 2: 429–441.

Beman JM, Chow C-E, King AL, Feng Y, Fuhrman JA, Andersson A, et al. 2011. Global declines in oceanic nitrification rates as a consequence of ocean acidification. Proc Natl Acad Sci. 108(1):208–13.

Beman JM, Popp BN, Alford SE. 2012. Quantification of ammonia oxidation rates and ammonia-oxidizing archaea and bacteria at high resolution in the Gulf of California and eastern tropical North Pacific Ocean. Limnol Oceanogr. 57(3):711–26.

Beman JM, Shih JL, Popp BN. 2013. Nitrite oxidation in the upper water column and oxygen minimum zone of the eastern tropical North Pacific Ocean. ISME J. 7(11):2192–205.

Birkeland C. 1997. Life and death of coral reefs. Chapman & Hall. 536 p.

Bonin PC, Michetoy VD. 2006. Nitrogen budget in a microbial mat in the Camargue (southern France). Mar Ecol Prog Ser Mar Ecol Prog Ser. 322:75–84.

Botting JP, Muir LA, Zhang Y, Ma X, Ma J, Wang L, et al. 2017. Flourishing Sponge-Based Ecosystems after the End-Ordovician Mass Extinction. Curr Biol. 27(4):556–62.

Bradley CJ, Madigan DJ, Block BA, Popp BN. 2014. Amino Acid Isotope Incorporation and Enrichment Factors in Pacific Bluefin Tuna, Thunnus orientalis. PLoS One. 9(1):e85818.

Bradley CJ, Wallsgrove NJ, Choy CA, Drazen JC, Hetherington ED, Hoen DK, Popp BN. 2015. Trophic position estimates of marine teleosts using amino acid compound specific isotopic analysis. Limnol Oceanogr Methods. 13:476-493.

Bryan, PG. 1973. Growth rate, toxicity, and distribution of the encrusting sponge *Terpios sp.*(*Hadromeridea: Suberitidae*) in Guam, Mariana Islands. Micronesica 9: 237-242.

Calleja ML, Batista F, Peacock M, Kudela R, McCarthy MD. 2013. Changes in compound specific $\delta^{15}N$ amino acid signatures and D/L ratios in marine dissolved organic matter induced by heterotrophic bacterial reworking. Mar. Chem. 149, 32–44.

Casciotti KL, Sigman DM, Hastings MG, Böhlke JK, Hilkert A. 2002. Measurement of the oxygen isotopic composition of nitrate in seawater and freshwater using the denitrifier method. Analytical Chemistry. 74, 4905–4912.

Cheshire AC, Wilkinson CR. 1991. Modelling the photosynthetic production by sponges on Davies Reef Great Barrier Reef Australia. Mar Biol. 109:13–18.

Christman GD, Cottrell MT, Popp BN, Gier E, Kirchman DL. 2011. Abundance, Diversity, and activity of ammonia-oxidizing prokaryotes in the Coastal Arctic Ocean in summer and winter. Appl. Environ. Microbiol. 77, 2026–2034.

Chikaraishi Y, Ogawa NO, Kashiyama Y, Takano Y, Suga H, Tomitani A, et al. 2009. Determination of aquatic food-web structure based on compound-specific nitrogen isotopic composition of amino acids. Limnol Oceanogr Methods. 7(11):740–50.

Coles SL, DeFelice RC, Eldredge LG, Carlton JT. 1999. Historical and recent introductions of non-indigenous marine species into Pearl Harbor, Oahu, Hawaiian Islands. Mar Biol. 135(1):147–58.

Coles SL, and Eldredge LG. 2002. Non- indigenous species introductions on coral reefs: A need for information. Pac. Sci. 56:191–209.

Coles SL, Eldredge LG, Kandel F, Reath PR, Longenecker K. 2004. Assessment of nonindigenous species on coral reefs in the Hawaiian Islands with emphasis of introduced invertebrates, Bishop Museum, Tech. Rep. No. 27, Honolulu.

Coles SL and Bolick H. 2006. Assessment of Invasiveness of the Orange Keyhole Sponge *Mycale Armata* in Kāneʻohe Bay, Oahu, Hawaiʻi Final Report Year 1.

Coles SL, Marchetti J, Bolick HA, Montgomery SL. 2007. Assessment of Invasiveness of the Orange Keyhole Sponge *Mycale armata* in Kāneʻohe Bay, Oʻahu, Hawaiʻi. Final Report, Year 2.

Corredor JE and Morell H. 1985. Inorganic nitrogen in coral reef sediments. Mar. Chem. 16: 379-384.

Corredor JE, Wilkinson CR, Vicente VP, Morell JM, Otero E. 1988. Nitrate release by Caribbean reef sponges. Limnol Oceanogr. 33(1):114–20.

Cox E, Ribes M, Kinzie RA. 2006. Temporal and spatial scaling of planktonic responses to nutrient inputs into a subtropical embayment. Mar Ecol Prog Ser. 324:19–35.

Cunning R, Muller EB, Gates RD, Nisbet RM. 2017. A dynamic bioenergetic model for coral-*Symbiodinium* symbioses and coral bleaching as an alternate stable state. J Theor Biol. 431:49–62.

Dale JJ, Wallsgrove NJ, Popp BN, Holland KN. 2011. Nursery habitat use and foraging ecology of the brown stingray *Dasyatis lata* determined from stomach contents, bulk and amino acid stable isotopes. Mar Ecol Prog Ser. 433:221–36.

De Carlo EH, Hoover DJ, Young CW, Hoover RS, Mackenzie FT. 2007. Impact of storm runoff from tropical watersheds on coastal water quality and productivity. Appl Geochemistry. 22:1777–97.

DeCarlo TM, Cohen AL, Barkley HC, Cobban Q, Young C, Shamberger KE, et al. 2015. Coral macrobioerosion is accelerated by ocean acidification and nutrients. Geology. 43(1):7–10.

de Goeij JM, Van Duyl FC. 2007. Coral cavities are sinks of dissolved organic carbon (DOC). Limnol Oceanogr. 52(6):2608–17.

de Goeij JM, van den Berg H, van Oostveen MM, Epping EHG, van Duyl FC. 2008a. Major bulk dissolved organic carbon (DOC) removal by encrusting coral reef cavity sponges. Mar Ecol Prog Ser ;357:139–51.

de Goeij JM, Moodley L, Houtekamer M, Carballeira NM, Van Duyl FC. 2008b. Tracing ^{13}C-enriched dissolved and particulate organic carbon in the bacteria- containing coral reef sponge *Halisarca caerulea*: Evidence for DOM feeding. Limnol Oceanogr. 53(4):1376–86.

de Goeij JM, De Kluijver A, Van Duyl FC, Vacelet J, Wijffels RH, De Goeij AFPM, et al. 2009. Cell kinetics of the marine sponge *Halisarca caerulea* reveal rapid cell turnover and shedding. J Exp Biol. 212(23):3892–900.

de Goeij JM, van Oevelen D, Vermeij MJA, Osinga R, Middelburg JJ, de Goeij AFPM, et al. 2013. Surviving in a marine desert: the sponge loop retains resources within coral reefs. Science. 342(6154):108–10.

De Laubenfels MW. 1950. The Sponges of Kāne‘ohe Bay, Oahu. Pacific Sci. 4(1):3–36.

De Laubenfels MW. 1951. The Sponges of the Island of Hawai‘i. Pacific Sci. 5(3):256–71.

Décima M, Landry MR, Bradley CJ, Fogel ML. 2017. Alanine δ^{15}N trophic fractionation in heterotrophic protists. Limnol Oceanogr. 62(5):2308–22.

Diaz MC, Ward BB. 1997. Sponge-mediated nitrification in tropical benthic communities. Mar Ecol Prog Ser. 156:97–107.

Doney SC. 2010. The growing human footprint on coastal and open-ocean biogeochemistry. Science. 328:1512-1516.

Dore JE and Karl DM. 1996. Nitrite distributions and dynamics at Station ALOHA. Deep Sea Res Part II Top Stud Oceanogr. 43(2–3):385–402.

Dore JE, Popp BN, Karl DM, Sansone FJ, 1998. A large source of atmospheric nitrous oxide from subtropical North Pacific surface waters. Nature. 396, 63–66.

Drupp P, De Carlo EHB, Mackenzie F, Bienfang P, Sabine C et al. 2011. Nutrient Inputs, Phytoplankton Response, and CO_2 Variations in a Semi-Enclosed Subtropical Embayment, Kāne‘ohe Bay, Hawai‘i. Aquat Geochem. 17:473–98.

Dubinsky Z and Jokiel PL. 1994. Ratio of energy and nutrient fluxes regulates symbiosis between zooxanthellae and corals. Pac. Sci. 48: 313–324.

Duckworth AR, West L, Vansach T, Stubler A, Hardt M. 2012. Effects of water temperature and pH on growth and metabolite biosynthesis of coral reef sponges. Marine Ecology Progress Series. 462: 67–77.

Dudgeon SR, Aronson RB, Bruno JF, Precht WF. 2010. Phase shifts and stable states on coral reefs. Mar Ecol Prog Ser. 413:201–16.

Eldredge LG, Smith CM. 2001. A Guidebook of Introduced Marine Species in Hawai‘i. Bishop Museum Tech Rep 21.

Eldredge LG, Carlton JT. 2002. Hawaiian Marine Bioinvasions: A Preliminary Assessment. Pacific Sci. 56(2):211–2.

Erwin PM, Thacker RW. 2007. Incidence and identity of photosynthetic symbionts in Caribbean coral reef sponge assemblages. Journal of the Marine Biological Association of the United Kingdom. 87: 1683–1692.

Erwin PM, Thacker RW. 2008. Phototrophic nutrition and symbiont diversity of two Caribbean sponge–cyanobacteria symbioses. Mar Ecol Prog Ser. 362:139–47.

Fabry VJ, Seibel BA, Feely RA, Orr JC. 2008. Impacts of ocean acidification on marine fauna and ecosystem processes. ICES J Mar Sci. 65(3):414–32.

Falkowski PG, Fenchel T, Delong EF. 2008. The Microbial Engines That Drive Earth's Biogeochemical Cycles. Science 320:1034–8.

Fernandes R, Nadeau M-J, Grootes PM. 2012. Macronutrient- based model for dietary carbon routing in bone collagen and bioapatite. Archaeological and Anthropological Sciences. 4, 291–301.

Fiore CL, Jarett JK, Olson ND, Lesser MP. 2010. Nitrogen fixation and nitrogen trans-formations in marine symbioses. Trends in Microbiology. 18, 455–463.

Fiore CL, Baker DM, Lesser MP. 2013. Nitrogen Biogeochemistry in the Caribbean Sponge, *Xestospongia muta*: A Source or Sink of Dissolved Inorganic Nitrogen? PLoS One. 8(8):1–11.

Fiore CL, Freeman CJ, Kujawinski EB. 2017. Sponge exhalent seawater contains a unique chemical profile of dissolved organic matter. PeerJ 5:e2870; DOI 10.7717/peerj.2870

Freeman CJ, Thacker RW. 2011. Complex interactions between marine sponges and their symbiotic microbial communities. Limnol Oceanogr. 56(5):1577–86.

Freeman CJ, Thacker RW, Baker DM, Fogel ML. 2013. Quality or quantity: is nutrient transfer driven more by symbiont identity and productivity than by symbiont abundance? ISME J. 7(10):1116–25.

Fukuda R, Ogawa H, Nagata T, Koike I. 1998. Direct determination of carbon and nitrogen contents of natural bacterial assemblages in marine environments. Appl Environ Microbiol. 64:3352–3358.

Fuller BT, Petzke KJ. 2017. The dietary protein paradox and threonine ^{15} N-depletion: Pyridoxal-5'-phosphate enzyme activity as a mechanism for the δ^{15} N trophic level effect. Rapid Commun Mass Spectrom. 31(8):705–18.

Furnas M, Mitchell A, Skuza M, Brodie J. 2005. In the other 90%: phytoplankton responses to enhanced nutrient availability in the Great Barrier Reef Lagoon. Mar Pollut Bull. 51:253–65.

Garrison DL, Gowing MM, Hughes MP, Campbell L, Caron DA, Dennett MR, et al. 2000. Microbial food web structure in the Arabian Sea: a US JGOFS study. Deep Sea Res Part II Top Stud Oceanogr. 47(7–8):1387–422.

Gerodette, T, and Flechsig, AO. 1979. Sediment-induced reduction in the pumping rate of the tropical sponge *Verongia lacunosa*. Mar Biol. 55: 103–110.

Glibert PM, Wilkerson FP, Dugdale RC, Raven JA, Dupont CL, Leavitt PR, et al. 2015. Pluses and minuses of ammonium and nitrate uptake and assimilation by phytoplankton and implications for productivity and community composition, with emphasis on nitrogen-enriched conditions. Limnol Oceanogr. 61:165–97.

Gloeckner V, Wehrl M, Moitinho-Silva L, Gernert C, Schupp P, Pawlik JR, et al. 2014. The HMA-LMA Dichotomy Revisited: an Electron Microscopical Survey of 56 Sponge Species. Biol Bull. 227:78–88.

Gómez C, Larsen T, Popp BN, Hobson KA, Cadena KD. 2018. Assessing seasonal changes in animal diets with stable-isotope analysis of amino acids: a migratory boreal songbird switches diet over its annual cycle. *Oecologia.* 187:1-13.

González-Rivero M, Yakob L, Mumby PJ. 2011. The role of sponge competition on coral reef alternative steady states. Ecol Modell. 222:1847–53.

Grasshoff K, Ehrhardt M, and Kremling K. 1983. *Methods of Seawater Analysis*, second revised and extended edition.

Gutiérrez-Rodríguez A, Décima M, Popp BN, Landry MR. 2014. Isotopic invisibility of protozoan trophic steps in marine food webs. Limnol Oceanogr. 59:1590–1598.

Hannides C, Popp BN, Landry MR, Graham BS. 2009. Quantification of zooplankton trophic position in the North Pacific Subtropical Gyre using stable nitrogen isotopes. Limnol Oceanogr. 54:50-61.

Hannides C, Popp BN, Choy CA, Drazen, JC. 2013. Midwater zooplankton and suspended particle dynamics in the North Pacific Subtropical Gyre: a stable isotope perspective. Limnol Oceanogr. 58:1931–1946.

Hayes JM, Freeman KH, Hoham CH, Popp BN. 1990. Compound-specific isotopic analyses, a novel tool for reconstruction of ancient biogeochemical processes. Org Geochem. 16:1115-1128.

Hayes JM. 200.1 Fractionation of carbon and hydrogen isotopes in biosynthetic processes. In Stable Isotope Geochemistry, vol. 43, Eds. Cole DR and Valley JW. Mineralogical Society of America, pp. 225–278.

Hentschel U, Hopke J, Horn M, Friedrich AB, Wagner M, Hacker J, et al. 2002. Molecular Evidence for a Uniform Microbial Community in Sponges from Different Oceans. Appl Environ Microbiol. 68(9):4431–40.

Hentschel U, Usher KM, Taylor MW. 2006. Marine sponges as microbial fermenters. FEMS Microbiol Ecol. 55(2):167–77.

Hoegh-Guldberg O, Mumby PJ, Hooten AJ, Steneck RS, Greenfield P, Gomez E, et al. 2007. Coral Reefs Under Rapid Climate Change and Ocean Acidification. Science. 318:1737–42.

Hoer DR, Gibson PJ, Tommerdahl JP, Lindquist NL, Martens CS. 2017. Consumption of dissolved organic carbon by Caribbean reef sponges. Limnol Oceanogr. doi: 10.1002/lno.10634.

Hoffmann F, Rapp HT, and Reitner J. 2006. Monitoring microbial community composition by fluorescence *in situ* hybridisation during cultivation of the marine cold-water sponge *Geodia barretti*. Mar Biotechnol. 8: 373–379.

Hoffmann F, Radax R, Woebken D, Holtappels M, Lavik G, Rapp HT, et al. 2009. Complex nitrogen cycling in the sponge *Geodia barretti*. Environ Microbiol. 11(9):2228–43.

Hofmann GE, Barry JP, Edmunds PJ, Gates RD, Hutchins DA, Klinger T, et al. 2010. The Effect of Ocean Acidification on Calcifying Organisms in Marine Ecosystems: An Organism-to-Ecosystem Perspective. Annu Rev Ecol Evol Syst. 41(1):127–47.

Houlbreque F and Ferrier-Pages C. 2009. Heterotrophy in tropical scleractinian corals. Biol. Rev. Camb. Philos. Soc. 84: 1–17

Hunter CL and Evans CW. 1995. Coral reefs in Kāneʻohe Bay, Hawaiʻi: Two centuries of western influence and two decades of data. Bull Mar Sci. 57(2):501–15.

Jackson JBC, Kirby MX, Berger WH, Bjorndal KA, Botsford LW, Bourque BJ, Bradbury RH, Cooke R, Erlandson J, Estes JA, Hughes TP, Kidwell S, Lange CB, Lenihan HS, Pandolfi JM, Peterson CH, Steneck RS, Tegner MJ, Warner RR. 2001. Historical overfishing and the recent collapse of coastal ecosystems. Science, 293, 629-638.

Jarman CL, Larsen T, Hunt T, Lipo C, Solsvik R, Wallsgrove NJ, Ka'apu-Lyons C, Close HG, Popp BN. 2017. Diet of the prehistoric population of Rapa Nui (Easter Island, Chile) shows environmental adaptation and resilience. American Journal of Physical Anthropology. 164:343-361.

Jiao N, Herndl GJ, Hansell DA, Benner R, Kattner G, Wilhelm SW, et al. 2010. Microbial production of recalcitrant dissolved organic matter: long-term carbon storage in the global ocean. Nat Rev Microbiol. 8(8):593–9.

Jiménez E, Ribes M. 2007. Sponges as a source of dissolved inorganic nitrogen: Nitrification mediated by temperate sponges. Limnol Oceanogr. 52(3):948–58.

Jokiel PL. 1987. Ecology, biogeography and evolution of corals in Hawaiʻi. Trends Ecol Evol. 2(7):179–82.

Kanda J, Laws EA, Saino T, Hattori A. 1987. An evaluation of isotope dilution effect from conventional data sets of ^{15}N uptake experiments. J Plankton Res. 9:79–90.

Kay AE, Palumbi SR. 1987. Endemism and evolution in Hawaiian marine invertebrates. Trends Ecol Evol. 2(7):183–6.

Keller K, Morel FMM. 1999. A model of carbon isotopic fractionation and active carbon uptake in phytoplankton. Mar Ecol Prog Ser. 182:295–8.

Kendall, C, Silva, SR, and Kelly, VJ. 2001. Carbon and nitrogen isotopic compositions of particulate organic matter in four large river systems across the United States. Hydrol. Process. 15: 1301–1346.

Kennedy J, Marchesi JR, Dobson ADW. 2007. Metagenomic approaches to exploit the biotechnological potential of the microbial consortia of marine sponges. Appl Microbiol Biotechnol. 75: 11–20.

Kerouel R and Aminot A. 1997. Fluorometric determination of ammonia in sea and estuarine waters by direct segmented flow analysis. Marine Chemistry. 57(3-4): 265-275.

Kirchman DL. 1994. The uptake of inorganic nutrients by heterotrophic bacteria. Microb Ecol. 28(2):255–71.

Kirchman DL, Wheeler PA. 1998. Uptake of ammonium and nitrate by heterotrophic bacteria and phytoplankton in the sub-Arctic Pacific. Deep-Sea Research I. 45: 347-365.

Lajtha K, and Michener RH. 1994. Stable isotopes in ecology and environmental science, Oxford: Blackwell Scientific Publications.

Larsen T, Taylor DL, Leigh MB, O'Brien DM. 2009. Stable isotope fingerprinting: a novel method for identifying plant, fungal, or bacterial origins of amino acids. Ecology. 90:3526-3535.

Larsen T, Ventura M, Andersen N, O'Brien DM, Piatkowski U, McCarthy MD. 2013. Tracing carbon sources through aquatic and terrestrial food webs using amino acid stable isotope fingerprinting. PLoS One 8:e73441.

Larsen T, Bach LT, Salvatteci R, Wang YV, Andersen N, Ventura M, McCarthy MD. 2015. Assessing the potential of amino acid $\delta^{13}C$ patterns as a carbon source tracer in marine sediments: effects of algal growth conditions and sedimentary diagenesis. Biogeosci Discuss. 12:1613-1651.

Laws EA, Popp BN, Bidigare RR, Riebesell U, Burkhardt S, Wakeham SG. 2001. Controls on the molecular distribution and carbon isotopic composition of alkenones in certain haptophyte algae. Geochemistry, Geophys Geosystems. 2(1).

Lotze HK, Lenihan HS, Bourque BJ, Bradbury RH, Cooke RG, Kay MC, Kidwell SM, Kirby MX, Peterson CH, Jackson JBC. 2006. Depletion, degradation, and recovery potential of estuaries and coastal seas. Science. 312: 1806-1809.

Lowe RJ, Falter JL, Monismith SG, Atkinson MJ. 2009. A numerical study of circulation in a coastal reef-lagoon system. J Geophys Res. 114.

Maliao RJ, Turingan RG, Lin J. 2008. Phase-shift in coral reef communities in the Florida Keys National marine Sanctuary, USA. Marine Biology. 154, 841-853.

McCarthy MD, Benner R, Lee C, Fogel ML. 2007. Amino acid nitrogen isotopic fractionation patterns as indicators of heterotrophy in plankton, particulate, and dissolved organic matter. Geochim Cosmochim Acta. 71(19):4727–44.

McClelland JW and Valiela I. 1998. Linking nitrogen in estuarine producers to land-derived sources. Limnol. Oceanogr. 43: 577–585.

McClelland JW, Montoya JP. 2002. Trophic relationships and the nitrogen isotopic composition of amino acids in plankton. Ecology. 83, 2173–2180.

McCook LJ, Jompa J, Diaz-Pulido G. 2001. Competition between corals and algae on coral reefs: a review of evidence and mechanisms. Coral Reefs. 19, 400–417.

McMurray SE, Blum AJE, Pawlik AJR. 2008. Redwood of the reef: growth and age of the giant barrel sponge *Xestospongia muta* in the Florida Keys. Mar Biol. 155:159–71.

McMurray SE, Pawlik JR, Finelli CM. 2014. Trait-mediated ecosystem impacts: how morphology and size affect pumping rates of the Caribbean giant barrel sponge. Aquat Biol Aquat Biol. 23:1–13.

Menden-Deuer S, Lessard EJ. 2000. Carbon to volume relationships for dinoflagellates, diatoms, and other protist plankton. Limnol Oceanogr. 45(3):569–79.

Merbt SN, Stahl DA, Casamayor EO, Nia Martí E, Nicol GW, Prosser JI. 2012. Differential photoinhibition of bacterial and archaeal ammonia oxidation. FEMS Microbiol Lett. 327(1): 41-46.

Mohamed NM, Colman AS, Tal Y, Hill RT. 2008. Diversity and expression of nitrogen fixation genes in bacterial symbionts of marine sponges. Environ Microbiol. 10(11):2910–21.

Mohamed NM, Saito K, Tal Y, Hill RT. 2010. Diversity of aerobic and anaerobic ammonia-oxidizing bacteria in marine sponges. ISME J. 4(1):38–48.

Mueller B, de Goeij JM, Vermeij MJA, Mulders Y, van der Ent E, Ribes M, et al. 2014. Natural Diet of Coral-Excavating Sponges Consists Mainly of Dissolved Organic Carbon (DOC). PLoS One. 9(2):e90152.

Murphy J and Riley IP. 1962. A modified single solution method for the determination of phosphate in natural waters. Anal. Chim. Acta. 27:31-6.

Muscatine L and Cernichiari E. 1969. Assimilation of photosynthetic products of zooxanthellae by a reef coral. Biol Bull. 137: 506–523.

Muscatine L and Porter JW. 1977. Reef corals: mutualistic symbioses adapted to nutrient-poor environments. Bioscience. 27, 454–460.

Muscatine L, Porter JW, Kaplan IR. 1989. Resource partitioning by reef corals as determined from stable isotope composition. Mar Biol. 100(2):185–93.

Núñez Pons L, Calcinai B, Gates RD. 2017. Who's there? – First morphological and DNA barcoding catalogue of the shallow Hawaiian sponge fauna. PLoS One. 12(12): e0189357.

O'Connell TC. 2017. 'Trophic' and 'source' amino acids in trophic estimation: a likely metabolic explanation. Oecologia. 184, 317–326.

Ostrander CE, McManus MA, DeCarlo EH, Mackenzie FT. 2008. Temporal and spatial variability of freshwater plumes in a semi-enclosed estuarine-bay system. Estuaries Coasts. 31:192–203.

Pawlik JR, Kernan MR, Molinski TF, Harper MK, Faulkner DJ. 1988. Defensive chemicals of the Spanish dancer nudibranch *Hexabranchus sanguineus* and its egg ribbons: macrolides derived from a sponge diet. J Exp Mar Bio Ecol. 119(2):99–109.

Pawlik JR, Loh T-L, Mcmurray SE, Finelli CM. 2013. Sponge Communities on Caribbean Coral Reefs Are Structured by Factors That Are Top-Down, Not Bottom-Up. PLoS One. 8(5).

Pawlik JR, McMurray SE, Erwin P, Zea S. 2015. A review of evidence for food limitation of sponges on Caribbean reefs. Marine Ecology Progress Series. 519: 265–283.

Pile AJ, Patterson MR, Savarese M, Chernykh VI, Fialkov VA. 1997. Trophic effects of sponge feeding within Lake Baikal's littoral zone. 2. Sponge abundance, diet, feeding efficiency, and carbon flux. Limnol Oceanogr. 42(1):178–84.

Pile AJ, Grant A, Hinde R, Borowitzka MA. 2003. Heterotrophy on ultraplankton communities is an important source of nitrogen for a sponge-rhodophyte symbiosis. J Exp Biol. 206(Pt 24):4533–8.

Plucer-Rosario G. 1987. The effect of substratum on the growth of *Terpios*, an encrusting sponge which kills corals. Coral Reefs. 5: 197-200.

Peterson BJ and Fry B. 1987. Stable isotopes in ecosystem studies. Annual Review of Ecology and Systematics. 18: 293–320.

Popp BN, Sansone FJ, Rust TM, Merritt DA. 1995. Determination of concentration and carbon isotopic composition of dissolved methane in sediments and nearshore waters. Analytical Chemistry. 67: 405–411.

Popp BN, Graham BS, Olson RJ, Hannides CCS, Lott MJ, Lopez-Ibarra GA, Galvan-Magana F, Fry B. 2007. Insight into the trophic ecology of yellowfin tuna, *Thunnus albacares*, from compound-specific nitrogen isotope analysis of proteinaceous amino acids. Eds: Dawson T, Siegwolf R. Stable Isotopes as Indicators of Ecological Change. New York: Elsevier Academic Press, Terrestrial Ecology Series. p 173-190.

Post DM. 2002. Using stable isotopes to estimate trophic position: Models, methods, and assumptions. Ecology. 83(3):703–18.

Post DM, Layman CA, Arrington DA, Takimoto G, Quattrochi J, Montaña CG. 2007. Getting to the fat of the matter: models, methods and assumptions for dealing with lipids in stable isotope analyses. Oecologia. 152:179–189.

Rädecker N, Pogoreutz C, Voolstra CR, Wiedenmann J, Wild C. 2015. Nitrogen cycling in corals: the key to understanding holobiont functioning? Trends Microbiol. 23(8):490–7.

Rees TAV. 2007. Metabolic and ecological constraints imposed by similar rates of ammonium and nitrate uptake per unit surface area at low substrate concentrations in marine phytoplankton and macroalgae. J. Phycol. 43: 197–207.

Reiswig HM. 1971. *In situ* pumping activities of tropical *Demospongiae*. Mar Biol. 9(1):38–50.

Reiswig, HM. 1974. Water transport, respiration and energetics of three tropical marine sponges. J. Exp. Mar. Biol. Ecol. 14: 231-249.

Reshef L, Koren O, Loya Y, Zilber-Rosenberg I, Rosenberg E. 2006. The coral probiotic hypothesis. Environ. Microbiol. 8: 2068–2073.

Richardson CM, Dulai H, Whittier RB. 2016. Sources and spatial variability of ground-derived nutrients in Maunalua Bay, O'ahu, Hawai'i. Journal of Hydrology: Regional Studies 11:178-193.

Richter C, Wunsch M, Rasheed M, Kötter I, Badran MI. 2001. Endoscopic exploration of Red Sea coral reefs reveals dense populations of cavity-dwelling sponges. Nature. 413:726–730.

Rix L, de Goeij JM, Mueller CE, Struck U, Middelburg JJ, van Duyl FC, et al. 2016. Coral mucus fuels the sponge loop in warm- and cold-water coral reef ecosystems. Sci Rep. 6(1):18715.

Rix L, de Goeij JM, van Oevelen D, Struck U, Al-Horani FA, Wild C, et al. 2017. Differential recycling of coral and algal dissolved organic matter via the sponge loop. Funct Ecol. 31(3):778–89.

Rutzler K. 1990. Association between Caribbean sponges and photosynthetic organisms. New Perspectives in Sponge Biology. Third International Conference on the Biology of Sponges, Smithsonian Inst. Press, Washington, D.C.: 455-466.

Rutzler K and Muzik K. 1993. *Terpios hoshinota*, a new cyanobacteriosponge threatening Pacific reefs *. Sci Mar. 57(4):395–403.

Santoro AE, Casciotti KL. 2011. Enrichment and characterization of ammonia-oxidizing archaea from the open ocean: phylogeny, physiology and stable isotope fractionation. ISME J. 558(10): 1796–808.

Scheffers SR, Nieuwland G, Bak RPM, van Duyl FC. 2004. Removal of bacteria and nutrient dynamics within the coral reef framework of Curaçao (Netherlands Antilles). Coral Reefs. 23(3):413–22.

Schläppy M-L, Schöttner SI, Lavik G, Kuypers MMM, De Beer D, Hoffmann F. 2010. Evidence of nitrification and denitrification in high and low microbial abundance sponges. Mar Biol. 157:593–602.

Schmitt, S, Wehrl M, Lindquist N, Weisz JB, and Hentschel U. 2007. Morphological and molecular analyses of microorganisms in Caribbean reef adult sponges and in corresponding reproductive material, p. 561–568. Eds: M. Custodio, G. Lobo-Hajdu, E. Hajdu, and G. Muricy, Porifera research: biodiversity, innovation & sustainability. Museo National, Rio de Janeiro, Brazil.

Schmitt S, Angermeier H, Schiller R, Lindquist N, Hentschel U. 2008. Molecular microbial diversity survey of sponge reproductive stages and mechanistic insights into vertical transmission of microbial symbionts. Appl Environ Microbiol. 74(24):7694–708.

Selph KE, Landry MR, Taylor AG, Yang E-J, Measures CI, Yang J, et al. 2011. Spatially-resolved taxon-specific phytoplankton production and grazing dynamics in relation to iron distributions in the Equatorial Pacific between 110 and 140°W. Deep Sea Res Part II Top Stud Oceanogr. 58(3–4):358–77.

Selph KE, Goetze E, Jungbluth MJ, Lenz PH, Kolker G. 2018. Microbial food web connections and rates in a subtropical embayment. Mar Ecol Prog Ser. 590:19–34.

Shantz AA, Lemoine NP, Burkepile DE. 2015. Nutrient loading alters the performance of key nutrient exchange mutualisms. Ecol. Lett. 19 (1), 20–28.

Sharp KH, Eam B, Faulkner DJ, Haygood MG. 2007. Vertical transmission of diverse microbes in the tropical sponge *Corticium sp.* Appl Environ Microbiol. 73(2):622–9.

Siegl A, Hentschel U. 2010. PKS and NRPS gene clusters from microbial symbiont cells of marine sponges by whole genome amplification. Environ Microbiol Rep 2: 507–513.

Sigman DM, Casciotti KL, Andreani M, Barford C, Galanter M, Bo JK. 2001. A Bacterial Method for the Nitrogen Isotopic Analysis of Nitrate in Seawater and Freshwater. Anal Chem. 73(17):4145–53.

Silfer J, Engel M, Macko S, Jumeau E. 1991. Stable carbon isotope analysis of amino acid enantiomers by conventional isotope ratio mass spectrometry and combined gas chromatography/isotope ratio mass spectrometry. Anal Chem. 63:370-374.

Silveira CB, Silva-Lima AW, Francini-Filho RB, Marques JSM, Almeida MG, Thompson CC et al. 2015. Microbial and sponge loops modify fish production in phase-shifting coral reefs. Environmental Microbiology. 17, 3832–3846.

Simion P, Philippe H, Baurain D, Jager M, Richter DJ, Di Franco A, et al. 2017. A Large and Consistent Phylogenomic Dataset Supports Sponges as the Sister Group to All Other Animals. Curr Biol. 27(7):958–67.

Smith JE, Shaw M, Edwards RA, Obura D, Pantos O, Sala E, et al. 2006. Indirect effects of algae on coral: algae-mediated, microbe-induced coral mortality. Ecol Lett. 9(7):835–45.

Smith JE, Hunter CL, Smith CM. 2010. The effects of top–down versus bottom–up control on benthic coral reef community structure. Oecologia. 163(2):497–507.

Southwell MW. 2007. Sponge impacts on coral reef nitrogen cycling, Key Largo, Florida. Ph.D. thesis, Univ. of North Carolina, Chapel Hill.

Southwell MW, Popp BN, Martens CS. 2008a. Nitrification controls on fluxes and isotopic composition of nitrate from Florida Keys sponges. Mar Chem. 108:96–108.

Southwell MW, Weisz JB, Martens CS, Lindquist N. 2008b. In situ fluxes of dissolved inorganic nitrogen from the sponge community on Conch Reef, Key Largo, Florida. Limnol Oceanogr. 53(3):986–96.

Steindler L, Huchon D, Avni A, Ilan M. 2005. 16S rRNA phylogeny of sponge-associated cyanobacteria. Appl Environ Microbiol. 71:4127–4131.

Stimson J and Larned ST. 2000. Nitrogen efflux from the sediments of a subtropical bay and the potential contribution to macroalgal nutrient requirements. J Exp Mar Biol Ecol. 252(252):159–80.

Stimson J and Conklin E. 2008. Potential reversal of a phase shift: the rapid decrease in the cover of the invasive green macroalga *Dictyosphaeria cavernosa* on coral reefs in Kane‘ohe Bay, Oahu, Hawai‘i. Coral Reefs. 27:717–726 DOI.

Stimson J. 2014. A long-term record of nutrient concentrations in Kāne’ohe Bay, Oahu, Hawai’i and its relevance to the onset and end of a phase shift involving an indigenous alga, *Dictyosphaeria cavernosa*. Pacific Sci. 69(3).

Sutka RL, Ostom NE, Ostrom PH, Phanikumar MS. 2004. Stable nitrogen isotopic dynamics of dissolved nitrate in a transect from the North Pacific Subtropical Gyre to the Eastern Tropical North Pacific. Geochimica et Cosmochimica Acta. 68(3): 517–527.

Taylor MW, Radax R, Steger D, Wagner M. 2007a. Sponge-associated microorganisms: evolution, ecology, and biotechnological potential. Microbiol Mol Biol Rev. 71(2):295–347.

Taylor MW, Hill RT, Piel J, Thacker RW, Hentschel U. 2007b. Soaking it up: the complex lives of marine sponges and their microbial associates. ISME J. 1(3):187–90.

Thacker RW. 2005. Impacts of shading on sponge-cyanobacteria symbioses: a comparison between host-specific and generalist associations. Integr Comp Biol. 45:369–376.

Thomas TRA, Kavlekar DP, LokaBharathi PA. 2010. Marine drugs from sponge-microbe association-a review. Marine Drugs. 8: 1417–1468.

Tolar BB, Powers LC, Miller WL, Wallsgrove NJ, Popp BN, Hollibaugh JT. 2016. Ammonia Oxidation in the Ocean Can Be Inhibited by Nanomolar Concentrations of Hydrogen Peroxide. Front Mar Sci. 3:237.

Ueda K, Morgan SL, Fox A, Gilbart J, Sonesson A, Larsson L, Odham G. 1989. D-alanine as a chemical marker for the determination of streptococcal cell wall levels in mammalian tissues by gas chromatography/negative ion chemical ionization mass spectrometry. Anal Chem. 61:265-270.

Vacelet J. 1975. Etude en microscopie electronique de l'association entre bacteries et spongiaires du genre *Verongia* (*Dictyoceratida*). J Microsc Biol Cell. 23: 271–288.

Verity PG and Landgon C. 1984. Relationships between lorica volume, carbon, nitrogen, and ATP content of tintinnids in Narragansett Bay. J. Plankton Res. 66: 859–868.

Vicente J, Silbiger NJ, Beckley BA, Raczkowski CW, Hill RT. 2016. Contribution to Special Issue: "Towards a Broader Perspective on Ocean Acidification Research" Impact of high pCO_2 and warmer temperatures on the process of silica biomineralization in the sponge *Mycale grandis*. ICES J Mar Sci. 73:704–14.

Vizzini S, Savona B, Chi T, Mazzola A. 2005. Spatial variability of stable carbon and nitrogen isotope ratios in a Mediterranean coastal lagoon. Hydrobiologia. 550:73–82.

Wang G, Yoon S-H, Lefait E. 2009. Microbial communities associated with the invasive Hawaiian sponge *Mycale armata*. ISME J. 3(3):374–7.

Ward BB, Kilpatrick KA, Renger EH, Eppley RW. 1989. Biological nitrogen cycling in the nitracline. Limnol Oceanogr. 34(3):493–513.

Webb KL, DuPaul WD, Wiebe W, Sottile W, Johannes RE. 1975. Enewetak (Eniwetok) Atoll: Aspects of the nitrogen cycle on a coral reef. Limnol Oceanogr. 20(2):198–210.

Webster NS, Taylor MW, Behnam F, Lücker S, Rattei T, Whalan S, et al. 2010. Deep sequencing reveals exceptional diversity and modes of transmission for bacterial sponge symbionts. Environ Microbiol. 12: 2070– 2082.

Weisz JB, Hentschel U, Lindquist N, Martens CS. 2007. Linking abundance and diversity of sponge-associated microbial communities to metabolic differences in host sponges. Mar Biol. 152(2):475–83.

Weisz JB, Lindquist N, Martens CS. 2008. Do associated microbial abundances impact marine demosponge pumping rates and tissue densities? Oecologia. 155(2):367–76.

Wild C, Huettel M, Klueter A, Kremb SG, Rasheed MYM, Jorgensen BB. 2004. Coral mucus functions as an energy carrier and particle trap in the reef ecosystem. Nature 428:66–70.

Wilkinson CR and Vacelet J. 1979. Transplantation of marine sponges to different conditions of light and current. J Exp Mar Bio Ecol. 37(1):91–104.

Wilkinson CR. 1983. Net primary productivity in coral reef sponges. Science. 219(4583):410–2.

Wilkinson CR. 1984. Immunological Evidence for the Precambrian Origin of Bacterial Symbioses in Marine Sponges. Proc R Soc B Biol Sci. 220(1221):509–18.

Wilkinson CR. 1987. Interocean Differences in Size and Nutrition of Coral Reef Sponge Populations. Source Sci New Ser. 236(4809):1654–7.

Wulff JL and Buss LW. 1979. Do sponges help hold coral reefs together? Nature. 281: 474–475.

Yahel G, Sharp JH, Marie D, Hase C, Genin A. 2003. *In situ* feeding and element removal in the symbiont-bearing sponge *Theonella swinhoei*: bulk DOC is the major source for carbon. Limnol Oceanogr. 48, 141–149.

Yahel G, Whitney F, Reiswig HM, Eerkes-Medrano DI, Leys SP. 2007. *In situ* feeding and metabolism of glass sponges (*Hexactinellida, Porifera*) studied in a deep temperate fjord with a remotely operated submersible. Limnol Oceanogr. 52: 428–440.

Yamaguchi YT, Chikaraishi Y, Takano Y, Ogawa NO, Imachi H, Yokoyama Y, Ohkouchi N. 2017. Fractionation of nitrogen isotopes during amino acid metabolism in heterotrophic and chemolithoautotrophic microbes across Eukarya, Bacteria, and Archaea: effects of nitrogen sources and metabolic pathways. Organic Geochemistry. 11, 101–112.

Yamaguchi YT, McCarthy MD. 2018. Sources and transformation of dissolved and particulate organic nitrogen in the North Pacific Subtropical Gyre indicated by compound-specific $\delta^{15}N$ analysis of amino acids. Geochim Cosmochim Acta. 220:329–47.

Zeebe RE and Wolf-Gladrow D. 2001. CO_2 in Seawater: Equilibrium, Kinetics, Isotopes, Elsevier Oceanography Series (Elsevier, Amsterdam).

Zehr JP, Ward BB. 2002. Nitrogen cycling in the ocean: new perspectives on processes and paradigms. Appl Environ Microbiol. 68(3):1015–24.

Zhu P, Li Q, Wang G. 2008. Unique Microbial Signatures of the Alien Hawaiian Marine Sponge *Suberites zeteki*. Microb Ecol. 55(3):406–14.